VLÁKNA a TEXTIL

1

Ročník 19.
2012

ISSN1335-0617

Indexed in:

Chemical Abstracts,

World Textile Abstracts

EMDASE

Elsevier Biobase

Elsevier GeoAbstracts

Fibres and Textiles (1) 2012
Vlákna a textil (1) 2012

Content

Textile materials

Obsah

Textilné materiály

Príspevky boli prijaté do tlače bez recenzie.
Za odbornú a jazykovú úroveň príspevkov zodpovedajú autori a prekladatelia.

COMPARISON OF WET MILLING ACTION FOR FIBROUS AND SOLID MATERIALS

Vijay Baheti, Miroslava Marsalkova, Rehan Abbasi and Jiri Militky

Department of Textile Materials, Technical University of Liberec, Studentská 2, 46117 Liberec, Czech Republic
vijaykumar.baheti@gmail.com

Abstract: *The objective of this work was to utilise the short fibres generated in textile processing for the preparation of nano particles as reinforcement in composite applications. Suitability of high energy planetary ball milling technique was studied for grinding these materials at nano scale in wet condition. Three different types of materials with different density and surface characteristics (i.e. fly ash, jute fibres and glass fibres) were selected for analysing severity of milling action.*

Keywords: *Short fibres, High energy planetary ball milling, Particle size distribution*.

1 INTRODUCTION

Nanotechnology has become the buzz-word in recent years. Materials at the nanoscale have enhanced mechanical, electrical, magnetic, optical and chemical properties to a level that cannot be achieved by large scale materials. A variety of ways have been reported to synthesize nano level materials such as plasma arcing, chemical vapour deposition, electro deposition, sol-gel synthesis, high energy ball milling etc. Among these methods high energy ball milling has advantages of being simple, relatively inexpensive to produce, applicable to any class of materials and can be easily scaled up to large quantities [1, 2, 3].
Ball milling process is a mechanical process which relies on the energy released at the point of collision between balls as well as on the high grinding energy created by friction of balls on the wall as shown in Figure 1. When the mill rotates, balls are picked up by the mill wall and rotate around the wall due to centrifugal force leading to grinding of material due to frictional effect. On the other hand there is also reverse rotation of disc with respect to mill which applies centrifugal force in opposite direction leading to transition of balls on opposite walls of mill giving impact effect. However most of the reduction is carried out by impact.

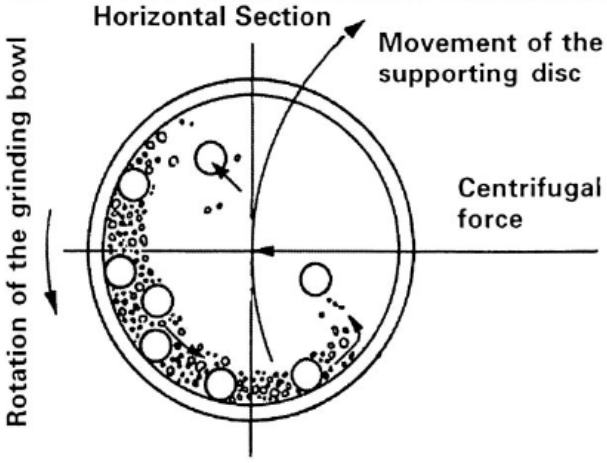

Figure 1 Principle of ball milling process

The purpose of this study is to determine severity of milling action for different types of materials. Jute fibres and glass fibres were selected from fibrous category whereas fly ash was selected from solid category.

2 MATERIALS AND METHODS

2.1 Materials

Jute fibres were obtained from Textile Technology department of IIT Delhi, India. The other materials like fly ash and glass fibres were available in Technical University of Liberec and used without any modification.

2.2 Methods

Pulverization of fly ash, jute fibres and E-glass fibres was carried out using a high-energy planetary ball mill of Fritsch Pulverisette 7 in a sintered corundum container with zirconia balls of Φ 10 mm for initial 10 min of dry milling and for further wet milling in deionised water. The ball mill was loaded with ball to material ratio (BMR) of 10:1. The rotation speed of the planet carrier was 850 rpm.

Particle size distributions of milled material was carried out after each one hour of milling on Malvern Zetasizer Nano series based on dynamic light scattering principle. Deionised water was used as dispersion medium and ultrasonicated for 5 min with Bandelin ultrasonic probe before characterisation. Refractive indexes of 1.52 (Jute), 1.52 (E-Glass) and 1.55 (Fly ash) were used to calculate particle size. Morphologies of jute and fly ash after wet milling was observed on scanning electron microscope TS5130-Tescan SEM at 30 KV accelerated voltage.

3 RESULTS AND DISCUSSIONS

3.1 Comparison of milling action between fibrous materials

For the initial dry milling of 10 min, glass fibres were pulverised into powder form faster than the jute fibres (Figure 2a and 2b). The size distribution was also observed uniform in case of glass with every individual fibre refined to powder. Whereas jute was partly refined to powder with small percentage in fibre stage. This was due to the brittle nature of glass fibres than the jute fibres.

Wet milling for extended duration of 3 hours resulted into multimodal size distribution for jute fibres and near unimodal size distribution for glass fibres (Figure 2a and 2b). This was due to abrasive nature of glass particles which prevented them from sticking to milling media as a result of heat generated during milling operation. Jute particles being soft in nature formed a layer on the wall of milling container with increased heat which stopped further pulverisation to result in multimodal distribution.

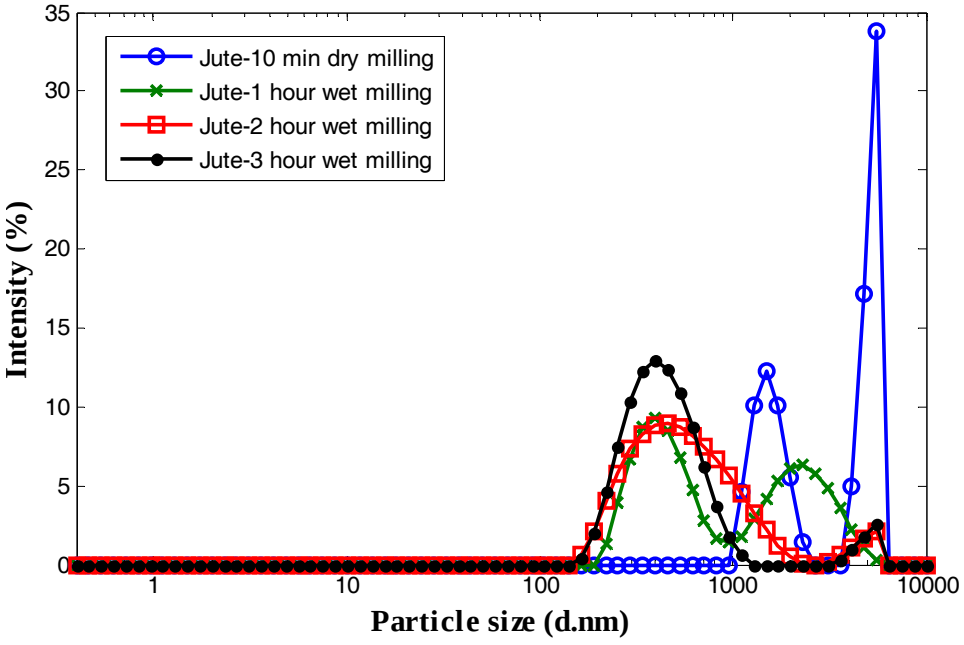

Figure 2a Particle size refinement of jute fibres

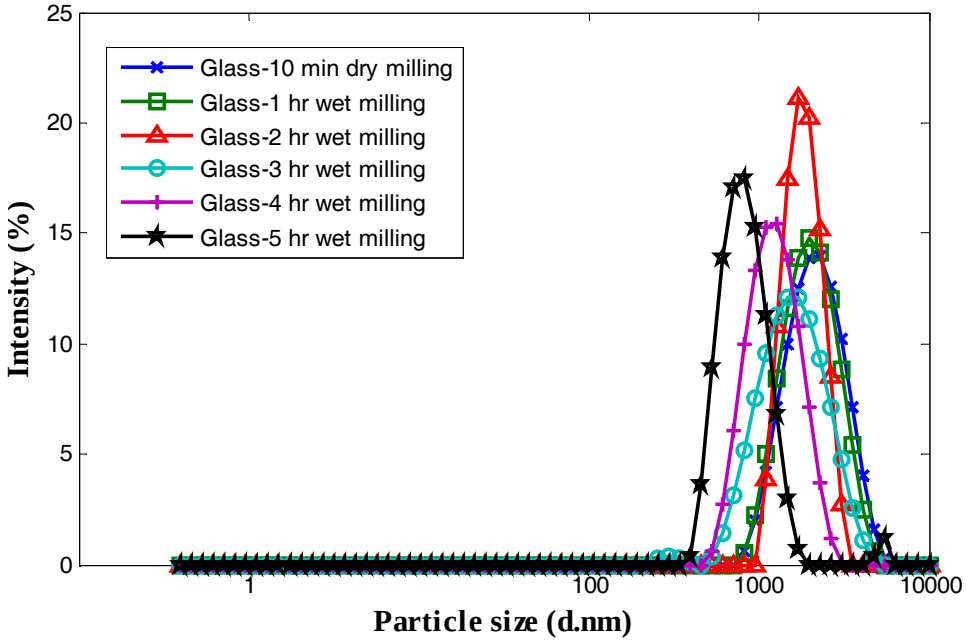

Figure 2b Particle size refinement of glass fibres

3.2 Comparison of milling action between fibrous and solid materials

When fly ash was pulverised in wet condition, the decrease in particle size was observed little slower than jute fibres due to higher density of fly ash (Figure 3a and 3b). However the milling action was more efficient and uniform throughout the duration of three hours for the fly ash due to non layering of material on the wall. This resulted in further size reduction even after 3 hours of milling (Figure 3b). On the other hand, jute particles were unable to undergo further refinement as peaks remained in the same position with only difference of reduction in multimodality with increase in milling time (Figure 3a).

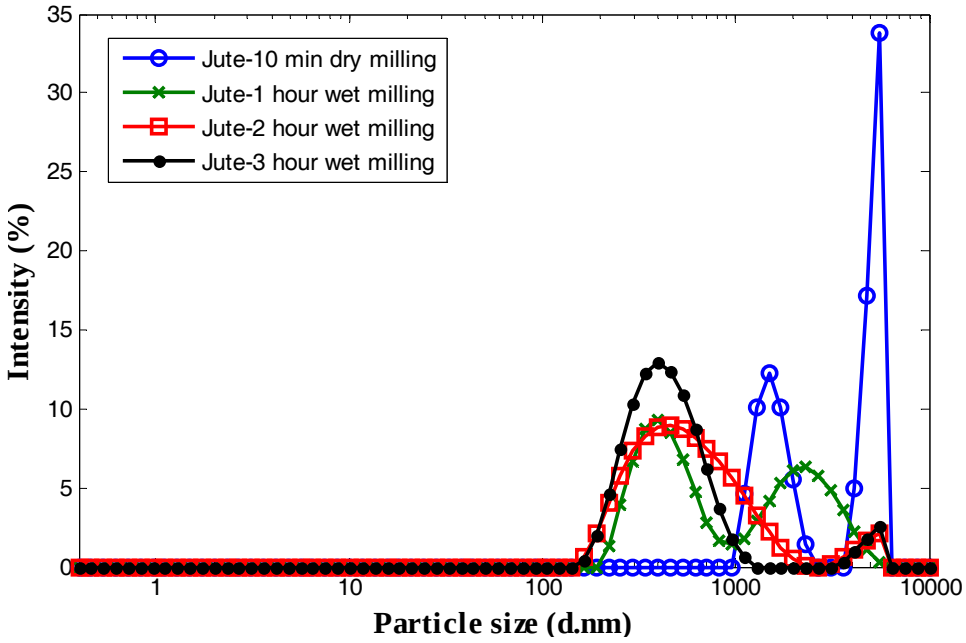

Figure 3a Particle size refinement of jute fibres

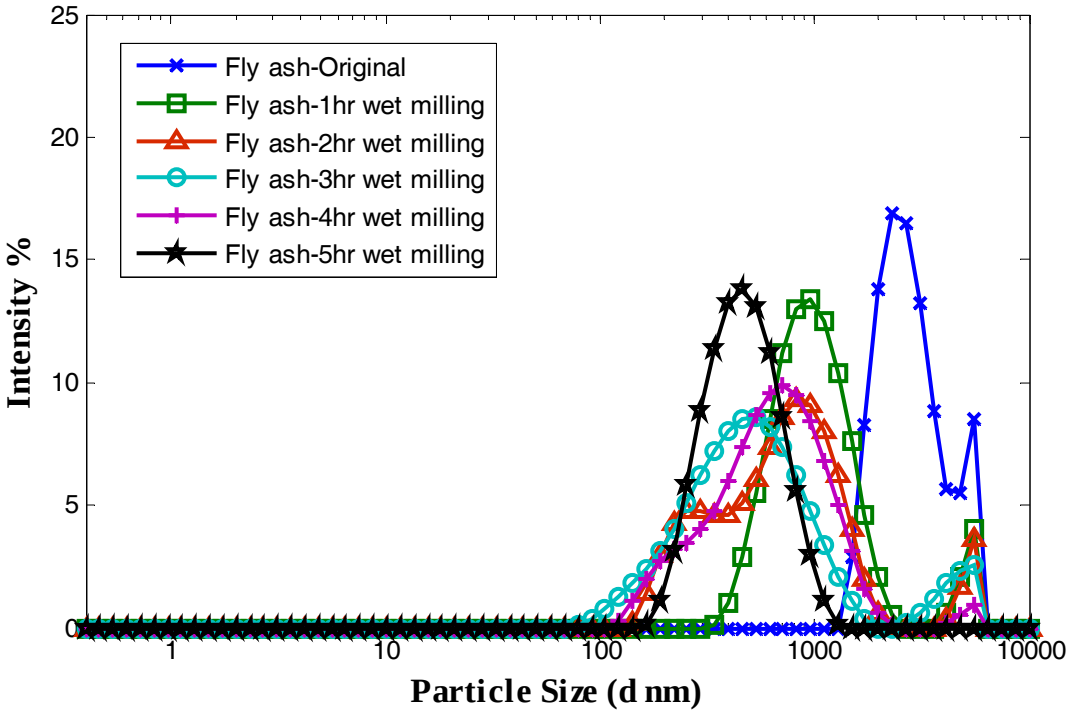

Figure 3b Particle size refinement of fly ash

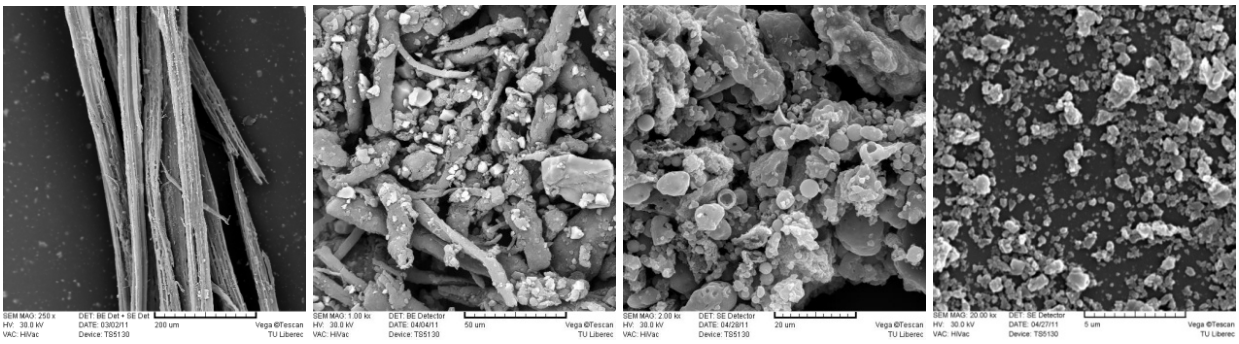

Figure 4a Unmilled jute fibre

Figure 4b Wet milled jute after 3 hours

Figure 4c Unmilled fly ash

Figure 4d Wet milled fly ash after 5 hours

The wider size distribution in case of jute milling than the fly ash milling was clearly seen under SEM as shown in Figure 4. The same reason of sticking of jute on the wall surface due to increase in temperature during milling operation was responsible to provide these large differences in size of particles.

3.3 Effect of milling time on average particle size

When average size of the particle was considered apart from size distribution, then all these three materials shown near about similar level of refinement in the size after 3 hours of wet milling (Figure 5). The rate in particle size reduction obtained for jute, glass and fly ash is near about same with the milling time. This confirmed the effectiveness of milling action regardless of density of material for finer refinement. Therefore, if rise in temperature is prevented during the milling operation, then the chances of wider size distribution as obtained in the jute milling can be avoided and milling can be performed for extended duration.

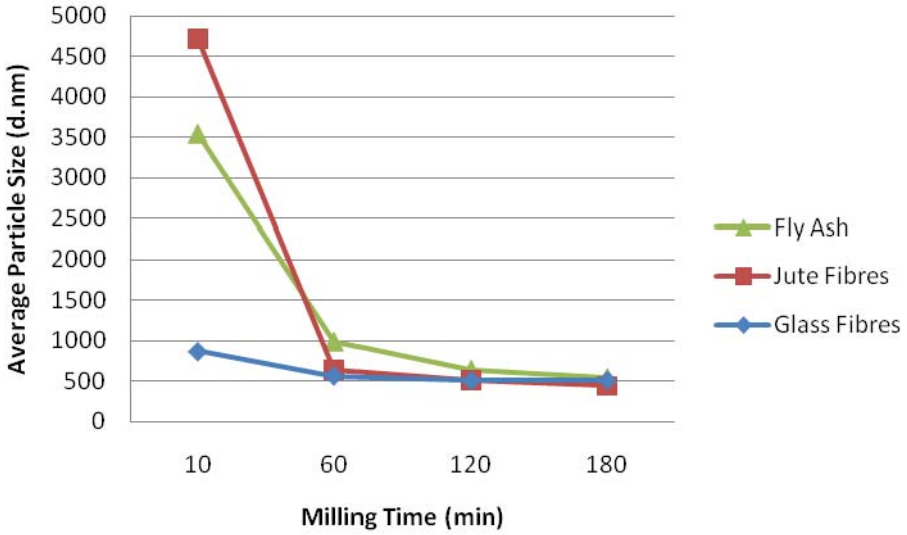

Figure 5 Average particle size with increase in milling time

4 CONCLUSION

The rate in particle size reduction obtained for jute, glass and fly ash is near about same with the milling time. Only concern is chances of sticking of material to the milling media as observed in jute fibres due to increase in temperature during milling which gives wider size distribution. This requires optimisation of milling conditions to increase the possible milling time without rise in temperature. As a result ball milling will have plenty of scope to become industrially applicable as it can produce nanoparticles in large quantity.

Acknowledgement: *This work was supported under the project SGS-4841 by Technical University of Liberec, Czech Republic.*

5 REFERENCES

1. Thomos Paul K., Satpathy S.K., Manna I., Chakraborty K.K., Nando G.B.: Preparation and characterisation of nano structured materials from fly ash: a waste from thermal power stations, by high energy ball milling, Nanoscale Research Letter 2, 2007, 397-404
2. Prasad B.M., Sain M.M., Roy D.N.: Properties of ball milled thermally treated hemp fibers in an inert atmosphere for potential composite reinforcement, Journal of Material Science 40, 2005, 4271-4278
3. Yuen C.W.M., Cheng Y.F., Li Y., Hu J.Y.: Preparation and characterisation of nano-scale cotton powder, The journal of Textile Institute 100, 2009, 165-172

Porovnání účinnosti mletí vlákenných materiálů a částic za mokra

Translation of the article
Comparison of wet milling action for fibrous and solid materials

Práce je zaměřena na přípravu nanočástic z vlákenných odpadů vhodných pro využití v kompozitních strukturách. Je použito techniky planetového mletí pomocí kuliček za mokra. Jsou použity tří výchozí materiály s různou měrnou hmotností a povrchovými charakteristikami (popílek, jutové odpady a skleněná odpadní vlákna). Je hodnocena účinnost přípravy nanočástic za různých podmínek.

A NEW WAY TO THE OBJECTIVE HAND EVALUATION

Vladimír Bajzík

Technical University in Liberec, Faculty of Textile Engineering, Department of Textile Evaluation, Liberec, Czech Republic
vladimir.bajzik@tul.cz

Abstract: *In present paper a new method named BM technique leading to the objective hand evaluation is presented. The method is based on the evaluation of 8 measurable properties using instruments occurring commonly in textile laboratories. The properties were selected from four basic groups of properties corresponding to the hand sensory centre. As prediction equation the ordinal logistic regression was applied. At first the total hand value (THV) of 90 men suits was evaluated subjectively using the panel of 40 respondents and median category M of eleven degree ordinal scale was calculated for each fabric. From 90 fabrics the set of 80 ones was applied for creation of the prediction formulae. The rest 10 fabrics served for verification of prediction ability. Prediction ability of BM techniques was compared with the same approach but on the properties obtained from KES system. Also 2 types of prediction equation derived on the basis of analysis from BM properties were compared. Results flowing from both sets of properties and 4 equations show the comparable results. The most of 10 fabrics was objectively classified to the category M±1 in comparison with subjective evaluation.*
Key Words: *objective hand evaluation, subjective hand evaluation, THV, ordinal logistic regression*

1 INTRODUCTION

The hand of textiles belongs among the basic tactile properties of textiles and is understood as the complex psychophysical property. It means that the subjective precept hand is weighted mean of single primary hand stimulus and personal knowledge of evaluator. Its definition still is not given clearly. Generally, hand can be understood as sensation evoked by contact between the skin and textile. Some definitions are presented in [1-4]. Before and during subjective hand evaluation it is necessary to solve several key problems which realization can affect the results:

- choice of respondents,
- choice of scale,
- choice of properties and its definition,
- the course and conditions of experiment,
- analysis of results.

Bishop [5] in his summary review presents the similar key elements:

- the judges,
- the criteria of judgement,
- the assessment conditions,
- the assessment technique,
- the method of ranking or scaling the assessment,
- analysis of results.

It is evident to prepare and realize experiment for subjective hand evaluation needs a lot of time.

During approximately last 40-50 years the big effort to objective hand evaluation was dedicated. As the main reason the prediction of subjective hand evaluation is. The research realized by Binns [6] and Peirce work [7] belongs among the first works in the field of subjective hand evaluation and its objective prediction. The introduced principles of objective hand evaluation according to applied methods and instruments can be divided to three groups:

- set of special instruments – e.g., here the most spread system KES [8] can be placed. It is consisted from 4 instruments where 15 characteristics is measured,
- special instrument, where the principle is based on pulling sample through round or conic hole [9, 10],

- standard instruments, which are mostly to disposal in a textile laboratory [11, 12].

Kawabata in his work [8] proved that primary hand hands are evaluated at first and then a total hand is expressed. In the present paper the technique (BM technique) at which the choice of properties was realized on the basis of idea of Lundgren [1] that evaluation of hand is connected with four centres:

- centre of surface smoothness and unevenness,
- centre of stiffness and compliance,
- centre of volume properties,
- centre of thermal phenomena.

Ordinal logistic regression (OLR) was applied for design of formula for objective hand evaluation. The application of OLR is presented in [13] and results indicated its application as suitable. Therefore, the results flowing from BM technique were compared with results built on the properties from KES.

2 ORDINAL LOGISTIC REGRESSION

Ordinal logistic regression can be applied in the case when depended variable *y* is ordinal. This is typical for subjective hand evaluation when fabrics are classified to *K* ordered categories – in this case *K* is mostly 11, *k*=1, 2,…*K*, from evaluation – hand is very bad (*k*=1, *y*=0) to the excellent one (*k*=*K, y*=*K*-1). The most suitable model is called proportional odds model [14]

$$CL_k = \ln\left[\frac{P(y \le k)}{P(y > k)}\right] \qquad (1)$$

The solution of the proportional odds model leads to *K-1* regression equations which differ only in the value of absolute member $b_{k,0}$ whose value grows

$$\ln\left[\frac{P(y \le k)}{P(y > k)}\right] = b_{k,0} + \mathbf{b}^{\mathrm{T}}\mathbf{x} \qquad (2)$$

The phenomenon is placed to category for which *P(y=k)* is maximum. Advantage of the model is that the effects of the vector of independent properties ***x*** are invariant in respect to the dependent variable [13].

Significance of the model was tested using the deviance G^2 and single regression parameters by means of Wald test.

3 EXPERIMENTAL PART

The prediction of the hand was made from eight objectively measurable characteristics selected from four basic groups of properties corresponding to the hand sensoric centre [1].

1. For characterisation of the fabric surface roughness
   - mean absolute deviance *MAD* [mN] has been selected.
2. The deformability has been characterised by the
   - tensile modulus in diagonal direction *Y45* [MPa],
   - initial tensile modulus *Y* [MPa],
   - stiffness *T* [mN cm].
3. Bulk behaviour has been expressed by the
   - area weight *M* [g m^{-2}]
   - compressibility *S* [-]
   - thickness *t* [mm].
4. Thermal part of hand has been characterised by the
   - thermal absorbtivity *b* [W $m^{-2}s^{1/2}K^{-1}$].

Experimental data were collected for 90 men suit fabrics. The basic parameters are shown in Table 1. In the next step data were divided to two groups. The first group (data representing 80 fabrics) called training group was used for the calculation of estimation of regression parameters *b* and the second group of the rest 10 fabrics helped for verification of prediction ability of the model. The estimated regression coefficients are in Table 3. The significant coefficients and properties are in bold format.

Table 1 The basic characteristics of fabrics

areal weight	g/m^2	140 - 370
sett - warp - weft	threads/10 cm	170 - 560 150 - 370
fibre composition	100% wool, 45/55 wool/polyester, wool/polyester/polyamide	
basic types of weaves	mostly different types of twills, plain weave	

To obtain the formula for objective hand evaluation the subjective evaluation of fabrics also had to be realized. The panel of 40 judgers classified samples to 11 degree ordinal scale in accordance with scale used in [8]. As result 40 evaluations of total hand value (THV) for 90 fabrics had been obtained. For prediction the estimation of the median category of ordinal scale *M* was chosen which is defined

$$F_{M-1} < 0{,}5 \qquad F_M \geq 0{,}5 \qquad (3)$$

where *Fz* cumulative relative frequency is (*z=M-1* or *M*). Number of median categories is presented in Table 2.

Table 2 Number of fabrics classified into the median categories *M*

median category	number of classified fabrics
1	0
2	2
3	11
4	8
5	16
6	17
7	19
8	8
9	5
10	4
11	0

It is evident from Table 2 that no fabrics has median category 1 or 11 and to the median categories 2, 9 and 10 was classified only a few fabrics. The final interpretation of results is affected by this situation.

The model created on the basis of BM technique is marked BM11 and compared model flowing from KES characteristics as KES11.

Relations among the single properties used in BM technique were investigated. The paired (above the main diagonal) and partial (below the main diagonal) coefficients of correlation are presented in Table 3. The bold is used for correlations in absolute value higher than 0.6. All correlations with value higher than $|\mathbf{0.2}|$ are statistically significant on the level of significance α=0.05.

The principal component analysis (PCA) was also applied for detection of relations among the properties. Scree plot (Figure 1a) indicates 3 important principal components. Components weight graphs (Figure 1b-d) show for the individual combinations of 3 principal components dependencies and relations of the single properties. As results in Table 3 as graphs in Figure 1 leads to conclusions that among area weight *M* and thickness *t* dependence exist. Less strong relation between properties tensile modulus in diagonal direction *Y45* and initial tensile modulus *Y* can be observed. Therefore properties were collected according to their character

$$\text{geom1} = \frac{\text{M}}{\text{t}} \text{ and } \text{tenacity1} = \frac{(\text{Y45} + \text{Y})}{2}$$

model is called BM11v1.

in accordance with results PCA

$$\text{geom2} = -0.91\text{t} - 0.86\text{M} \text{ and}$$

$$\text{tenacity2} = 0.8945\,\text{Y45} + 0.68\,\text{Y}$$

model is called BM11v2.

Table 3 Paired and partial coefficients of correlation

	b	T	t	M	S	MAD	Y45	Y
b	1.00	-0.45	-0.58	-0.45	0.19	-0.55	0.01	-0.24
T	-0.12	1.00	**0.72**	**0.71**	-0.56	0.44	0.02	0.34
t	-0.24	0.22	1.00	**0.86**	-0.43	**0.65**	-0.07	0.33
M	0.11	0.18	**0.67**	1.00	-0.48	0.49	-0.14	0.31
S	-0.10	-0.33	0.02	-0.17	1.00	-0.23	-0.23	-0.42
MAD	-0.26	-0.02	0.38	-0.07	0.06	1.00	0.09	0.25
Y45	0.06	0.01	-0.03	-0.26	-0.20	0.18	1.00	0.51
Y	-0.09	0.02	0.04	0.14	-0.14	-0.05	0.54	1.00

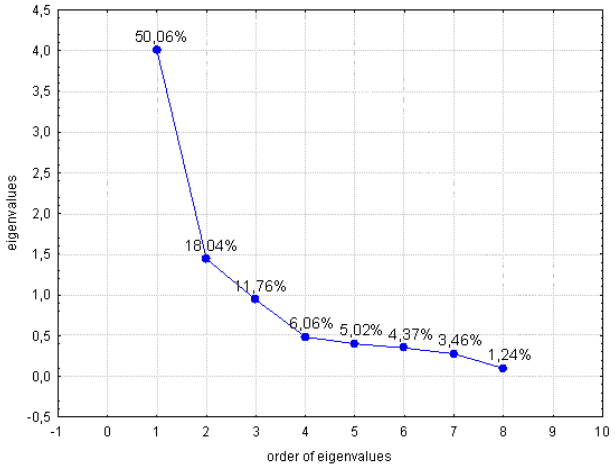

a.

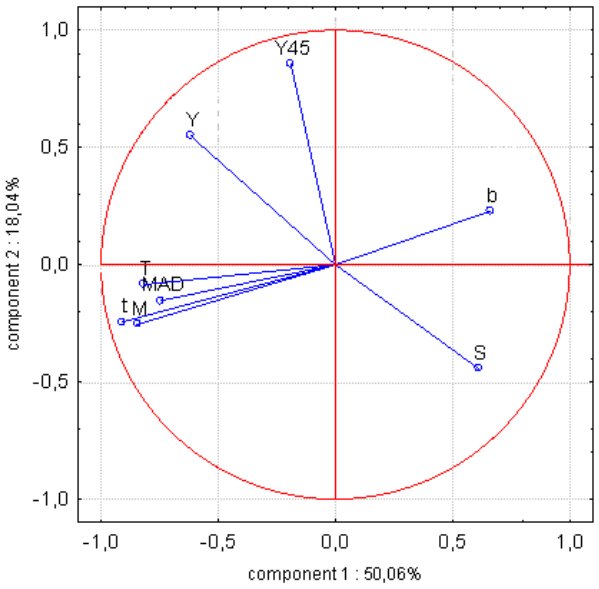

b.

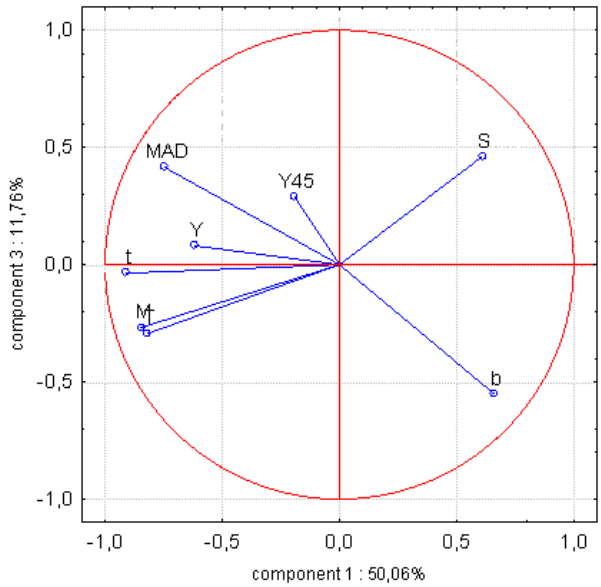

c.

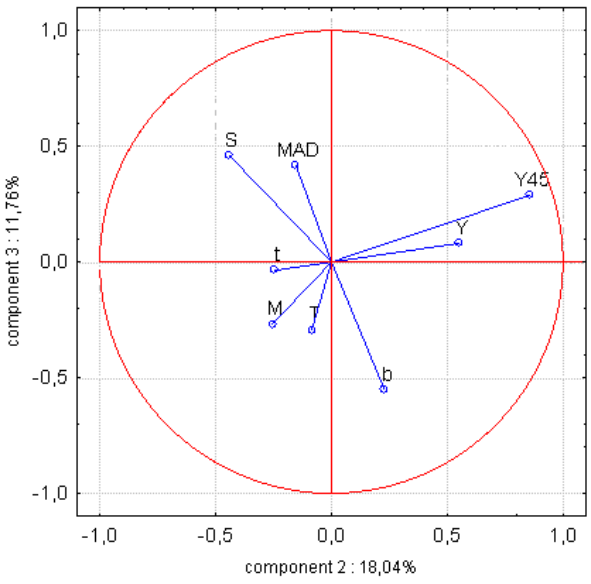

d.

Figure 1 Scree plot (a) and components weight graphs – (b) the 1st principal component vs the 2nd principal component; (c) the 1st principal component vs the 3rd principal component; (d) the 2nd principal component vs the 3rd principal component

Table 4 Comparison of models

characteric	KES11	BM11	BM11v1	BM11v2
G^2	147.06	157.55	**114.86**	152.93
p	<0.01	<0.01	<0.01	<0.01
R^2_{MF}	0.47	**0.49**	0.36	0.48
R^2_N	0.92	**0.93**	0.78	0.87
BIC	**81.55**	124.8	88.57	126.67
AIC	-2.35	**-2.44**	2.94	2.46

Table 5 Comparison of predicted and measured values of median categories of THV

Sample No.	THV	Predicted value by BM11	Diff.	Predicted value by BM11v1	Diff.	Predicted value by BM11v2	Diff.	Predicted value by KES11	Diff.
T117	6	7x	+1	5x	-1	7	+1	6	
T118	4	4		4		4		2	-2
T135	3	3		5x	+2	4	+1	4	+1
T136	9	8x	-1	8x	-1	8	-1	8	-1
T153	5	5		5		5		5	
T154	3	3		5x	+2	3		4	+1
T171	6	6		6		5	-1	5	-1
T172	7	7		7		6	-1	9	+2
T189	10	9x	-1	8x	-2	8	-2	9	-1
T190	7	6x	-1	6x	-1	6	-1	6	-1

The models were compared using Bayesian (*BIC*) and Akaike (*AIC*) information criterions, McFaden coefficient of determination (R^2_{MF}) and Nagelkerke statistic (R^2_N). It is valid for both criterions that lower value means better model. Advantage of these criterions is that adding new independent variable does not mean automatically better model in comparison with deviance G^2. McFaden coefficient of determination and Nagelkerke statistic indicate better model when its value is higher.

Proposed models based on BM technique are compared with the similar model in which the KES properties were used [8].

Results in Table 4 indicate that no model is significantly better. Parameter *p* shows that all models are significant and can be used for prediction.

The verification of prediction ability of the proposed models was realized on the second group of 10 textiles. Results presented in Table 5 show that model BM11 predicted 6 samples in accordance with the results of sensory analysis and the rest of samples with the mistake 1 category. All other models classified at least one sample with the difference 2 categories. On other hand, as variability in subjective hand evaluation of THV exists, difference 1 category is acceptable. From this point of view all of samples were classified well by model BM11, and 90% by model BM11v2, 80% by model KES11 and 70% by model BM11v1. No fatal classification (e.g., the excellent classification instead of very bad) was predicted.

4 CONCLUSION

Presented paper show objective hand evaluation using properties which are possible to measure in the textile laboratory by means of standard instruments. The ordinal logistic regression for the prediction of total hand – THV was introduced. For prediction the median category of THV was applied. The median category indicates that about 50% judgers will evaluate THV to median category and better (or worse). However, it is necessary take to

consideration that to the terminal categories No. 1, 2, 9, 10 and 11 was sorted less textiles than it is necessary.
Results show that application of the ordinal logistic regression is possible. Proposed model called BM designed from 8 properties provided very similar prediction ability as model based on KES characteristics. Applied properties mean absolute deviance *MAD*, initial tensile modulus in diagonal direction *Y45*, initial tensile modulus *Y*, stiffness *T*, area weight *M*, compressibility *S*, thickness *t* and thermal absorbtivity *b* are suitable for building of formula for objective hand evaluation.

Acknowledgement: *This work was supported by project of MŠMT of Czech republic No. 1M06047.*

5 REFERENCES

1. Lundgren H.P: New Concepts in Evaluating Fabric Hand. Textile Chemists and Colorists Vol.1, No. 1, 1969, 35-45
2. Matsuo T., Nasu N., Saito M.: Study on the Hand. Journal of the Textile Machinery Society of Japan Vol.17, No.3, 1971, 92-104
3. McIntyre J.E.: Textile Terms and Definitions, The textile Institute, Manchester, England, 10th edition, 1995
4. Fabric Hand: Guidelines to Subjective Evaluation of. AATCC evaluation procedure 5, 2001
5. Bishop D.P. Fabric: Sensors and Mechanical Properties, The Textile Progress Vol. 26, No. 1, 1996, 1-62
6. Binns H.: The Discrimination of Wool Fabrics by the Sense of Touch, British Journal of Psychiatry Vol.16, 1926, 237-247
7. Peirce F.T.: The 'Handle' Of Cloth As a Measurable Quantity, The Journal of The Textile Institute Vol. 21, 1930, 377-416
8. Kawabata S.: The Standardisation and Analysis of Hand Evaluation, The Textile Machinery Society of Japan, Osaka, 1980
9. Meie L., Xiaoan S., Li Z.A.: Study of Method of Measuring and Evaluating Fabric Handle, Proceedings of Textile Science 91, Technical university in Liberec, 1991, 41-50
10. Pan N.: Quantification and Evaluation of Human Tactile Sense Towards Fabrics, Int. Journal of Design & Nature Vol.1, No.1, 2006, 1-13
11. Raheel M., Lin J.: An Empirical Model for Fabric Hand. Part I: Objective Assessment of Light Weight Fabrics, Textile Research Journal Vol. 61, No., 1991, 1, 31-36
12. Pan N., Yen K.C., Zhao S.J., Yang S.R.: A New Approach to the Objective Evaluation of Fabric Handle from Mechanical Properties. Part I: Objective Measure for Total Handle, Textile Research Journal Vol. 58, No. 8, 1998, 438-444
13. Bajzík V. Hand Prediction using Ordinal logistic Regression, Proceeding of Innovation in Clothes and Footwear, Radom, 2010, 191-198
14. Powers D. Xie Y.: Statistical Methods for Categorical data Analysis, San Diego: Academic Press, 2000

NOVÝ PŘÍSTUP K OBJEKTIVNÍMU HODNOCENÍ OMAKU

Translation of the article
A new way to the objective hand evaluation

V příspěvku je představena nová metoda (BM technika) pro objektivní hodnocení omaku. Je použito 8 vlastností. Pro konstrukci predikční rovnice byla použita ordinální logistická regrese. Výsledné predikce byly porovnány s výsledky z obdobné predikční rovnice, kde však byly pro konstrukci použity vlastnosti ze systému KES.
Výsledky ukazují na dobrou predikční schopnost navrženého modelu.

PREDICTION OF POLYPROPYLENE YARN PROPERTIES

Dana Křemenáková and Dagmar Pivoňková

Abstract: *The models for prediction of polypropylene yarn packing density and strength are described. These models are based on the characteristics of fibers and yarns and also on the technological and material parameters of yarns. Groups of polypropylene yarns were spun in the pilot plant from the smallest to the greatest possible twist factor. Polypropylene fibers with different fineness, strength and deformation at break were used for yarn production. Radial and effective packing density were measured based on yarn cross-section analysis. For prediction of yarn packing density Neckar model was used. For prediction of yarn strength the fiber bundle strength, fiber elongation factor, yarn packing density and fiber orientation factor can be used. While studying the effect of the twist coefficient on the strength of polypropylene yarn the mechanism different from cotton yarn strength was found. Influence of fiber fineness on yarn packing density and strength was illustrated, too.*
Keywords: *Yarn packing density, twist factor, strength, orientation factor, inter fiber slipping.*

1 INTRODUCTION

Technical textiles are currently produced from special synthetic fibers with increased resistance to mechanical stress, thermal stress etc. For the prediction of technical textiles properties the fiber properties depending on their chemical composition should be known. It is also necessary to know the mechanism of textile structures creation. There exist experiences related to the classic natural materials. For predicting the properties of gray cotton fabric the "LibTex" system was prepared [2]. This system allows prediction of the properties in line fiber - yarn - fabric. Set of relations which are valid for cotton fibers can be applied for synthetic fibers as well. Staple synthetic fibers are usually longer, with lower bending rigidity and have much higher break elongation than cotton fibers. Generally, yarns from synthetic fibers are denser and more regularly arranged. In this work, the possibilities of yarn packing density prediction and strength are described.

2 THEORETICAL PART

Fiber fineness *t*, defined as the ratio of fiber mass m_f and fiber length l_f, is the function of fiber cross-section area *s* (*d* is effective fiber diameter [1]) and fiber mass density ρ

$$t = m_f / l_f = s\rho = \pi d^2 \rho / 4 \qquad (1)$$

Fiber relative macro surface *a* (defined as fiber surface divided by mass) is function of fiber fineness *t*, fiber mass density ρ and fiber shape factor *q*

$$a = 2\sqrt{\pi}(1+q)/\sqrt{\rho t} \qquad (2)$$

When two fibers with the same mass density ρ and different fineness t_1, t_2 are compared cross-section areas s_1, s_2 or diameters d_1, d_2 and macro surfaces a_1, a_2 are different according relation

$$s_2 = s_1 t_2 / t_1;\ d_2 = d_1\sqrt{t_2/t_1};\ a_2 = a_1 t_2 / t_1 \qquad (3)$$

For example fiber with lower fineness has lower cross-section area, lower diameter and higher fiber macro surface. Yarn fineness is ratio between yarn mass m_y and yarn length *ly*

$$T = m_y / l_y = S\rho = \pi D_L^2 \rho / 4 \qquad (4)$$

where *S* is effective yarn cross-section area (sum of fiber areas in yarn cross-section) and ρ is fiber mass density. Diameter of effective yarn cross-section area *S* (used in equation (4)) is denoted as the limit yarn diameter D_L that means the ideal yarn diameter without air gaps. For definition of real yarn diameter it is possible to define yarn packing density μ as ratio between fiber volume V_f and whole yarn volume V_y [1]

$$\mu = V_f / V_y = D_L^2 / D^2 = 4T / \pi D^2 \rho \qquad (5)$$

Real yarn diameter D is derived from equation (5)

$$D = \sqrt{4T / \pi \mu \rho} \qquad (6)$$

Packing density μ can be calculate by using the following relationship [1]

$$\frac{\left(\frac{\mu}{\mu_m}\right)^{5/2}}{\left[1-\left(\frac{\mu}{\mu_m}\right)^3\right]^3} = \frac{M\sqrt{\pi}}{2\mu_m^{5/2}\sqrt{\rho}}\left(ZT^{1/4}\right)^2 \qquad (7)$$

where *T* is the yarn fineness, *Z* the yarn twist, ρ the fiber density, *M* the material and technology parameter and μ_m the limit packing density. A suitable value of parameter *M* for ring and rotor cotton yarns was evaluated in [1] and for cotton compact yarns in [2, 3]. It is clear, that yarn packing density is increasing function of twist coefficient to the limit state which is represent by the limit packing density μ_m.

Relative yarn strength σ_y is frequently expressed as product of relative fiber strength σ_f and correction factor ϕ_{fy} expressing utilization of fibers strength in yarn.

$$\sigma_y = \sigma_f \phi_{fy} = \sigma_b \phi_{by} = \sigma_f \phi_{fb} \phi_{by} \qquad (8)$$

Utilization of fibers strength in yarn is product of fiber strength utilization in bundle ϕ_{fb} and utilization of bundle strength in yarn ϕ_{by}. The σ_b denotes bundle strength. These factors are computed according to the various relations.

The fiber strength distribution of Weibull two-parameter type was proposed by Pan [4, 5]. The mean fiber strength, the mean bundle strength and corresponding standard deviations are defined in [4]. For large bundles where number of fibers in cross-section is more that 100 is bundle strength approaching to normal distribution (Daniel's result [5]). Simple approximate relation for utilization of fiber strength in bundle was derived in [3]

$$\phi_{fb} = u^u \exp(-u) / \Gamma(1+u), u = 0.909 v_{\overline{\sigma_f}} \qquad (9)$$

In eqn. (9) the symbol $\Gamma()$ is gamma function and $v_{\overline{\sigma_f}}$ is variation coefficient of fiber strength. It was shown that utilization of fiber strength in bundle is function of variation coefficient of fiber strength, only. Utilization of bundle strength in yarn was derived by Pan [4, 5] as product of volume ratio and orientation factor. It is suitable used packing density defined in eq. (7) instead of volume ratio defined by Pan

$$\phi_{by} = \mu n_\beta \qquad (10)$$

The random distribution of fibers helical angles is used for computation of orientation factor η_β. Migration of fibers is negligible. Orientation factor η_β is function of surface fiber helix angle β_D and yarn Poisson ratio η [5]

$$\eta_\beta = \frac{2\beta_D(1-\eta)+(1+\eta)\sin 2\beta_D}{4\beta_D} \qquad (11)$$

Tangents of surface fiber helix angle β_D is well-known twist intensity defined as

$$\mathrm{tg}\beta = \pi D Z \qquad (12)$$

Poisson ratio η has the form [5]

$$\eta = \frac{\sin^5 \beta_D}{2\left(1-\cos^3 \beta_D\right)\left(\frac{1}{2}\beta_D - \frac{1}{4}\sin 2\beta_D\right)} \qquad (13)$$

Based on the careful inspection of above mentioned models the modified relation for prediction of yarns strength σ was proposed [7]

$$\sigma = \sigma_t \phi_{fb} \phi_{by} = \sigma_f (1+\varepsilon_f) \phi_{fb} \mu \eta_\beta \qquad (14)$$

In practical applications the assumption of constant volume during deformation is used and true stress is expressed in the simple form [6]

$$\sigma_t = \sigma_f(1+\varepsilon_f) \quad (15)$$

where ε_f is fiber deformation at break. By using of equation (14) is yarn strength function of fiber strength, variation coefficient of fiber strength, fiber deformation at break, fiber mass density, yarn twist coefficient and material and technology parameter *M*. Utilization of fiber bundle strength in yarn is product of packing density and orientation factor. Higher packing density means higher pressure between fibers and higher number of inter-fiber contacts. An important factor is the orientation of fibers in the yarn. With the increasing twist the orientation factor is decreasing.

3 EXPERIMENTAL PART

For testing of the influence of the twist factor on the yarn packing density and strength three groups of polypropylene yarns of the same fineness 25 tex with different twist were spun. Three types of polypropylene fibers were used. Fiber fineness, length and deformation at break of fiber type 1 and 2 were the same (nominal value 2.2 dtex, 50 mm length), but strength of fiber type 1 was statistical significantly higher then strength of fiber type 2. Fiber type 3 was finer with lower length (nominal value 1.7 dtex, 40 mm length) and with statistical significantly higher strength (see Table 1, Figure 1).

Yarns were produced in the pilot plant conditions in the range from the smallest to greatest possible twist. The same fineness 25 tex for all yarns type 1 (13 yarns, twist factor from 34 to 105 m^{-1} $ktex^{2/3}$), type 2 (13 yarns, twist factor from 30 to 98 m^{-1} $ktex^{2/3}$), type 3 (14 yarns, twist factor from 32 to 101 m^{-1} $ktex^{2/3}$) was used. The yarn packing density, diameter, strength and deformation at break were measured.

Yarn packing density was evaluated from yarn cross-sections by using of image analysis. Secant method based on the reconstruction of fiber sections around their centers [1, 8] was used. For evaluation of yarn packing density 30 cross-sections were prepared from each sample of yarns. The mean radial course of packing density which represents packing density from yarn axis to yarn surface (Figures 2, 3) was calculated. We assumed that the border between yarn core and a surface layers are approximately at the radial packing density value 0.15. The curve of the radial packing density was evaluated and core yarn diameter $D_{0.15}$, which correspond to the packing density μ=0.15 was computed.

Table 1 Polypropylene fibers properties

Fiber properties	fiber type	mean value	95% conf. interval	var. coef. [%]
Fineness [tex]	1	0.232	0.218 - 0.243	15.93
	2	0.225	0.213 - 0.236	17.66
	3	0.182	0.174 - 0.190	14.46
Length [mm]	1	51.12	50.49 – 51.75	-
	2	48.84	48.19 - 49.49	-
	3	40	-	-
Strength [N/tex]	1	0.356	0.344 - 0.370	12.73
	2	0.308	0.301 - 0.315	7.69
	3	0.399	0.389 - 0.409	8.11
Deformat.at break [%]	1	60.06	52.76 - 67.36	42.79
	2	55.15	48.78 - 61.53	40.68
	3	36.08	34.11 - 38.05	17.7

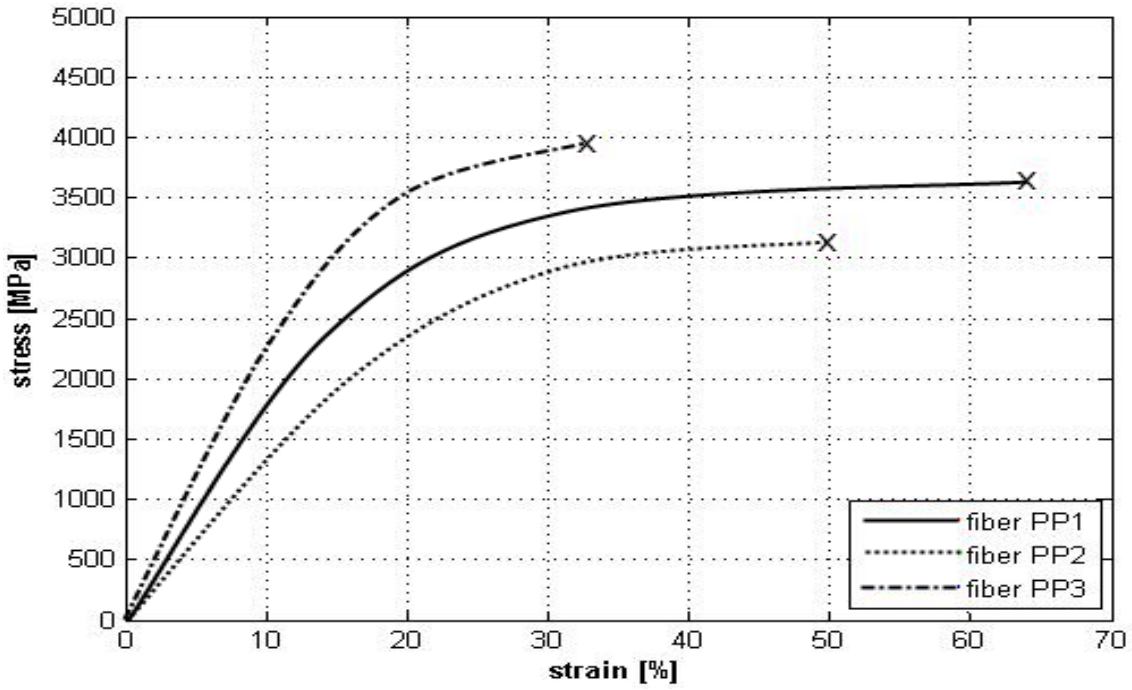

Figure 1 Fibers mean stress – strain curves

Radial packing density trace was replaced by constant value calculated from a yarn cross-section as ratio between sum of fiber areas of circle having diameter $D_{0.15}$ and areas of this circle. Packing density calculated based on the above mentioned principle can be called core packing density $\mu_{0.15}$. For all yarns types core yarn packing density (mean value and 95% confidence interval) as function of twist coefficient was evaluated (see Figure 4). Material and technology parameter M and limit packing density μ_m was optimized according eq. (1) for three group of yarn (Figure 4). Core yarn diameter was predicted by using of packing density (7) and relation (6). An orientation factor of these yarns was calculated from relation (11) and (13) as function of yarn twist intensity (12). Utilization of fiber in bundle (9) and utilization of bundle in yarns was calculated for prediction of yarn strength (14).

4 RESULTS AND DISCUSSION

Influence of yarn twist coefficient on the radial yarn packing density for selected yarns type 2 is shown in the Figure 2. For all yarns it is valid that increase of twist coefficient leads to the higher packing density in yarn core, fibers are more squeezed and core yarn diameter is decreasing.

Influence of fiber fineness on the radial packing density for selected yarns spun with the same twist coefficient is shown (type 1 - 55 $m^{-1}ktex^{2/3}$, type 2 - 53 $m^{-1}ktex^{2/3}$, type 3 - 54 $m^{-1}ktex^{2/3}$) in Figure 3. Yarns type 1 and 2 have the same structure and differences between radial packing density are statistically non significant. Yarns spun from finer fibers type 3 have statistically significant higher radial packing density in yarn core.

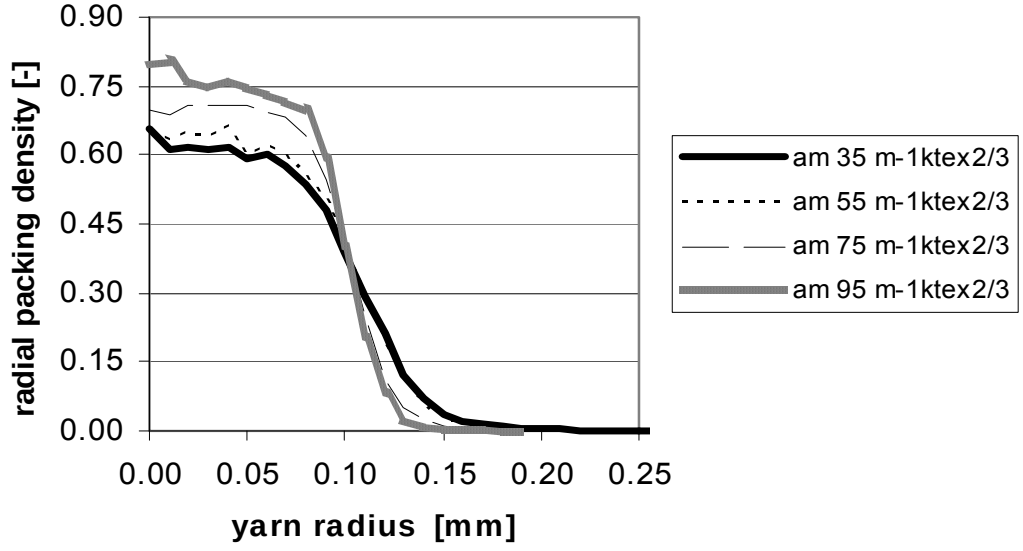

Figure 2 Influence of twist coefficient on the radial packing density (yarns type 2)

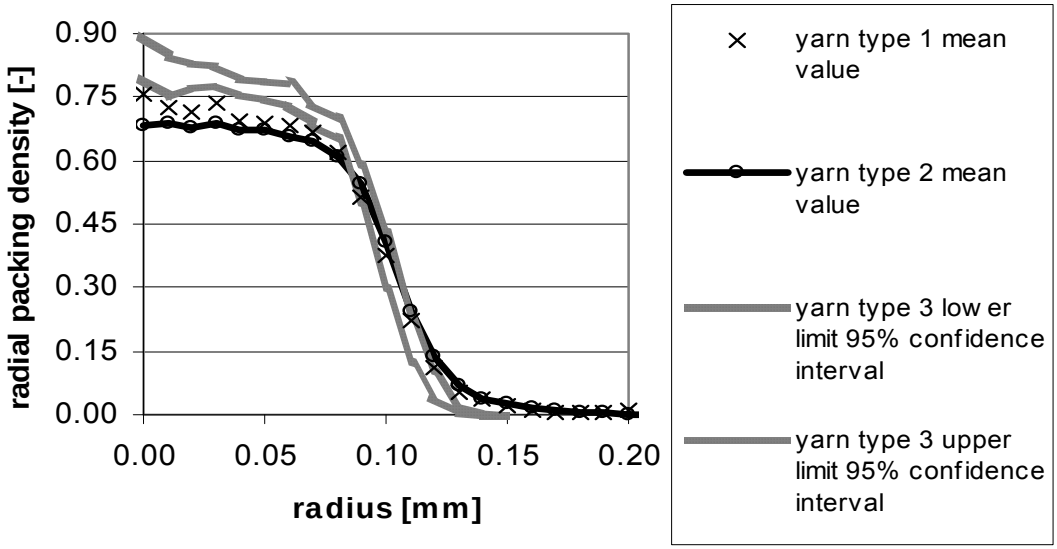

Figure 3 Influence of fiber fineness on radial packing density of yarn; type 1 - 55 $m^{-1}ktex^{2/3}$, type 2 - 53 $m^{-1}ktex^{2/3}$, type 3 - 54 $m^{-1}ktex^{2/3}$

Core packing density of yarn type 1, 2, 3 as function of twist coefficient are visible in Figure 4. These results are generally imaged in Figure 4. Experimental core packing density of yarns type 1, 2, 3 can be described by equation (7). The optimal value of limit packing density μ_m = 0.7 and optimal value of parameter M = 0.0919 m for yarns of type 1 and 2 were found. The same optimal value of limit packing density μ_m = 0.7 and higher optimal value of parameter M = 0.99 m for yarns of type 3 were found, too.

It is clear, that the same core packing density and core diameter are obtained for yarns spun from polypropylene fibers type 1 and 2, higher core packing density and lower core diameter is for yarn type 3 spanned from finer fibers. The measured yarns type 1, 2, 3 relative strength (mean value with 95% confidence intervals) and predicted values of yarns strength as function of twist coefficient are shown in the Figure 5. Strength of yarns type 1 is statistically significant higher than strength of yarns type 2 due to higher fiber

strength, only. Strength of yarns type 3 spun from finer fiber is statistically significantly higher in comparison with yarns type 1 and 2. This is a logical consequence of fact, when finer fibers have higher specific surface, the yarn with the same fineness has higher number of fibers and inter-fiber contacts.

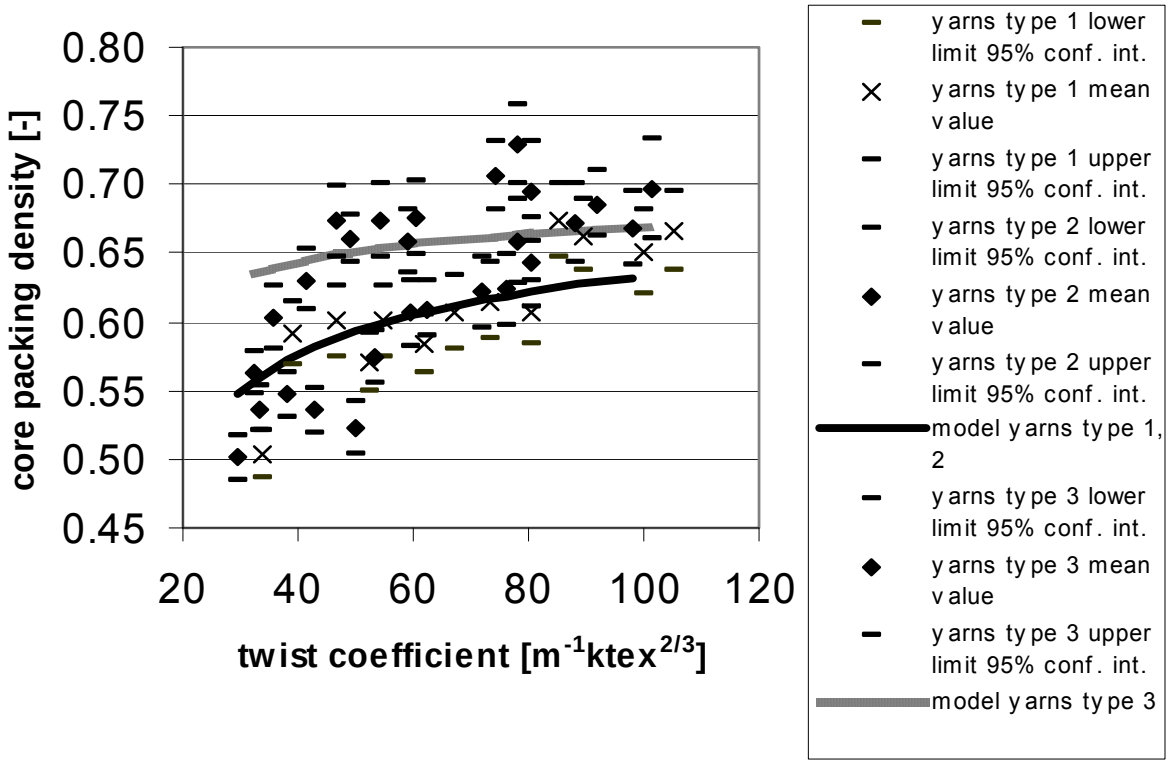

Figure 4 Influence of twist coefficient on the core packing density (predicted and experimental values)

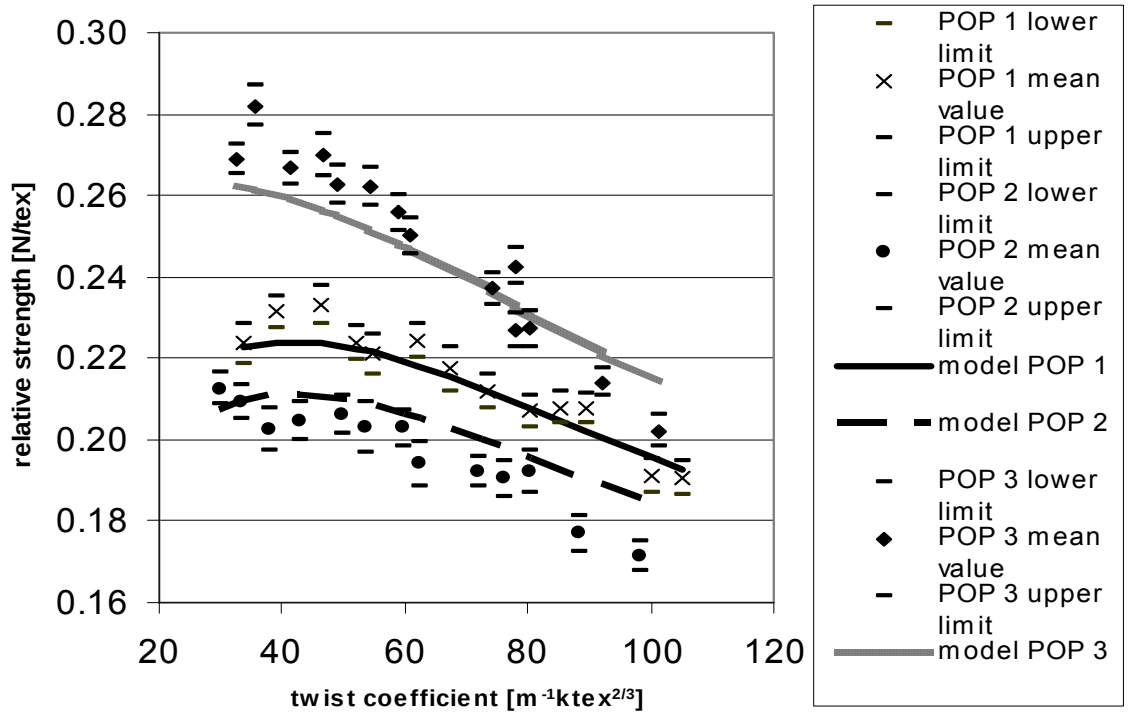

Figure 5 Influence of twist coefficient on the yarn strength (predicted and experimental values)

5 CONCLUSION

On the base of yarn cross-section analysis relation between fiber properties, yarn structure parameters and yarn strength was illustrated. Parameter of material and technology *M* is one from the important ones. This parameter includes set of factors, it is inter-fiber slipping, number of interfiber contacts, fiber bend rigidity, etc. According to the result of this work it is clear that influence of fiber fineness on this parameter must be included. Currently, the other group of viscose and polyester yarns are evaluated. Influence of different fiber mass density and fiber bending rigidity on the packing density and strength as function of twist coefficient is studied.

This methodology was prepared as part of a complex system for fabric design LibTex and ModSimTex. LibTex system offers a computer based method for the virtual design of fabrics and computation of their properties. ModSimTex is system for modelling and simulation of fabric properties connected with machine setting.

Acknowledgement: *This work was supported by research projects of Research Center Textile II No. 1M0553 and 7 FP EU ModSimTex Development of a rapid configuration system for textile production machinery based on the physical behaviour simulation of precision textile structure 214181 NMP2-SL-2008-214181.*

6 REFERENCES

1. Neckář B.: Yarns - Creation, structure, properties, SNTL, ISBN 80-03-00213-3, Praha, Czech Republic, 1990
2. Křemenáková D., Mertová I., Kolčavová-Sirková B.: Computer aided textile design 'LibTex', Indian Journal of Fiber & Textile Research Vol.33, December 2008
3. Křemenáková D., Militký J.: Comparisson of cotton yarn strength prediction method, Chap. 10 in Textiles for sustainable development, NOVA publishes 2007, New York USA, , 2007,.103-115
4. Pan N.: Prediction of Statistical Strengths of Twisted Fiber Structure,. J. Mater. Sci. 28, 1993, 6107
5. Pan N.: Development of a Constitutive Theory for Short – fiber Yarns. PART IV. The Mechanics of blended Fibrous Structures, Text. Res. J., 1995
6. Militký J.: Failure of PET Fibers, Chapt.4 in book Fiber Failure, Edited by Bunsell A., Schwatz P., Woodhead Publ. Cambridge, 2009
7. Křemenáková D., Militký J.: Modelling of polypropylene yarn properties, ICCE-17 Hawaii-Honolulu, July 26 to August 1, 2009
8. Křemenáková D. at all: Internal standards, Research center Textile 2004, Faculty of Textile Engineering Technical University of Liberec

NUMERICAL AND EXPERIMENTAL STUDY OF THE SHIELDING EFFECTIVENESS OF HYBRID FABRICS

J. Militký and V. Šafářová

Technical University of Liberec, Faculty of Textile Engineering, Czech Republic
jiri.militky@tul.cz

Abstract: *The electromagnetic interference shielding efficiency measurement needs to use special devices and in addition results are dramatically affected by applied measuring method. Measurements of surface or volume resistivity are simpler. It is known from theory that it is possible to measure characteristics of electrical part of electromagnetic field only at sufficiently high frequencies and therefore there should be mathematical relation between total shielding effectiveness SE [dB] and fabric resistivity or conductivity. One of modern application of materials with increased electromagnetic shielding efficiency is not only technical protection, but also protection of human being while operating specific electric equipments. The main aim of this work is investigation of the form of relation between electrical characteristics and total shielding effectiveness SE for special types of fabrics containing extremely thin metal fibers in its structure.*
Key words: *electromagnetic shielding efficiency, electric conductivity, correlation.*

1 INTRODUCTION

According to World Health Organization [1], exposure to electromagnetic fields is not a new phenomenon. However, during the 20th century, environmental exposure to man-made electromagnetic fields has been steadily increasing as growing electricity demand, ever-advancing technologies and changes in social behavior.

Everyone is exposed to a complex mix of weak electric and magnetic fields, both at home and at work. Sources of such emissions could include generation and transmission of electricity, domestic appliances and industrial equipment, telecommunications and broadcasting. If the electromagnetic waves are not isolated effectively, they will cause interference with each other and result in technical errors. If somebody gets exposed under the electromagnetic, radiate environment, physical harms may occur on human body [2, 3].

Metal is considered to be the best electromagnetic shielding material due its conductivity and permeability, but it is expensive, heavy, and may also have thermal expansion and metal oxidation, or corrosion problems associated with its use. In contrast, most synthetic fabrics are electrically insulating and transparent to electromagnetic radiation [4].

In recent years, conductive fabrics have obtained increased attention for electromagnetic shielding and anti-electrostatic purposes. This is mainly due to their desirable flexibility and lightweight [5]. One way how conductive fabrics can be created is by using minute electrically conductive fibers. They can be produced in filament or staple lengths and can be incorporate with traditional non-conductive fibers to create yarns that possess varying degrees of conductivity. Another way represents conductive coatings which can transform substrates into electrically conductive materials without significantly altering the existing substrate properties. They can be applied to the surface of fibers, yarns or fabrics. The most common are metal and conductive polymer coatings.

Direct measurement of fabrics electromagnetic shielding effectiveness is quite complicated especially because of need of special devices and time consuming preparation of samples. There are several methods available for shielding effectiveness

(SE) measurement. However, for thin planar structures, there are no standards defining the evaluation of small samples of only a several tens of centimeters in size. Therefore, comparing presented research results is not easy.
Utilization of presumption that "electrical part of electromagnetic field dominates for sufficiently high frequencies" seems to be simpler. Knowledge of the electrical characteristics which are easily measurable could be therefore used for establishment of electromagnetic shielding effectiveness of textile samples.
The main aim of this work is an investigation of the form of relation between electrical characteristics and total shielding effectiveness SE for special types of fabrics containing extremely thin metal fibers in its structure

2 THEOREY ON SHIELDING ELECTROMAGNETIC INTERFERENCE

An electromagnetic field is built up from various electric E and magnetic field H components. An electric field is created by a voltage difference and magnetic field is created by a moving charge, i.e. by a current. Every current is thus accompanied by both an electric and a magnetic field. Electromagnetic radiation consists of waves, see Figure 1.
EMI shielding consists of two regions, the near field shielding region and far field shielding region. The amount of attenuation due to shield depends on the electromagnetic waves reflection from the shield surface, absorption of the waves into the shield and the multiple reflections of the waves at various surfaces or interfaces in the shield. The multiple reflections require the presence of large surface area (porous or foam) or interface area (composite material containing fillers with large surface area) in the shields. The loss connected with multiple reflections can be neglected when the distance between the reflecting surfaces or an interface is large compared to the skin depth δ [m] (the penetration depth) defined as:

$$\sigma = \frac{1}{\sqrt{\pi\varphi\mu K}} \qquad (1)$$

where f [Hz] is the frequency; μ is the magnetic permeability equal to $\mu_0.\mu_r$; μ_0 is the absolute permeability of free space (air = $4.\pi.10^{-7}$) and K [$S.m^{-1}$] is the electrical conductivity. An electric field at a high frequency penetrates only the near surface region of a conductor. The amplitude of the wave decreases exponentially as the wave penetrates the conductor. The depth at which the amplitude is decreased to 1/e of the value at the surface is called the "skin depth" and the phenomenon is known as the "skin effect" [6].

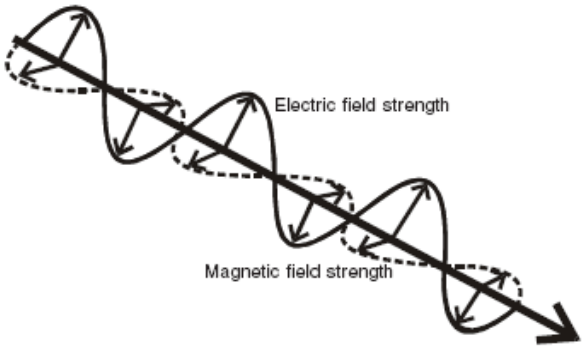

Figure 1 Electromagnetic wave

Efficiency of electromagnetic shields is commonly expressed by the total shielding effectiveness *SE* [dB], which represents the ratio between power P_2 [W] received with the shield is present and power P_1 received without the shield is present:

$$SE = -10\log\left(\frac{P_2}{P_1}\right) \qquad (2)$$

where log(x) is decimal logarithm.
The electromagnetic shielding efficiency of element is characterized by its electric conductivity, permittivity, and permeability, parameters of source and properties of ambient surrounding. Basic proposed

numerical models of fabrics *SE* are based either on electrical properties (especially volume conductivity) of element or on analysis of leakage through of opening in textile.
Shielding effectiveness *SE* of the conductive materials can be explained by the following expression [7, 8]

$$SE = 50 - 10\log\left(\frac{f}{K}\right) + 1.7t\sqrt{f\,K} \qquad (3)$$

where *K* [S cm^{-1}] is the volume conductivity of the conductive material and *f* [MHz] is the frequency.
The usefulness of this model can be ascertained by comparison with the model of White [6], which is usually used to predict the shielding effectiveness of a conductive sample of thickness *t* [cm] to an electromagnetic wave of frequency *f* (Hz), given as

$$SE = 168 - 10\log\left(\frac{K_C f}{K}\right) + 1.315t\sqrt{f\frac{K}{K_C}} \qquad (4)$$

where *K* [S cm^{-1}] is the volume conductivity and K_c is copper conductivity (5.82 10^5 S cm^{-1}).
The analysis of leakage through openings in conductive yarn fabric shields is based on transmission line theory [9]. The shielding effectiveness is given by the equation

$$SE = A_a + R_a + B_a + K_1 + K_2 + K_3 \qquad (5)$$

where A_a [dB] is attenuation introduced by a particular discontinuity, R_a [dB] is a fabric aperture with single reflection loss, B_a [dB] is a multiple reflection correction term, K_1, K_2, K_3 are correction terms. The empiric relations for these attenuation are published e.g. in the work of Perumalraja [9]. In order to approximate the mesh nature of the fabrics, the following assumptions are used:

1) The conductive fibers are wound together in a bundle in the center of the bundle of nonmetallic fibers. These two bundles together form the fabric strands.
2) The only influence of the nonmetallic fibers is to space the bundles of metallic fibers apart.
3) The pores in the fabric are square.

The fabric should contain as few portions of pores as possible for the most effective shielding.
The shield effectiveness *SE* of materials with (carbon) filler depends on the volume percent of the filler material *V* [%] [10]

$$SE = 2.46\,V \qquad (6)$$

For a single conductive layer, the theoretical value *SE* can be written as [11]

$$SE = 20\log\left(1 + \frac{K\,t\,Z_0}{2}\right) \qquad (7)$$

where *K* is conductivity; *t* the thickness of the sample; and Z_0 the free-space wave impedance, 377Ω. For low electrically conductive materials are these models in original form not useful [11].

3 EXPERIMENTAL

3.1 Hybrid Yarns

Hybrid yarns were composed of polypropylene and different content of staple stainless steel metal fiber (1-75 %). The aspect ratio (length/diameter ratio, l/d) of the SS is 6250 used in this study, since the diameter of the SS is 8 μm and the fiber length of the SS is 50 mm. See Figure 2 for microscopic image of hybrid yarn.

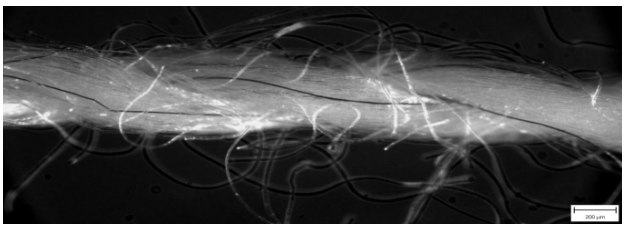

Figure 2 Microscopic image of chosen hybrid yarn containing 5% of stainless steel fibre (diameter of fibre is around 8 μm)

3.2 Hybrid Fabrics

The nine fabrics with the same structure were used. Samples were twill weaves with

weft and warp fineness 51 tex - warp sett 20 1/cm, weft sett 19 1/cm made of the hybrid yarn containing different portion of conductive phase. Weight per unit area of woven samples was 220 g m^{-2}. More details about fabrics are given in the Table 1. Microscopic figures of chosen studied samples are at Figure 3.

Table 1 Studied fabrics details

Sample	Composition	Thickness [mm]
1	99% POP/ 1% SS	0.78
2	97% POP/ 3% SS	0.75
3	95% POP/ 5% SS	0.77
4	90% POP/ 10% SS	0.75
5	85% POP/ 15% SS	0.73
6	80% POP/ 20% SS	0.71
7	60% POP/ 40% SS	0.70
8	40% POP/ 60% SS	0.63
9	25% POP/ 75% SS	0.57

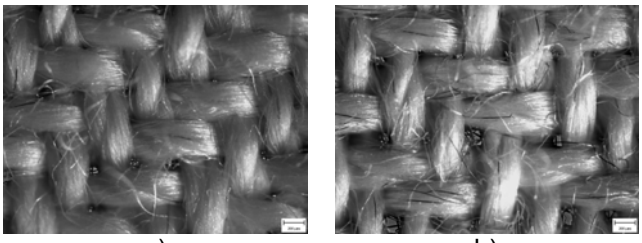

a) b)

Figure 3 Microscopic images of chosen studied fabrics: a) sample 1, b) sample 4

3.3 Characterization

Electric resistivity

Volume resistivity was measured according to the standard ČSN 34 1382, at the temperature T=22.3°C and relative humidity RH=40.7 %. Volume resistivity is measured by applying a voltage potential between two electrodes of specified configuration that are in contact with the opposite side of a material under test. Volume resistivity ρ_V [Ω.cm] was calculated from relation:

$$\rho_V = R_V \frac{\pi R_1^2}{4t} \qquad (8)$$

where R_V [Ω] is volume resistance reading, R_1 outer radius of electrode [cm], t thickness of sample [cm]. The mean values of ρ_V are listed in Table 2.

Table 2 Mean values of ρ_V and *SE*

Sample	ρ_V [Ω.cm]	SE [dB]
1	1.51E+03	19.26
2	1.56E+03	26.69
3	5.47E+03	29.16
4	1.789E+04	31.83
5	3.642E+04	33.54
6	7.749E+04	36.02
7	2.840E+05	36.10
8	7.339E+06	37.55
9	1.424E+07	38.30

Electromagnetic shielding efficiency

Electromagnetic shielding for higher frequencies was characterized by the attenuation of electromagnetic field power density by using simple device (see Figure 4).

Basic parts of device are two waveguides. One waveguide is connected with receiving wire (antenna). Textile sample is placed on the entrance of second waveguide. The end of this waveguide is filled by foam saturated by carbon absorbing the electromagnetic field passed through sample. Sample is oriented perpendicularly to the electromagnetic waves. Transmitting antenna is placed in front of first the waveguide input. As a source of electromagnetic field the ZigBee module working at frequency 2.4 GHz is used. The total shielding effectiveness S_T [dB], is calculated from (2) where P_1 [W.m^{-2}] is input power density and power P_2 is power density after passing through sample. The mean values of *SE* are given in the last column of Table 2.

Standard ASTM D4935-99 was used for reference measurement in a frequency range of 30 MHz to 1.5 GHz.

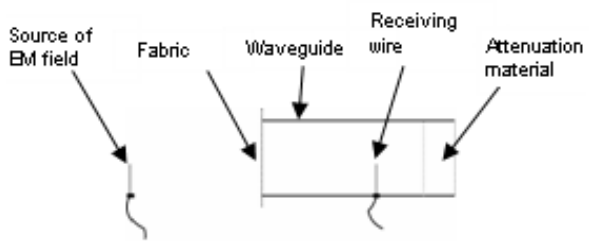

Figure 4 Scheme of device for measurement of electromagnetic shielding efficiency

4 RESULTS AND DISCUSSION

Electromagnetic shielding efficiency

The dependence of total shielding effectiveness *SE* on the percentage of conductive component *P* is shown in Figure 5.

The solid line in this graph corresponds with the logarithm model with parameters obtained by the minimizing sum of squared differences. A relatively good fit is visible. This model can be used for prediction of the value of *P* for sufficient shielding:

$$P = e^{\frac{SE-21.45}{4.18}} \qquad (9)$$

For example the *SE*=35 can be obtained at conductive component concentration *P*=33.1 %.

The percolation threshold can be observed. It is about 3 % of conductive component.

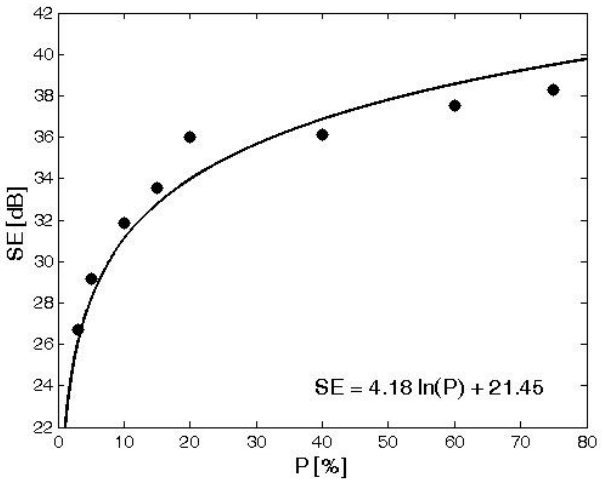

Figure 5 The dependence between *SE* and *P* for woven samples

Correlation between electric resistance and electromagnetic shielding

The dependence of total shielding effectiveness *SE* on logarithms of volume resistivity ln(R_V) above percolation threshold is shown in Figure 6.

The approximate linearity is visible. The solid lines in this graph correspond to the linear model with parameters obtained by the minimizing sum of squared differences. This graph clearly indicates that it is sufficient to measure only the electric field characteristics for sufficiently high frequencies.

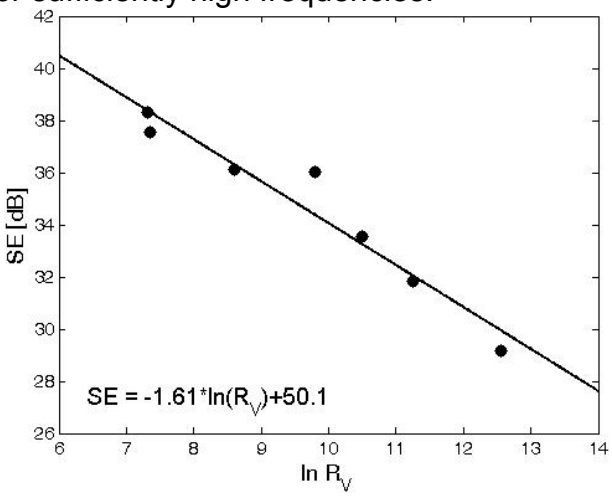

Figure 6 The dependence between *SE* and ln (R_V) for woven samples – above percolation threshold

Numerical estimation of special fabrics electromagnetic shielding efficiency

Suitability of different numerical models proposed in literature was studied. It was found that models based on the White model provide the best results for hybrid fabrics especially above percolation threshold:

$$SE = A - B\,log\left(\frac{K_C\,f}{K}\right) C\,t\sqrt{\frac{K}{K_C}}\,f \qquad (10)$$

where A,B,C are constants, K [S cm^{-1}] is the volume conductivity and K_c is copper conductivity (5.82 10^5 S cm^{-1}).

By optimizing the constants in (10), the numerical model for hybrid fabrics made of 100% of antistatic yarn was proposed:

$$SE = 88 - 4\log\left(\frac{K_C f}{K}\right) 1.315t\sqrt{\frac{K}{K_C}f} \qquad (11)$$

Comparison of calculated and measured values of electromagnetic shielding effectiveness for sample with relatively low conductive component content (below percolation threshold – sample 1) and for sample with conductive component above percolation threshold (sample marked 6) in a more extensive frequency range is shown in Figure 7. It is clear, that the proposed model fits better for samples with higher conductivity, more precisely for samples with conductive component content above percolation threshold. In Figure 8 there is a comparison of measured and calculated values of electromagnetic shielding efficiency for whole group of samples with different portion of conductive phase for frequency 2.4 GHz (measured by waveguide method). The model fits very well and therefore it was confirmed that the frequency 2.4 GHz is sufficient for predicting the electromagnetic shielding efficiency of textiles structures based on electric characteristics knowledge.

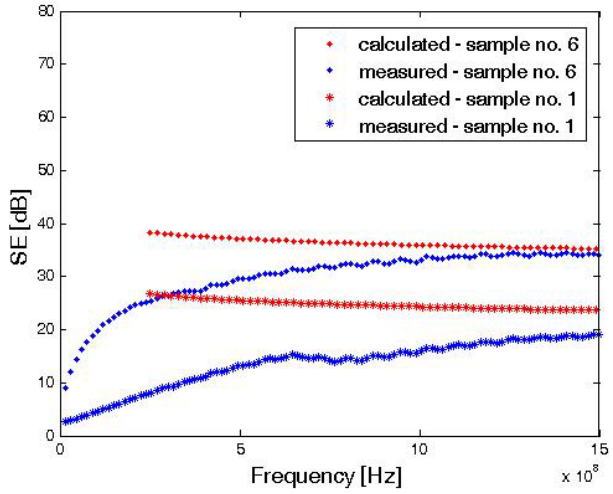

Figure 7 The dependence between *SE* (measured and calculated) and frequency for 2 types of samples

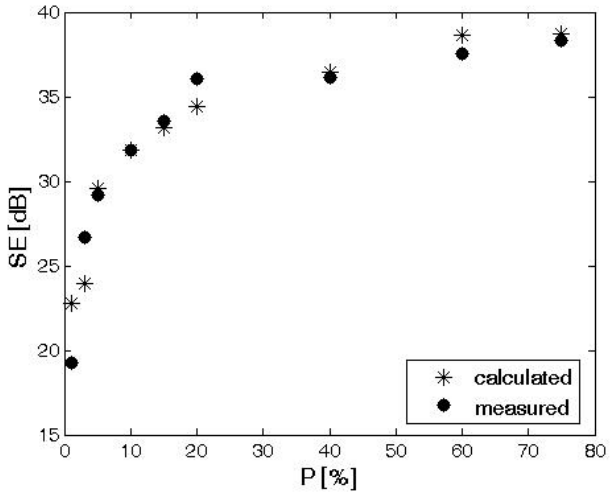

Figure 8 The dependence between *SE* and *P* – comparison of measured and calculated data

5 CONCLUSION

Low cost conductive fabrics with sufficient electromagnetic shielding efficiency conserving the main properties, e.g. drapability and process ability characteristics were created.

Fabrics with the same structure and different portion of conductive phase in hybrid yarn were studied. Hybrid yarns forming weaves and knitted fabrics were composed of polypropylene and staple stainless steel fiber. Samples were characterized by its volume resistivity (standardized method) and its electromagnetic shielding efficiency was measured by means of simple waveguide type device on frequency 2.4 GHz.

So called percolation threshold, dependence of total shielding effectiveness *SE* on the amount of conductive component *P* in hybrid yarn and dependence of total shielding effectiveness S_T on volume resistivity was examined. It is clear that the portion of conductive component has a significant effect on increasing conductivity (decreasing resistivity) and improvement of electromagnetic shielding efficiency.

The dependence between total shielding effectiveness and volume resistivity above percolation threshold is possible to express by linear function at the frequency of 2.4 GHz. Model for prediction of the value *P* for desired shielding was proposed.

Numerical models for calculation of shielding effectiveness based on electrical properties knowledge were studied. It was shown that modified White model is useful for prediction of hybrid fabrics electromagnetic shielding. The prediction ability of this line model is restricted to the relatively high frequency – above 1.5 GHz.

***Acknowledgement**: This work was financially supported by the research project TIP – MPO VaV 2009 "Electromagnetic field protective textiles with improved comfort" of Czech Ministry of Industry and student project 2011 "Comparison of methods for evaluating the shielding effectiveness of textiles" of Technical university of Liberec.*

NUMERICKÁ A EXPERIMENTÁLNÍ STUDIE EFEKTIVNOSTI STÍNĚNÍ HYBRIDNÍCH TEXTILIÍ

Translation of the article
Numerical and experimental study of the shielding effectiveness of hybrid fabrics

Hodnocení efektivity stínění proti elektromagnetickým polím vyžaduje obecně použití speciální aparatury a výsledky závisí na použitém principu měření. Jednodušší je měření povrchového resp. objemového elektrického odporu. Z teorie plyne, že pro oblast vysokých frekvencí postačuje měření pouze elektrické složky elektromagnetických polí. Existuje zde tedy přímá souvislost mezi efektivitou stínění SE [dB] a elektrickým odporem. Cílem této práce je sledování vztahů mezi elektromagnetickým stíněním a elektrickým odporem u speciálních typů textilií obsahujících velmi jemná kovová vlákna zabudovaná v přízích.

GEOMETRICAL MODELING OF 3D WOVEN FABRICS

R. Mishra[1], B. P. Dash[2], B. K. Behera[2] and J. Militky[1]

[1]*Faculty of textile engineering, Technical University of Liberec, Czech Republic*
[2]*Department of textile technology, Indian Institute of Technology Delhi, India*

Abstract: *The present research focuses on understanding the geometry of 3D orthogonal woven fabrics for suitability in composite reinforcement applications. The elliptical cross-section of glass tows is considered for more accurate prediction of fabric parameters. A simple MATLAB program is employed for calculating fabric parameters responsible for mechanical performance of a composite system. The predicted results are in good agreement with experimental values.*

1 INTRODUCTION

The unit cell represents the smallest repeat unit of the weave architecture. When the unit cell is tiled out it describes the whole reinforcing fabric. It is generally accepted that the predicted behaviour of the unit cell is representative of the 3D fabric as a whole. The unit cell of a 3D woven structure can be divided into two distinct sections [1-5]. These sections include the Side view, which gives information on the number of layers, thickness and binder path and Plan view, the face layer of the reinforcement that gives information on the number of repeats in the fabric structure [6, 7]. These sections fully describe the weave or pattern that is repeated through the thickness of the reinforcement and over the area of the reinforcement by providing all the information required for calculation of the geometric properties of the unit cell. In this research, a geometrical is suggested to establish relationship between various constructional and dimensional parameters of 3D woven fabrics [8, 9].

2 FABRIC MANUFACTURING

2.1 Orthogonal structure

Fibre used	Multifilament glass tow
Tow count warp	600 tex
Tow count weft	600 tex
Reed count /cm	10
Denting order	3/1/1
Stuffer ends / cm	5
Binder ends /cm	4
Width of fabric	40 cm
Picks /cm	13

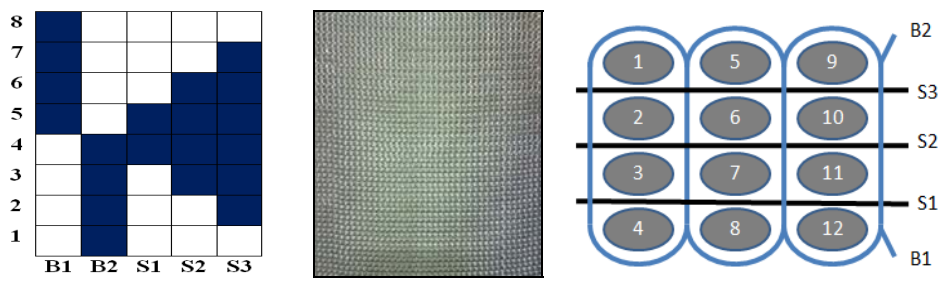

Figure 1 Orthogonal structure

2.2 Angle interlock structure

Fibre used	Multifilament glass tow
Tow count warp	600 tex
Tow count weft	600 tex
Reed count /cm	8
Denting order	3/2/3
Stuffer ends / cm	8
Binder ends /cm	2
Width of fabric	40 cm
Picks /cm	9

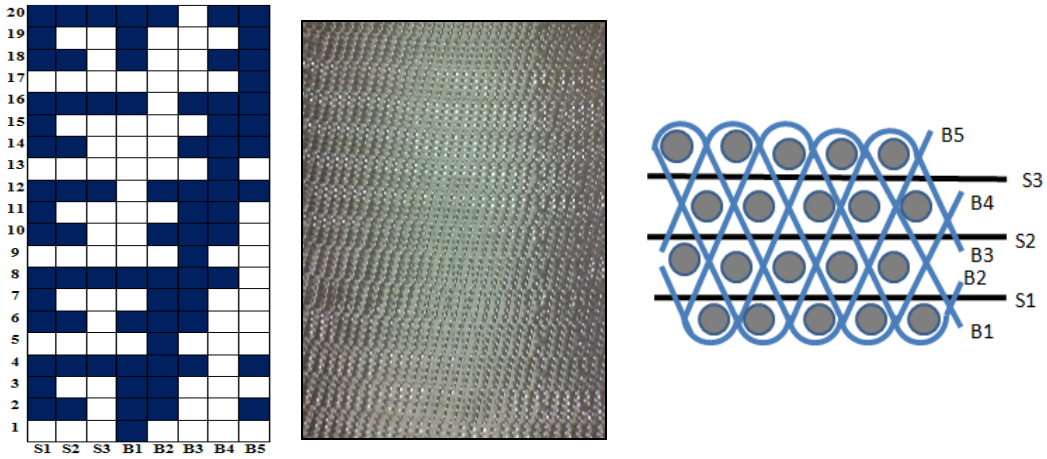

Figure 2 Angle Interlock structure

2.3 Multilayer structure

Fibre used	Multifilament glass tow
Tow count warp	600 tex
Tow count weft	600 tex
Reed count /cm	8
Denting order	3/3
Stuffer ends / cm	8
Binder ends /cm	4
Width of fabric	40 cm
Picks /cm	8

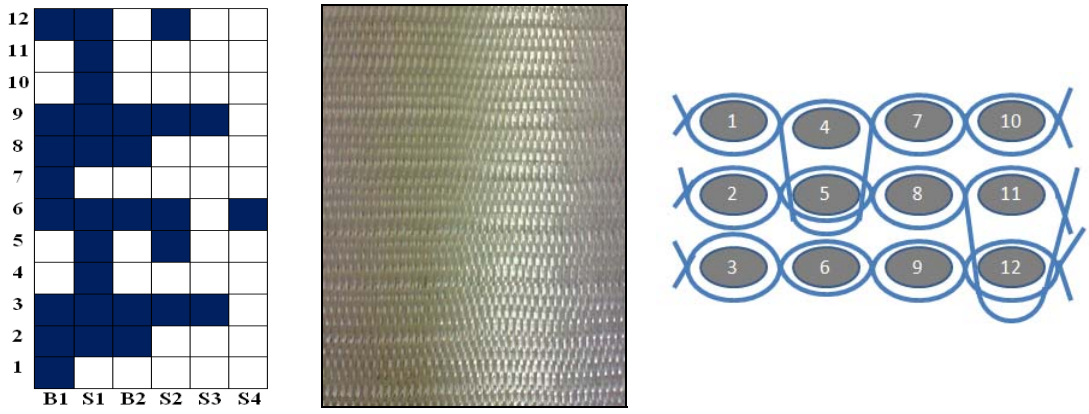

Figure 3 Multilayer structure

2.4 2D plain woven structure

Fibre used	Multifilament glass tow
Tow count warp	600 tex
Tow count weft	600 tex
Reed count /cm	8
Width of fabric	50 cm
Ends /cm	4
Picks /cm	3

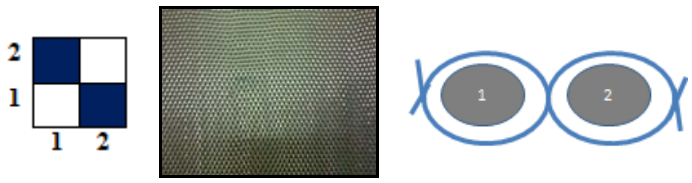

Figure 4 2D plain woven structure

2.5 Unidirectional structure

Fibre used	Multifilament glass tow
Tow count warp	600 tex
Tow count weft	33 tex
Reed count /cm	14
Width of fabric	50 cm
Ends /cm	7
Picks /cm	1

Figure 5 Unidirectional structure

Table 1 Measured parameters of fabric samples

Fabric type	Unidirectional (Glass)	2D Plain woven (Glass)	3D Orthogonal (Glass)	3D Interlock (Glass)	3D Multilayer (Glass)
Thickness (mm)	0.40	0.51	1.4	1.45	1.48
Areal mass (g/m^2)	425	413	1248	1221	1256
Fibre Volume Fraction	0.41	0.32	0.35	0.33	0.335

3 MODELING APPROACH

The 3D structures possess very low levels of waviness in the warp stuffer and weft filler tows and as a consequence have a high overall Fiber Volume Fraction (FVF) [10]. For this reason the model assumes that no waviness or nominally straight tows exists. An analytical method for calculating the geometric description of the composite unit cell based on the summation of volumes of tows in the three principal directions has been developed. The cross-sectional shape and aspect ratio of the warp stuffers, weft fillers and warp binder tows have been taken into consideration. Three different cross sectional shapes e.g., ellipsoidal (A.R.=11), racetrack (A.R.=3) and circular (A.R.=1) have

been considered. The model uses readily available data from the weaver and the constituent material manufacturers as inputs into the model.

The model accepts basic weaver and material manufacturer data as inputs in order to calculate the geometric characteristics of the 3D woven unit cell. This model enables to play with yarn linear density, thread density, number of tow layers, binding structure, packing factor of tows, and aspect ratio for predicting areal density, thickness and volume fraction, of the perform fabric even before actually manufacturing it [11].

An aspect ratio of 1 signifies a circular tow shape where increasing the aspect ratio results in flattening of the tow. All the parameters required for the geometric description of the unit cell can be taken from the manufacturer's and the weaver's specifications. The weaver's specification details all the processing variables related to weaving the fabric, which are required inputs for the model [12].

The unit cell of a 3D woven structure can be divided into two distinct sections such as side view and plan view as shown below. Side view provides information on the number of layers, thickness and binder path whereas plan view depicts the face layer of the reinforcement that gives information on number of repeats in the fabric structure [13]. These views fully describe the pattern that is repeated through the thickness of the reinforcement and over the area of the reinforcement by providing all the information required for calculating the geometrical properties of the unit cell.

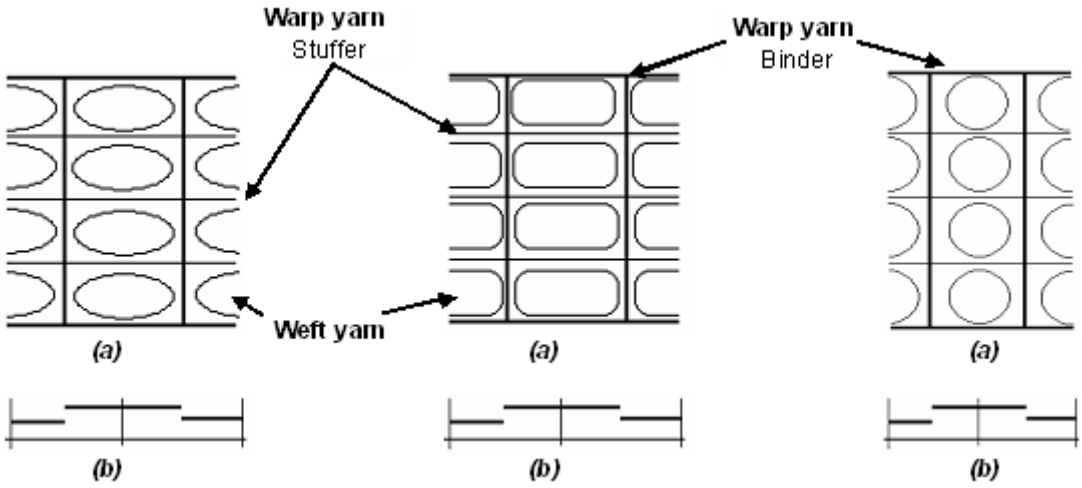

Figure 6 Orthogonal structure showing elliptical, racetrack and circular yarn cross section. (a) Side view, (b) Top view

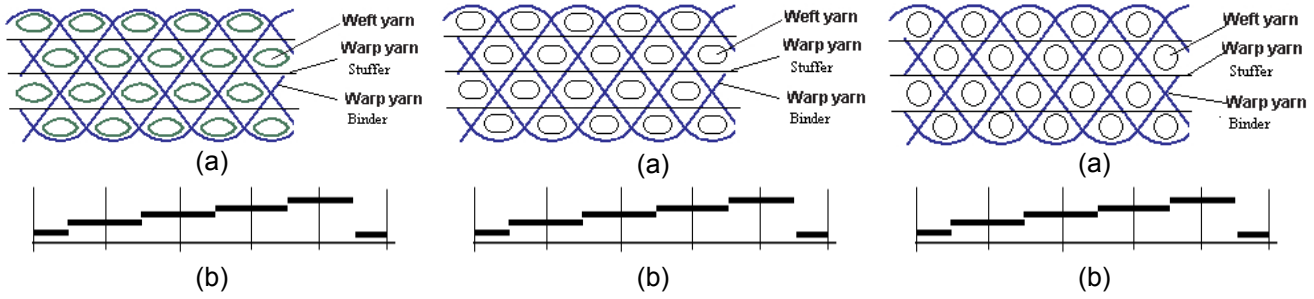

Figure 7 Angle Interlock Structure showing ellipsoidal, racetrack and circular yarn cross section. (a) Side view, (b) Top view

4 MODEL PARAMETERS

4.1 Manufacturer-specified parameters

μ_s, μ_f, μ_b Linear density of the stuffer, filler and binder tows (kg/m)
ρ Density of stuffer, filler and binder tows (kg/m^3)

4.2 Weaver-specified parameters

n^{uc}_s Number of stuffers along the weft direction (Y) in the unit cell
n^{uc}_f Number of fillers along the warp direction (X) in the unit cell
n^{uc}_b Number of binders along the weft direction (Y) in the unit cell
$\lambda_s, \lambda_f, \lambda_b$ Number of stuffers, fillers and binders per unit length perpendicular to tow direction (s/m, f/m and b/m).
n_s, n_f, n_b Number of stuffer, filler and binder layers in the unit cell
AR_s, AR_f, AR_b Aspect ratio of stuffer, filler and binder tows

4.3 Calculated parameters

h_s, h_f, h_b Thickness of stuffer, filler and binder tows (m).
H Thickness of unit cell (m)
l_s, l_f, l_b Length of one stuffer, filler and binder tow in the unit cell (m)
L_s, L_f, L_b Total length of stuffer, filler and binder tows in the unit cell (m)
V_s, V_f, V_b Total volume of stuffer, filler and binder tows in the unit cell (m^3)
L_x, L_y Length of unit cell in the X and Y directions (m)
M_{uc} Mass of the unit cell (kg)
S_{uc} Areal density of unit cell (kg/m^2)
FVF Fibre Volume Fraction of unit cell

5 MATHEMATICAL ANALYSIS

To determine the calculated parameters listed previously the model requires input values of the manufacturer and weaver-specified parameters. Knowing the linear density and assumed packing factor along with the aspect ratio, the thickness of the tows can be calculated via Equation (1)

$$h_i = 2(\mu_i/\rho A_R P_f \pi)^{1/2} \qquad (i = \text{s, f, b})$$

The filaments within the tow are circular and as such cannot be 100% packed together with no gaps in-between as such a tow-packing (P_f) factor is incorporated.
$P_f = \pi/4 \approx 0.7854$ (for rectangular packing array)
Having calculated the thickness of the stuffer, filler and binder tows, the full thickness of the consolidated unit cell may be determined using

$$H = n_s h_s + n_f h_f + 2h_b \qquad (1)$$

As evident from Equation (1), no contribution is assumed from the binder tows to the overall thickness of the unit cell. When the fabric reinforcement is consolidated prior to liquid moulding, tow nesting takes place. Next to be calculated is the length of one layer of stuffer, filler and binder tows

$$l_s = n^{uc}_f / \lambda_f \qquad (2)$$
$$l_f = n^{uc}_s / \lambda_s \qquad (3)$$

(For orthogonal structure)
$$l_b = n^{uc}_f (h_f AR_f) + 2H \qquad (4i)$$

(For angle interlock structure)
$$l_b = 2[h_f AR_f + \{(l_s/2)^2 + H^2\}^{1/2}] \qquad (4ii)$$

The dimensions of the unit cell are illustrated in Figure 3, where L_x and L_y are equal to l_s and l_f respectively.
From the calculated lengths of individual stuffer, filler and binder tows, the total length and subsequent volume can be formulated where subscript i is exchanged for each of

the representative values for subscripts s, f and b:

$L_i = l_i n_i n^{uc}_i$ (i = s, f, b) (5)

The cross-sectional area (A_i) of each tow is

$A_i = (\mu_i/\rho P_f)$ (6)

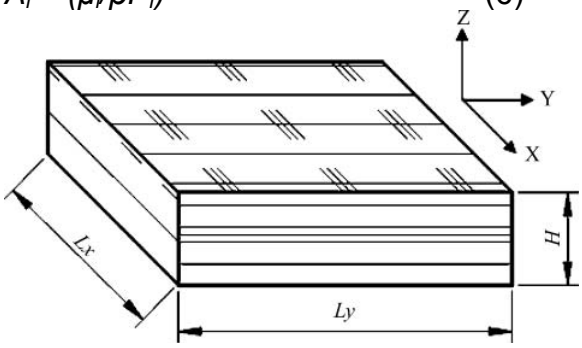

Figure 8 Dimensions of unit cell

The total volume of each tow is

$V_i = L_i A_i$ i = s, f, b (7)

The mass of the unit cell Muc can be calculated by the aggregation of all the linear masses

$M^{uc} = \sum L_i \mu_i$ i=s, f ,b (8)

The areal density can be calculated as

$S^{uc} = M^{uc}/L_x L_y$ (9)

The overall FVF can be calculated as

$FVF = (V_s+V_f+V_b)P_f/L_X L_Y H$ (10)

6 COMPARISON OF THEORETICAL AND EXPERIMENTAL RESULTS

All the fabrics are prepared by making suitable arrangement in a conventional loom, using 600 tex glass tow as stuffer, filler and binder. Thickness, Areal mass and Fiber Volume Fraction were calculated both from the prepared samples and computed by theoretical model provided above has been shown in Table1.

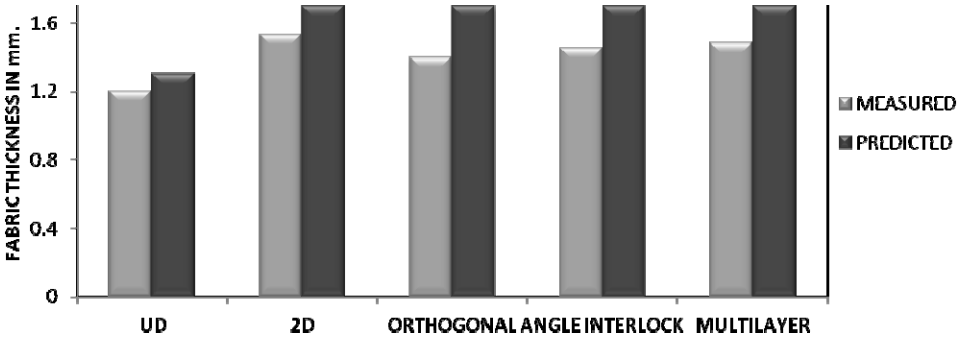

Figure 9 Comparison of measured and predicted values of fabric thickness

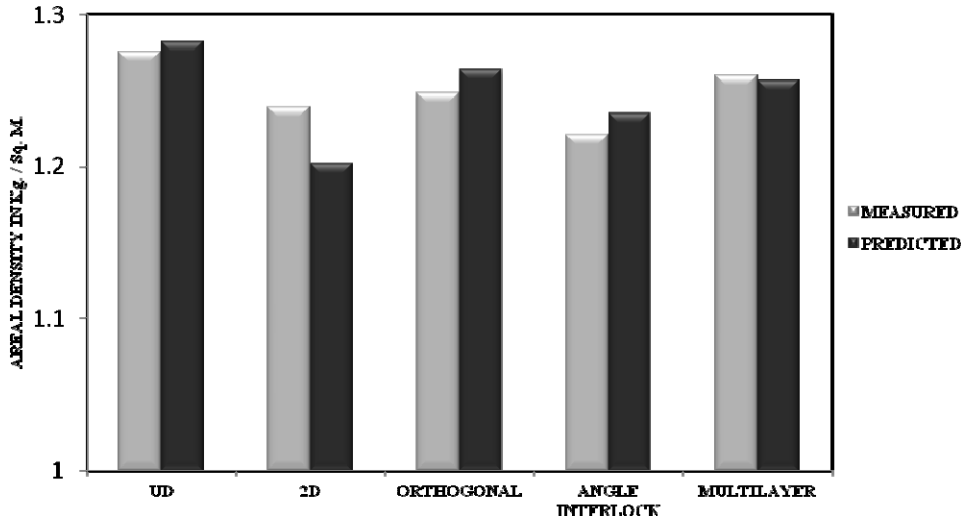

Figure 10 Comparison of measured and predicted values of fabric areal density

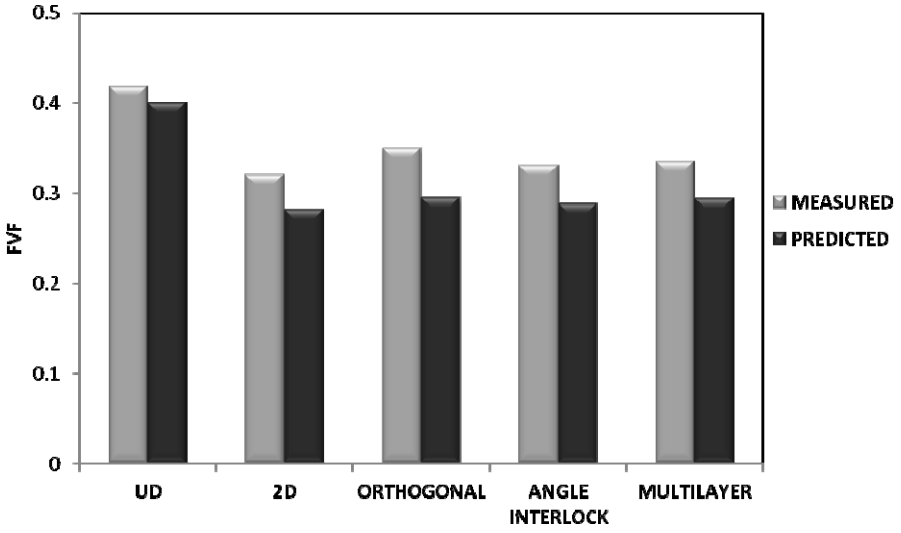

Figure 11 Comparison of measured and predicted values of FVF

For calculating the parameters from model the weaver and manufacture specified parameters have been shown below.

Orthogonal Structure

λ_s	λ_f	λ_b	n_s	n_f	n_b	μ_s, μ_f, μ_b	P_f	AR
158	315	158	3	4	2	$0.6\text{x}10^{-3}$	π/4	11

Angle interlock structure

λ_s	λ_f	λ_b	n_s	n_f	n_b	μ_s, μ_f, μ_b	P_f	AR
98	315	98	3	4	5	$0.6\text{x}10^{-3}$	π/4	11

Multilayer structure

λ_s	λ_f	n	μ_s, μ_f	P_f	A_R
394	275	3	$0.6\text{x}10^{-3}$	π/4	11

2D 3-layered structure

λ_s	λ_f	n	μ_s, μ_f	P_f	A_R
472	315	3	$0.6\text{x}10^{-3}$	π/4	11

UD 3-layered structure

λ_s	λ_f	n	μ_s	μ_f	P_f	A_R
709	79	3	$0.6\text{x}10^{-3}$	$0.033\text{x}10^{-3}$	π/4	11

7 PREDICTION OF 3D FABRIC PARAMETERS BY USING THE MODEL

The three important parameters such as thickness, areal density and fiber volume fraction could be predicted by this model, if the weaver and manufacturer specified parameters are known. It is revealed that as the tow linear density increases from $0.6x10^{-3}$ kg/m to $1.2x10^{-3}$ kg/m, and with increase in number of stuffer layers from 2 to 5, the fabric thickness, areal density and fiber volume fraction changes.
It has also been shown with increase in density of warp yarns how thickness, areal density and fiber volume fraction changes. It's been found that the number of stuffer yarn layers has very little effect on fiber volume fraction. The other parameters like thickness and areal density increase with increase in either towlinear density, or number of layer or warp yarn density or all. In the figures A, B, C, and D legends have been used for tows of linear density $0.6\ x10^{-3}$ kg/m, $0.8x10^{-3}$ kg/m, $1x10^{-3}$ kg/m, and $1.2x10^{-3}$ kg/m respectively.

8 CONCLUSION

The results indicate that the model provides a close approximation of the 3D woven orthogonal structure analyzed here. The model assumes elliptical tows and provides prediction of geometrical characteristics of the unit cell. The error of measurement between calculated and measured results may be due to measurement error or assumptions made regarding straight tow path with zero crimp. In order to model the geometric characteristic more accurately, better control over the weaving process is essential.

9 REFERENCES

1. Adanur S.: Wellington Sears Handbook of industrial textiles, USA: Technomic Publishing Co.,1995
2. Watson W.: Advanced Textile Design, Longmans, Green and Company, Third Edition, 1955
3. Wolff E.G.: Introduction to the Dimensional Stability of Composite Materials. USA: Destech Publications, Inc., 2004
4. Flemming M. et al: Faserverbundbauweisen, Fertigungsverfahren mit duroplastischer Matrix, Berlinpringer, 1999
5. Bogdanovich A.E., Pastore, C.M.: Mechanics of Textile and Laminated Composites, London, UK: Kluwer Academic Publishers, 1996
6. Mallick P.K.: Composites Engineering Handbook, New York, USA: Marcel Dekker, 1997
7. Vigo T., Turbak A.: High-tech fibrous materials, Washington, DC, USA: American Chemical Society, 1991
8. Antonio M.: 3-D textile reinforcements in composite materials, Cambridge, UK: Woodhead Publishing, 1999
9. Khokar N.: J. Textil. Inst. 92(2) Part 1, 2001, 193
10. Khokar N.: J. Textil. Inst. 90 Part I, 1999, 570
11. Fleury G.A., Lavalle R.L., Ohnstad, T.S.: Apparatus for weaving spheroidally contoured fabric, Ciba-Geigy AG, Switzerland, EP 00302 012 B1, 1991
12. Busgen A.: Tech. Textil. Int., 1995, 18
13. Busgen A.: Woven fabric having a bulging zone and method and apparatus of forming same, USP. 3 446 251, 1999

GEOMETRICKÉ MODELOVÁNÍ 3D TKANIN

Translation of the article
Geometrical modeling of 3D woven fabrics

Cílem práce je popis geometrie 3D ortogonálních tkanin určených pro výrobu kompozitních struktur. Tyto tkaniny jsou vyrobeny ze skleněných kabílků s přibližně eliptickým průřezem. Je popsán program v jazyce MATLAB umožňující výpočet základních geometrických parametrů těchto tkanin, které souvisí s mechanickými projevy kompozitních struktur. Vypočtené výsledky jsou v dobrém souladu s experimentálními hodnotami.

THERMAL RESISTANCE OF COTTON DENIM FABRIC UNDER VARIOUS MOISTURE CONDITIONS

Muhammad Mushtaq Mangat[1], Jiří Militký[2] and Luboš Hes[1]

[1]*Dep. of Evaluation of Textiles, Textile Faculty, TU Liberec, Liberec, Czech Republic*
[2] *Dep. of Textile Materials, Textile Faculty, TU Liberec, Liberec, Czech Republic*

Abstract: *This study is an effort to develop a mathematical model for the prediction of thermal resistance of cotton type textile fabrics under dynamic wet conditions. Thermal resistance was tested with the help of Alambeta at various moisture percentages. Mathematical model was developed based on simulation of the interaction between the main ingredient of fabric, fibre air and moisture. Model has a high correlation with the measured values and follows the trend line. Moreover, results show that there is a systematic decrease in thermal resistance with the increase of moisture. But it does not obey a linear relationship. Rather drastic change occurs at initial stage and thereafter, less change in thermal resistance has been observed.*
Keywords: *thermal conductivity, thermal resistance, moisture in fabric.*

1 INTRODUCTION

Nowadays people are more and more interested in clothing assuring the physiological comfort. Physiological comfort is strongly connected with the thermal comfort, which is defined as a state of satisfaction with the thermal conditions of environment. Thermal comfort can be defined as "that condition of mind which expresses satisfaction with the thermal environment" [16-18].
Thermal comfort is generally connected with sensations of hot, cold dry cold or dampness in clothes and is usually associated with environmental factors, such as moisture transport, thermal conductivity and air permeability.
One of the first attempts for specification of thermal comfort was introduction of special units *clo* or *tog* dealing with thermal resistivity *R* [m^2 K W^{-1}]. The *clo* and *tog* are measure of thermal resistance and includes the insulation provided by any layer of trapped air between skin and clothing and insulation of clothing itself. One *tog* is equal to 0.1 m^2 K W^{-1} and *clo* is equal to the 1.55 *tog*. One *clo* corresponds to intrinsic insulation of business suit worn by sedentary resting male in a normally ventilated room at 21°C and 50% RH and air ventilation of 0.1 m/s. In these conditions are man feelings as quite comfortable. For winter clothes is suitable *clo* around 0.8 and for summer conditions is *clo* around 0.5 (generally, lower *R* leads to state to be more cool).
Thermal resistivity *R* is defined as fabric thickness *h* [m] divided by fabric thermal conductivity λ [W K^{-1} m^{-1}].

$$R = \frac{h}{\lambda}$$

The prediction of the thermal resistivity or thermal conductivity of fibrous structures is therefore important for design purposes of new fabrics and prediction of their thermal comfort.
It is well known that thermal conductivity of dry fabric is mainly influenced by their porosity. The fabric porosity is function of construction parameters as yarn fineness and set of weft and warp. There are many other factors which can alter thermal conductivity of clothing. One crucial factor is presence of moisture in fabric.
Increase of moisture percentage in clothing increases the thermal conductivity, which creates a cool effect. Increase in moisture percentage in clothing may be due to internal reason e.g. sweat of human or any external

reason like, higher humidity in atmosphere or direct contact of clothing with water.

Presence of water in cotton fabric is due to the following factors:

- Hydrophilic nature of cellulose which is able to create strong hydrogen bonds with water molecules.
- Micro porous organization of cotton fibers with porosity sufficient for water molecules penetration.
- High radial swelling due to separation of cellulose sheets in cotton by water molecules.
- Macro porosity due to fabrics weave, sett of yarns and their fineness.

The most important factor in above-mentioned factors are the spaces between the fibres and yarns. Water moves through yarn obeying the capillary action. Moreover, amorphous region of fibres also plays a crucial role in absorbing the water. It shows that porosity of fabric is most significant factor to change the thermal resistance of fabric.

There is a drastic decrease in thermal insulation (*clo*) of the fabric if the moisture increases in fabric. It is mainly due to higher thermal conductivity of water as compared to fibres (polymers). Resultantly it negatively affects the thermal comfort due to less thermal insulation [1]. Research reports on experimentally determined thermal comfort properties of fabrics in the wet state are not many. The reason of this situation probably depends on the fact, that common measuring instruments lack in measuring thermal parameters of wet fabrics, due to long time of measurement, during which the fabrics becomes partially dry [2-5]. The instrument used in this study is the commercial PC evaluated Alambeta thermal comfort tester, which provides reliable non-destructive measurement of thermal insulation and thermal contact properties of fabrics in the dry and wet state, thanks to very short time of measurement [6].

There exists a plenty of various models for prediction of thermal conductivity of multiphase materials which can be used for prediction of textile fabrics thermal conductivity [19, 20]. Militký [19] used the plain weave cell model for computation of volume porosity and then various two phase models for prediction of cotton type fabrics thermal conductivity. The best according to the experimental data was simple linear mixture model corresponding to the parallel arrangements of phases. The main aim of this work is to generalisation of work [19, 20] for the case of wet cotton fabrics and including density porosity as one step of prediction from fibres to fabric.

2 THERMAL CONDUCTIVITY OF FIBRES

Thermal conductivity is the intensive property of a material that indicates its ability to conduct heat (see Figure 1).

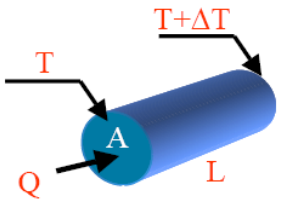

Figure 1 Thermal transport though solid body

One-dimensional steady state heat flow through body of cross sectional area *A* and length *L* in the x-direction due to thermal difference ΔT can be expressed by Fourier equation [25]

$$Q = -\lambda A \frac{\Delta T}{L} \qquad (1)$$

where *Q* [W] is heat flux in the x-direction per unit area perpendicular to the heat flow and λ [W m^{-1} K^{-1}] is thermal conductivity The thermal conductivity λ is then heat flux transported through a material due to a temperature gradient. The non-stationary one dimensional transient heat conduction in a semi-infinite stationary medium without heat production is described by parabolic differential equation [25]

$$\frac{\partial T}{\partial t} = D_T \frac{\partial^2 T}{\partial x^2} \qquad (2)$$

The heat transfer coefficient or thermal diffusivity D_T [m^2 s^{-1}] is defined as [25]

$$D_T = \frac{\lambda}{\rho\, c_p} \tag{3}$$

where ρ [kg m^{-3}] is density and c_p [J kg^{-1} K^{-1}] is specific heat capacity at constant pressure.

Thermal conductivity of solid particles is about 1-5 [W m^{-1}K^{-1}], Thermal conductivity of water is λ_{water} = 0.6 [W m^{-1}K^{-1}] and for ice it is λ_{ice} = 2.24 [W m^{-1}K^{-1}]. Thermal conductivity of dry air is λ_a = 0.024 [W m^{-1}K^{-1}].

An adequate theory for prediction accurately the thermal conductivity of polymeric melts or solids does not exist [21]. Simple phonon model of thermal conductivity is described by Van Krevelen [21]. Most of the semi empirical expressions for prediction of the thermal conductivity are based on the Debye equation [26]

$$\lambda = C_P\ \rho\ u\ L \tag{4}$$

where L [m] is the distance between the molecules in "adjacent isothermal layers" and u [m s^{-1}] is velocity of elastic waves (sound velocity). Assuming that L is nearly constant and independent on temperature, it may be expected that a direct proportionality exists between the thermal diffusivity D_T and the sound velocity u.

The process of thermal transport is supposed to occur in such a way that energy is passed quantum wise from layer to layer with sonic velocity and the amount of energy transferred is assumed to be proportional to density and heat capacity. No large-scale transfer of molecules takes place.

The thermal conductivity of polymers is temperature-dependent. This dependence can be approximated by two phase empirical model [24]

$$\frac{\lambda(T)}{\lambda(T_g)} = \left(\frac{T}{T_g}\right)^{0.22} \quad \text{for } T \le T_g$$
$$\frac{\lambda(T)}{\lambda(T_g)} = 1.2 - 0.2\left(\frac{T}{T_g}\right) \quad \text{for } T > T_g \tag{5}$$

This model is in good agreement with experimental data. For amorphous Polyethylene terephthalate it was found value 0.218 [Wm^{-1}K^{-1}] and for amorphous Polypropylene (atactic) it was found value 0.172 [Wm^{-1}K^{-1}] [21].

In crystalline solids, and therefore also in highly crystalline solid polymers, the thermal conductivity is enlarged by a concerted action of the molecules. Crystalline polymers show a much higher thermal conductivity dependent strongly on temperature T [K]. Eiermann [23] derived the simple relationship for polymers such as polyethylene polypropylene of "100% crystallinity".

$$\lambda = \frac{210}{T} \tag{6}$$

Therefore the thermal conductivity at room temperature of these highly regular polymers is found to be approximately 0.71 [Wm^{-1}K^{-1}] as compared with about 0.17 [Wm^{-1}K^{-1}] for the same polymers in the amorphous state. For the highly regular polymers the following empirical relationship can be used

$$\frac{\lambda_c}{\lambda_a} \approx \left(\frac{\rho_c}{\rho_a}\right)^6 \tag{7}$$

The heat conductivity at room temperature of fully crystallized polymers can be then simply predicted if it is known the ratio $\rho c/\rho a$. For the standard less regular, crystalline polymers the following relationship can be used [23]

$$\frac{\lambda_c}{\lambda_a} = 1 + 5.8\left(\frac{\rho_c}{\rho_a} - 1\right) \tag{8}$$

Calculated heat conductivity of semi-crystalline Polyethylene terephthalate at a common degree of crystallinity of 0.40 is in

very good agreement with the experimental value 0.272 [21].

Thermal conductivity of textile fibres is generally dependent on theirs chemical composition, technology of preparation (spinning and heat treatment), porosity and content of water. The results are scattered in some publications without description of measurements conditions. For standard atmosphere it is relative humidity of air *RH* = 65 % which can influence the moisture content in fibres. Very rough approximation of moisture content in cotton fibres expressed as regain *RE* [%] at various temperatures can be expressed by relation [27]

$$RE = (0.8067 + 0.02912\ RH)\sqrt[4]{100 - T} \quad (9)$$

This relation can be used till *RE* < 85 %. Regain *RE* is defined as the weight of water (*W* = wet weight - dry weight) in a material expressed as a percentage of the oven dry weight *D*

$$RE = 100\frac{W}{D} \quad (10)$$

Regain is closely connected with water content *MC* defined as the weight of water in a material expressed as a percentage of the total wet weight.

$$MC = 100\frac{W}{D+W} \quad (11)$$

It is simple to derive relationship

$$MC = \frac{RE}{1+(RE/100)} \quad (12)$$

For standard conditions is from eqn. (9) regain equal to the 8.0734 %. Due to higher thermal conductivity of water it will be the thermal conductivity of cotton in standard conditions higher in comparison with dry state.

Haghi [22] published thermal conductivity for some typical fibres. For practically nonporous polypropylene fibre he found λ = 0.518 [$Wm^{-1}K^{-1}$] and for porous acrylic fibre λ = 0.288 [$Wm^{-1}K^{-1}$]. For hydrophilic fibres is thermal conductivity based on the moisture content characterized by regain RE [%]. Haghi [22] found the dependence of λ on RE for cotton fibres in the form of simple linear model. This model has error in order of conductivity because Rengasamy and Kawabata [28] found for dry cotton the value λ_{cot} = 0.352 [$Wm^{-1}K^{-1}$].

We proposed simple rule of mixing for prediction of cotton fibers thermal conductivity as function of moisture content in the form

$$\lambda_{cot}(MC) = (1 - MC/100)\,\lambda_{tot} + \\ + \lambda_{water}\ MC/100 \quad (13)$$

where λ_{cot} is conductivity of dry cotton found in [28] and λ_{watter} =0.6 is thermal conductivity of water. The influence of moisture content on cotton thermal conductivity calculated from eqn (13) is shown on the Figure 2. Denote that *MC* = 12.358 % correspond to the relative humidity of air *RE* =90 %.

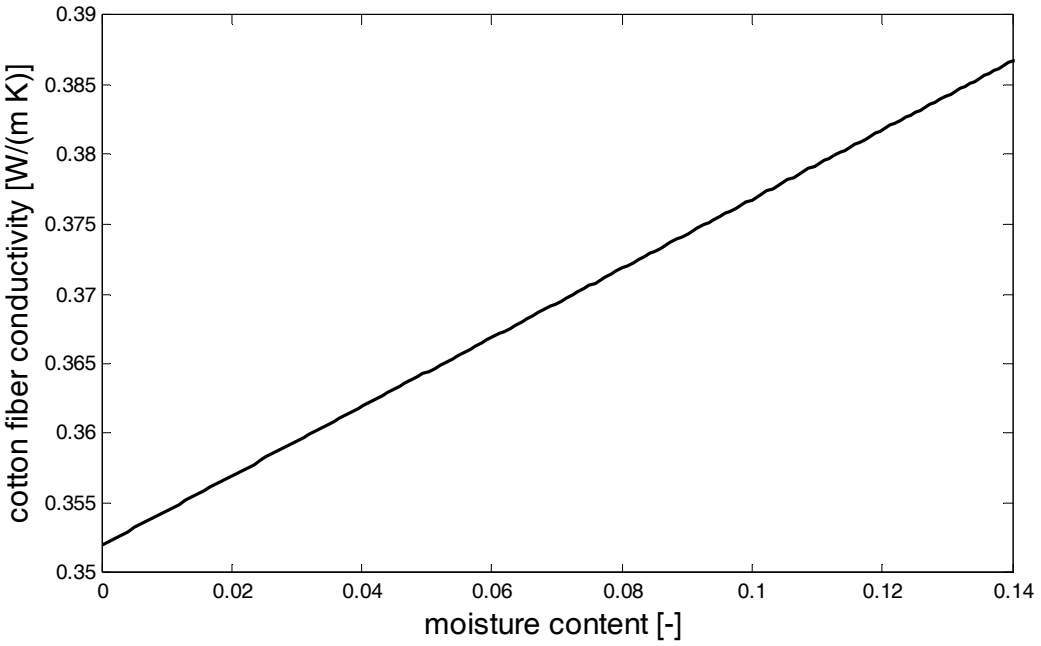

Figure 2 Influence of moisture content on cotton thermal conductivity

In the case when the two fibres A an B are blended (blending ratio i.e. proportion of fibre A in blend is equal to b_r) is their conductivity λ_{AB} estimated as upper limit defined as

$$\lambda_{AB} = b_r \lambda_A + (1 - b_r)\lambda_B \qquad (14)$$

If the mixture will be composed from wet fibers it is necessary to replace dry conductivities by wet conductivities calculated by analogy with eqn. (14) for cotton.

3 FABRIC POROSITY

There exist a lot of models characterizing the idealized porosity P_O from some construction parameters of textile fabrics [29]. Classical parameters are sett (texture) of weft D_C [1/m], sett of warp D_M [1/m], fineness of weft yarn T_C [tex], fineness of warp yarn T_M [tex], planar weight of weave W_P [kgm^{-2}], density of fibres ρ_F [kgm^{-3}] and thickness of fabric t_W [m]. For the idealized arrangement of yarns in fabric is $t_I = d_C + d_M$, where d_C is diameter of weft yarn and d_M is diameter of warp yarn. In the case when $t_W \approx t_I$ the yarns in fabric are roughly circular. This type of arrangements is assumed in sequel.

Porosity of fabric can be divided into main three categories:

- Macro porosity consists of spaces between the warp and weft yarns and spaces between warp and weft yarns.
- Meso porosity consists of the inner parts of the yarn, spaces between fibre to fibre, openings due to textured structure of yarn.
- Micro porosity composed by spaces in the inner side of fibre (void, pores and free spaces in amorphous regions of fibre).

The total porosity can be estimated by the „density“ porosity of fabrics which can be computed from relation [8]

$$P_D = 1 - \rho_W / \rho_F \quad \text{where} \quad \rho_W = \frac{W_P}{t_W} \qquad (15)$$

From the measured planar weight W_P, fabric thickness t_W and known density of fibres ρ_F it is the simple to compute the „density“ porosity from relationship

$$P_D = 1 - \frac{W_P}{\rho_F \; t_W} \qquad (16)$$

Second possibility of porosity evaluation is based on the definition of hydraulic pore for the filtration purposes [29].
The macro porosity can be estimated by the „volume“ porosity defined as [29]

$$P_V = 1 - \frac{volume\ covered\ by\ yarns}{whole\ accessible\ volume}$$

For the case of negligible yarns dimensional changes in fabrics can be porosity P_V expressed by the relation [29]

$$P_V = 1 - \frac{[D_C\ T_C + D_M\ T_M]}{525\ 10^3\ \rho_F\ t_W} \qquad (17)$$

More accurate determination of volume porosity is based on the idealized fabric surface structure projection shown on the Figure 3.
The unit cell (element of structure) shown by solid line contains a part of curved weft and warp yarns portions. Volumes and lengths of these portions are computed from equation derived by Militký et all. [29].

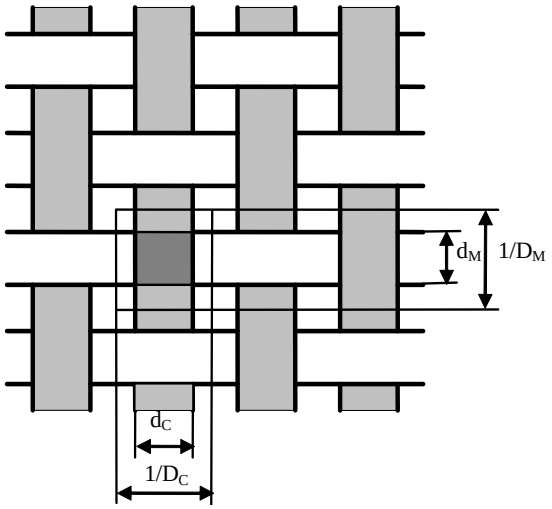

Figure 3 Idealized surface of fabrics projection (solid lines bound the unit cell)

The unit cell (element of structure) shown on solid line contains a part of curved weft and warp yarns portions. Volumes and lengths of these portions are computed from equation derived by Militký [12]. Corrected volume porosity is then defined as:

$$P_V^* = 1 - \frac{\pi}{4*(d_M + d_C)\left[\begin{array}{l} d_C^2 * D_C\sqrt{1.16*d_C^2*D_C^2+1} \\ +d_M^2 * D_M\sqrt{1.16*d_M^2*D_M^2+1}\end{array}\right]} \qquad (18)$$

From pure geometrical point of view can be defined the surface porosity [11]

$$P_S = 1 - CF \qquad (19)$$

The CF is the cover factor of fabric defined as $CF = D_C\ d_C + D_M\ d_M - d_C\ d_M\ D_C\ D_M$.
The meso porosity can be evaluated from packing density μ_c of yarns. For the moderate level of twist it has been empirically found that $\rho_C/\rho_F = \mu_C \approx 0.525$ and then 1- μ_c is equal to the yarns internal porosity [29].
Higher porosity means that fabric can trap more amount of air. Higher porosity means that fabric can have more space for air and water. Amount of water and air in fabric has a significant impact of thermal conductivity and thermal resistance. It shows that porosity plays a significant role in thermal resistance [7-9].
Other than porosity effect of surface roughness of fibre in wicking is quite significant [10]. Rough surface will complement in wicking and ultimately moisture absorbency will be increased.
For the case of wet fabrics it is necessary to use „density“ porosity which can be calculated from wet planar weight and wet thickness. It is only necessary to calculate the density of wet fibres. The harmonic mean should be used for this purpose. For example the cotton fibre density in wet state is calculated as harmonic mean

$$\frac{1}{\rho_w} = \frac{MC}{1000} + \frac{1-MC}{\rho_d} \qquad (20)$$

The influence of moisture content on cotton fiber density calculated from eqn (20) is shown on the Figure 4. Denote that *MC* = 12.358 % correspond to the relative humidity of air *RE* =90 %.

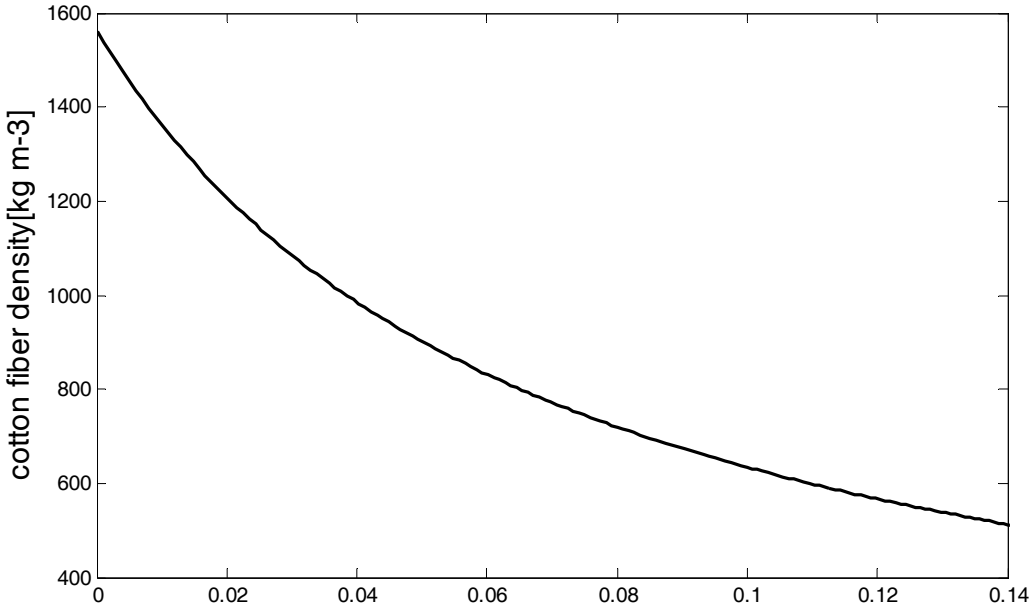

Figure 4 Influence of moisture content on cotton fiber density

4 THERMAL RESISTANCE OF MOIST FABRIC

Fabric has a certain structure and a finite thickness. Measurement of fabric thickness is quite sensitive mainly due to the compressibility attribute of fabric. There could be drastic change in the thickness due to pressure. During this experiment we have noticed that there is a decrease in thickness of fabric due to increase of moisture. This is also a fact that there is a swelling effect but at the same time there is an adhesion of protruding fibres, which decrease the thickness of fabric.

Effect of moisture on thermal resistance and porosity of the fabric plays significant role in thermal resistance [3]. Moreover structure of fabric is more important for higher thermal resistance than polymers.

When pores are filled with water completely, it means that height of water column is equal to fabric thickness. The attachments forces are very low and water is easily removed due to gravitational forces. In the case of hydrophilic fibres is water included into their structure mainly. Moreover, there is a layer of moisture on both sides of fabric, which will promote evaporation process and this process also creates changes in the temperature of fabric.

Another problem attached with moisture is amount of water inside the fibre and water on the surface of fibres. Moreover, there is change in the volume of the fabric due to swelling of fibre. There is an obvious change in the volume of hydroscopic fibres and this leads towards increase of volume and holding capacity of the fibre as well as decrease the gaps between warp and weft.

These changes of total porosity will be estimated by density porosity P_D (see eqn. (16)) replacing dry fibre density ρ_F by wet fibre density ρw calculated from eqn. (20) and planar weight of dry weave W_P by planar weight of wet weave W_w.

For expression of thermal conductivity of wet cotton fabric is then simple to use two phase model consist from fibres (moist) having thermal conductivity $\lambda_{cot}(MC)$ and air with thermal conductivity λ_a in serial (lower limit) or parallel (upper limit) arrangements as is shown on the Figure 5. Relative portion of air phase is equal to porosity P_D and relative portion of fibrous phase is $1 - P_D$.

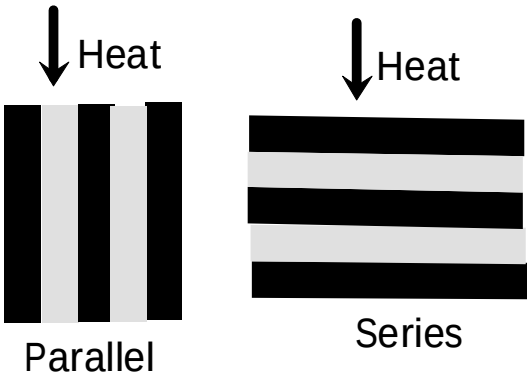

Figure 5 Limit arrangement of yarns (black) and air (white) in conductivity model

The thermal conductivity for parallel arrangement λ_P (higher limit) is equal to

$$\lambda_P = P_D \ \lambda_a + (1 - P_D) \ \lambda_{\cot}(MC) \qquad (21)$$

For serial arrangements is thermal conductivity λ_S (lower limit) defined as

$$\lambda_s = \frac{\lambda_a \ \lambda_{\cot}(MC)}{P_D \ \lambda_{\cot}(MC) + (1 - P_D) \ \lambda_a} \qquad (22)$$

Actual composition of a fibres and air phases can be presented by linear combination of parallel and series structures of its constituents' thermal resistance [30]. The compromise is to compute the mean porosity λ_{PS} as arithmetic mean between upper and lower limit.

$$\lambda_{Ps} = \frac{\lambda_P + \lambda_S}{2} \qquad (23)$$

This might not give an accurate prediction of the fabrics thermal conductivity due to the specific orientations the fibres take within the yarns as well as the distribution, shape, and size of the pores. However, the parallel/series structure gives a first hand prediction and would give reasonable prediction accuracy for practical application due to its simplicity.

5 EXPERIMENTAL PART

The denim samples composed from 100% cotton yarns were produced and their thermal resistance was measured with the help of Alambeta device under different moisture content in the range 0-45 %. Table 1 contains the sample description.

Table 1 Specifications of denim fabric

Description	units	Denim 1
Warp fineness	Tex	49.25
Warp sett	m^{-1}	2401
Weft fineness	Tex	49.25
Weft set	m^{-1}	1732
Weight after washing	g m^{-2}	351

Alambeta has two settings for pressure, 200 Pa and 1000 Pa. During initial testing it was found that there is a significant difference in the height of fabric when it is measured under two different weights (Table 2) and due to the difference in heights, there is big difference in thermal resistance.
By taking close pictures of the fabrics, it was observed that there are many protruding fibres on the surface of the fabric, which play a significant role in the measurement, whereas, by increasing pressure we found the actual values of the height which were closer to the values of sum of the diameter of warp and weft yarn (Figure 5). Moreover, this change also leads towards the change in the porosity. Considering these factors, thermal resistance was measured by keeping Alambeta pressure at 1000 Pa. Variation in results shows that arrangement of fibers, their compressibility has a significant impact on thermal properties. It confirms the work of Bogaty [14].

Table 2 Differences in height and porosity due to change in pressure of Alambeta

Porosity 200 Pa	Porosity 1000 Pa	Difference %	Fabric thickness (200 Pa)	Fabric thickness (1000 Pa)	Difference %
0.8447	0.8192	3.02	0.000850	0.00073	14.12

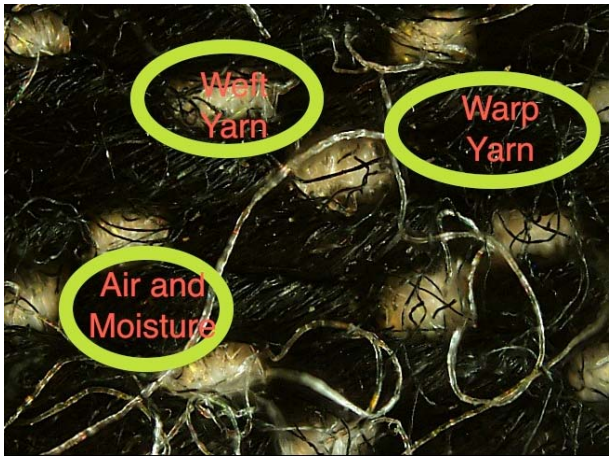

Figure 6 Surface of denim

6 DISCUSSION

Measured thermal conductivity of 100% denim for various level of moisture content is marked in Figure 7 by stars. The solid line is mean porosity λ_{PS} calculated from eqn. (23) for the case of mean (constant) thickness equal to the 0.00073 m.

The prediction is relatively good. Better results can be obtained if the thickness for all moisture levels is measured. The thermal conductivities for this case are shown in the Figure 8.

It is clearly visible that the prediction is generally better but due to measured thickness the curve is not smooth in the whole range.

Measured thermal resistance of 100% denim for various level of moisture content is marked in Figure 9 by stars. The solid line is calculated thermal resistance as measured fabric thickness divided by mean porosity λ_{PS} calculated from eqn. (23).

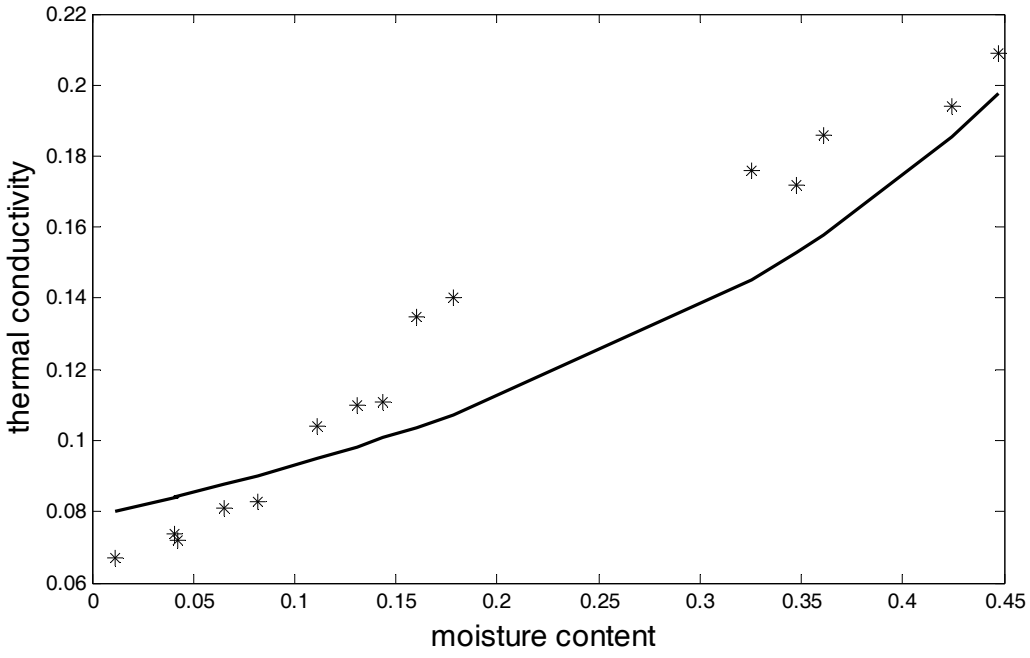

Figure 7 Dependence of calculated and measured thermal conductivity of 100% cotton denim on moisture content (case of constant thickness)

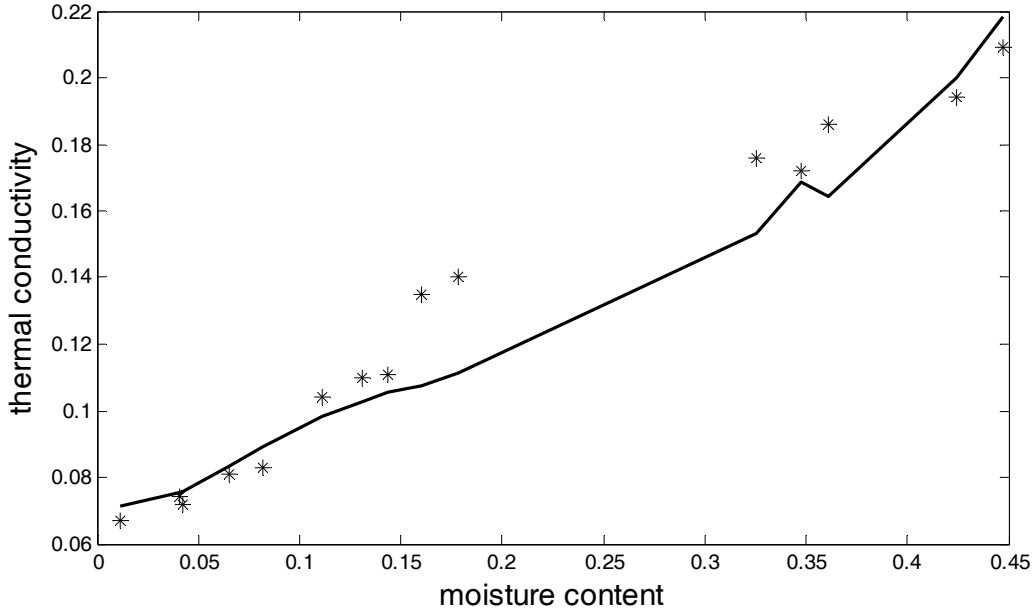

Figure 8 Dependence of calculated and measured thermal conductivity of 100% cotton denim on moisture content (case of measured thickness)

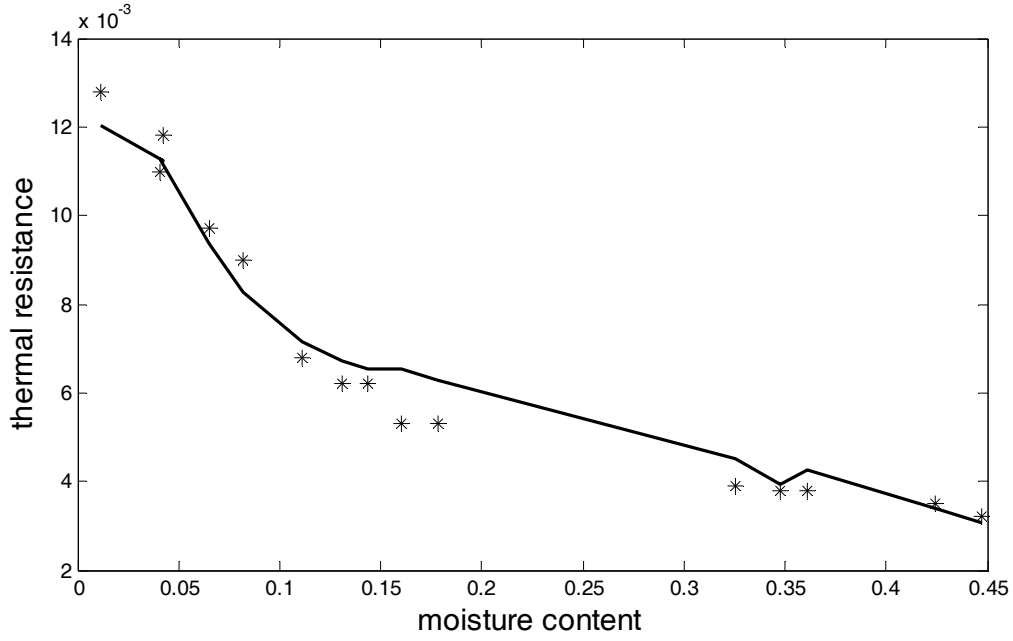

Figure 9 Dependence of calculated and measured thermal resistance of 100% cotton denim on density porosity

It is clearly visible that the prediction is very good.

In case of denim used in this study, there is only about 30% area of denim fabric is filled with polymers (P_D of dry sample is 0.7367) and the rest is composed of air. Air has thermal conductivity 10-15 times less than polymers and offers high resistance. In such case, heat flow is stopped by air but when this air is replaced with water, thermal resistance of the whole fabric reduces drastically.

In this study our focus is change in thermal resistance of fabric due to presence of water in cotton structure.

7 CONCLUSION

Thermal resistance is one of crucial factors in thermo physiological comfort and primary characteristic of clothing. Thermal resistance of clothing decreases due to the presence of water since water has low thermal resistance. Consequently, human body loses its heat and a cool effect is created, which leads towards discomfort [1]. For this study the thermal resistances and conductivities of denim having various moisture content were simulated and measured. And finally a mathematical equation has been developed to predict thermal resistance and conductivity of denim made by using cotton. The developed model has a substantial agreement with actual values.
Results show that more than 70% reduction in thermal resistance happened during moisture content in the range 0.00 to 0.30, which shows that minor amount of moisture in fabric, is responsible for the major reduction in thermal resistance. Nevertheless, further increase in moisture has a little effect on thermal resistance.

8 REFERENCES

1. Hes L.: Fast Determination of Surface Moisture Absorptivity of Smart Underwear Knits, in International Textile Conference Terrassa, 2001
2. Barker R.L.: Effects of Moisture on the Thermal Protective Performance of Firefighter Protective Clothing in Low-level Radiant Heat Exposures, Textile Research Journal 76, 2006, 27-31
3. Hes L.: Thermal comfort properties of textile fabrics in wet state, in Proc. Izmir Internat. Textile and Apparel Symposium, Cesme (Turkey) 2007
4. Hu J., Li Y., Yeung K.W., Wong A.S., Xu W.: Moisture Management Tester: A Method to Characterize Fabric Liquid Moisture Management Properties, Textile Research. Journal 75, 2005, 57-62
5. She F., Kong L.: Theoretical Investigation of Heat and Moisture Transfer through Porous Textile Materials, Research Journal of Textile and Clothing 4, 2000, 37-41
6. Hes L.: Thermal properties of nonwovens, Congress Index 87, Genf, 1987
7. Militky J., Matusiak M.: Complex Characterization of Cotton Fabric Thermo Physiological Comfort, in 3rd International Textile, Clothing and Design Conference. Croatia, 2006
8. Militký J., Havrdová J.: Porosity and air permeability of composite clean room textiles, International Journal of Clothing Science and Technology 13, 2001, 280-289
9. Militký J., Rubnerová J., Klička V.: Surface appearance irregularity of nonwovens, International Journal of Clothing Science and Technology 11(2/3), 1999, 141-152
10. Hes L.: Fundaments of design of fabrics and garments with demanded thermophysiological comfort, in International Round Table «Clothing Comfort – Condition of Life Quality», Romania, 2009
11. Çay A., Atav R., Duran K.: Effects of Warp-Weft Density Variation and Fabric Porosity of the Cotton Fabrics on their Colour in Reactive Dyeing, Fibres & Textiles in Eastern Europe. 15, 2007, 91-94
12. Militky J.: Prediction of Textile Fabrics Thermal Conductivity, in Thermal Manikins and Modelling, J. Fan, Editor, 2006
13. Crow R.M.: Heat and moisture transfer in clothing systems. Transfer through materials, a literature review Part 1., Ottawa, Ontario, Defence Research Establishment, 1974
14. Bogaty H., Hollies N.R.S., Harris M.: Some Thermal Properties of Fabrics. The Effect of Fiber Arrangement :Part 1957, Textile Research Journal 27, 1957, 445-449
15. Ullmann's Fibers, ed. Fibers. Vol. 1, Wiley-VCH Verlag GmbH&Co, KGaA, Weinheim, 2008
16. ASHRAE Standard 55-66, Thermal Comfort Conditions, American Society of Heating, Refrigerating and Air Conditioning Engineers, New York, 1966
17. Parsons K.C.: Ergonomics Assessment of Environments in Buildings, Proceedings of the CIBS Technical Conference, 1985
18. Fanger P.O.: Thermal Comfort, Danish Technical Press, Copenhagen, 1970
19. Militký J., Křemenáková D.: Prediction of textile fabric thermal conductivity, Proc.5th HEFAT Conf, Sun City, June 2007
20. Militký J., Křemenáková D.: Prediction of textile fabric thermal conductivity, Proc.7th HEFAT Conf, Pretoria, June 2009
21. Van Krevelen D.W.: Properties of Polymers, Correlations with Chemical Structure, Elsevier 1992
22. Hagi A. K.: Factors effecting water vapor transport through fibers, Theor. Appl. Mech. 30, 2003, 277 -309
23. Eiermann K: Kolloid-Z 201, 1965, 3-15

24. Bicerano J.: Prediction of Polymer Properties, Marcel Dekker, New York, 3rd Ed, 2002
25. Carslaw H.S., Jaeger J.C.: Conduction of Heat in Solids, Clarendon Press, Oxford, 2nd Ed, 1959
26. Sakiadis B.C., Coates J.: AICHE Journal 21956, 88
27. Kukin G.N. et all.: Učenie o voloknistych materialach, Legkaja promyšlenost, Moskva, 1949 (in Russian)
28. Rengasamy R.S., Kawabata S.: Computation of thermal conductivity of fibre from thermal conductivity of twisted yarn, Indian Journal of Fibre & Textile Research 27, 2002, 342-345
29. Militký J., Trávníčková M., Bajzík V.: Air Permeability and Light Transmission of Weaves, Fibres and Textiles No. 5, 1998, 125-132
30. Al Sulaiman F.A. et all: Numerical prediction of thermal conductivity of fibres, Heat Mass Transfer 42, 2006, 449-456

TEPELNÝ ODPOR BAVLNĚNÉHO DENIMU S RŮZNÝM OBSAHEM VLHKOSTI

Translation of the article
Thermal Resistance of Cotton Denim Fabric under various Moisture Conditions

Abstrakt: Cílem práce je vývoj matematického modelu pro predikci tepelného odporu tkanin bavlnářského typu s různým obsahem vlhkosti. Tepelný odpor je testován pomocí zařízení Alambeta. Matematický model je založen na vícefázovém modelu textilní struktury složené z fáze vlán, vody a vzduchu. Vícefázový model je vytvořen jako průměr sériového a paralelního uspořádání fází. Tepelný odpor klesá výrazně s obsahem vlhkosti ve tkaninách zejména pro nízké obsahy vlhkosti.

ELECTRICAL AND THERMAL PROPERTIES OF POLYPYRROLE COATED COTTON FABRIC

A.M. Rehan Abbasi, M. Mushtaq Mangat, V. K. Baheti and J. Militky

Technical University of Liberec, Faculty of Textile Engineering
Studentská 2, Liberec 46117, Czech Republic
rehan.abbasi@tul.cz

Abstract: *Polypyrrole can be chemically synthesized on cotton fabrics, giving rise to textiles with high electric conductivity. These textiles are suitable for several applications from antistatic films to electromagnetic interference shielding devices. The value of adhesion of conductive polymer into fibers by scanning electron microscope (SEM) was determined. Then assessments were made on physical properties specially focused towards electrical and thermal conductivities and their relationship for the present experiment.*
Key words: *Polypyrrole, cotton denim fabric, electrical conductivity, thermal conductivity.*

1 INTRODUCTION

Several works have been devoted to the coating of fibers or fibrous materials with conducting electroactive polymers (CEP). All these works involve a vapor-phase treatment of oxidant-containing carriers with the monomers [1]. Polymers with conjugated π-electron backbones can be oxidized or reduced more easily and more reversibly than conventional polymers. Dopants, which act as charge transfer agents, affect this oxidation or reduction process and render these polymers conductive.
The ultimate goal of electrically conductive polymer research is to combine the process-ability of polymers with the electronic properties of metal or semi-conductors [2]. Unfortunately, most of these conductive polymers are intractable and cannot be processed into useful articles. This is particularly true for polypyrrole (PPy) and polyaniline (PANi), which are preferred for their high conductivity and stability under environmental conditions [3, 4].
In the mid-1970s, the first polymer capable of conducting electricity was discovered in a new form of polyacetylene. The announcement of this discovery quickly rang around scientific community, and the intensity of the search for others magnified dramatically [5-7].
Among the first commercial products incorporating conductive polymers there was Contex®, a line of conductive textile products originally manufactured by Milliken [8], starting around 1990, and now produced by Eeonyx Corp., under the trade name of EeonTex ™.
There has been little attention devoted to the determination of the thermal conductivity of polypyrrole. Kanazawa et al. [9] reported a thermal conductivity value of 3.77 $Wm^{-1}K^{-1}$ for a copolymer of pyrrole and N-methylpyrrole. No information was given regarding the measurement technique or temperature at which the test was made.
For metals the Wiedemann-Franz law states that the ratio of thermal to electrical conductivity is proportional to temperature. The proportionality constant is the Lorenz number and is constant for a wide range of metals. This behavior may be explained by applying Fermi Dirac statistics to the "free" electrons in the material [10, 11]. Hence, it can be shown that the ratio of the electronic component of thermal conductivity λ ($W\ m^{-1}K^{-1}$) to electrical conductivity σ (Sm^{-1}) is given by:

$$N\sigma = \left(\pi^2 / 3\right)\left(k / e\right)^2 T \qquad (1)$$

where *k* is the Boltzmann constant ($J.K^{-1}$), *e* the charge on an electron (C) and *T* is the

absolute temperature (K). Hence the Lorenz number for metals is given by $(\pi^2/3).(k/e)^2$ and is equal to $2.45x10^{-8}$ $W\Omega K^{-2}$.
In this study PPy was chemically polymerized in different concentrations on cotton denim fabric by surfactant dopant. Cotton fiber surface was characterized by SEM. Volume and surface electrical conductivity of fabric samples was measured together with thermal conductivity.

2 METHODOLOGY

Cotton denim fabric was desized and washed thoroughly for complete removal of finishing additives. Construction of the fabric sample is mentioned in the Table 1.

Table 1 Description of the fabric sample

Description	
Warp Yarn	Cotton Dyed, Tex 49.25
Weft Yarn	Cotton, Tex 49.0
Weave	Twill 3/1 Z
gram per sq. meter (GSM)	248

Sample preparation

PPy was chemically synthesized in different concentrations on cotton denim fabric by in situ polymerization in the presence of surfactant dopant. Five different aqueous emulsions of Pyrrole (Sigma) with concentrations 0.3, 0.6, 0.9, 1.2 and 1.5 M were prepared by adding Dodecyl benzenesulphonate (DBSA) (Sigma) 0.05 M in each solution.
Five samples of fabric were immersed completely in each emulsion for 5 hours. Each sample was then taken out from emulsion and immersed in 0.1 M $FeCl_3$ (Sigma) for further 10 hours in order to complete polymerization of PPy. Each sample was then washed with ethanol followed by distilled water several times in order to remove surfactant from the fabric surface. Fabric samples were then dried at 25±4°C for 24 hours and marked as A1 to A5 with respective concentrations 0.3 to 1.5 M of Pyrrole and untreated sample was marked as A0.

SEM micrographs

Fibers coated with PPy were collected from each fabric sample and analyzed from SEM (WEGA TESCAN Inc. USA) at 30 kV.Samples were not coated with gold deliberately in order to take contrast image of shiny PPy particles.

Electrical conductivity

Surface as well as volume electrical conductivity were measured from both face and back of each fabric sample and average was recorded with the help of HP Agilent 4339A High Resistance Meter. Concentric ring electrodes were used for this purpose in order to avoid errors caused by textural unevenness of denim fabric.

Thermal conductivity

All treated and untreated fabric samples were conditioned for 24 hours at 25±2°C and 65% R.H before measuring thermal conductivity. It was measured with the help of ALAMBETA which is based on hot plate principle.

3 RESULTS

The Figure 1 shows the deposition of PPy on cotton fibers of fabric samples. It can be seen that with increase in pyrrole concentration in the polymerizing emulsion, there is a significant increment in the amount of particles on the fiber surface, Figure 1(b-f).

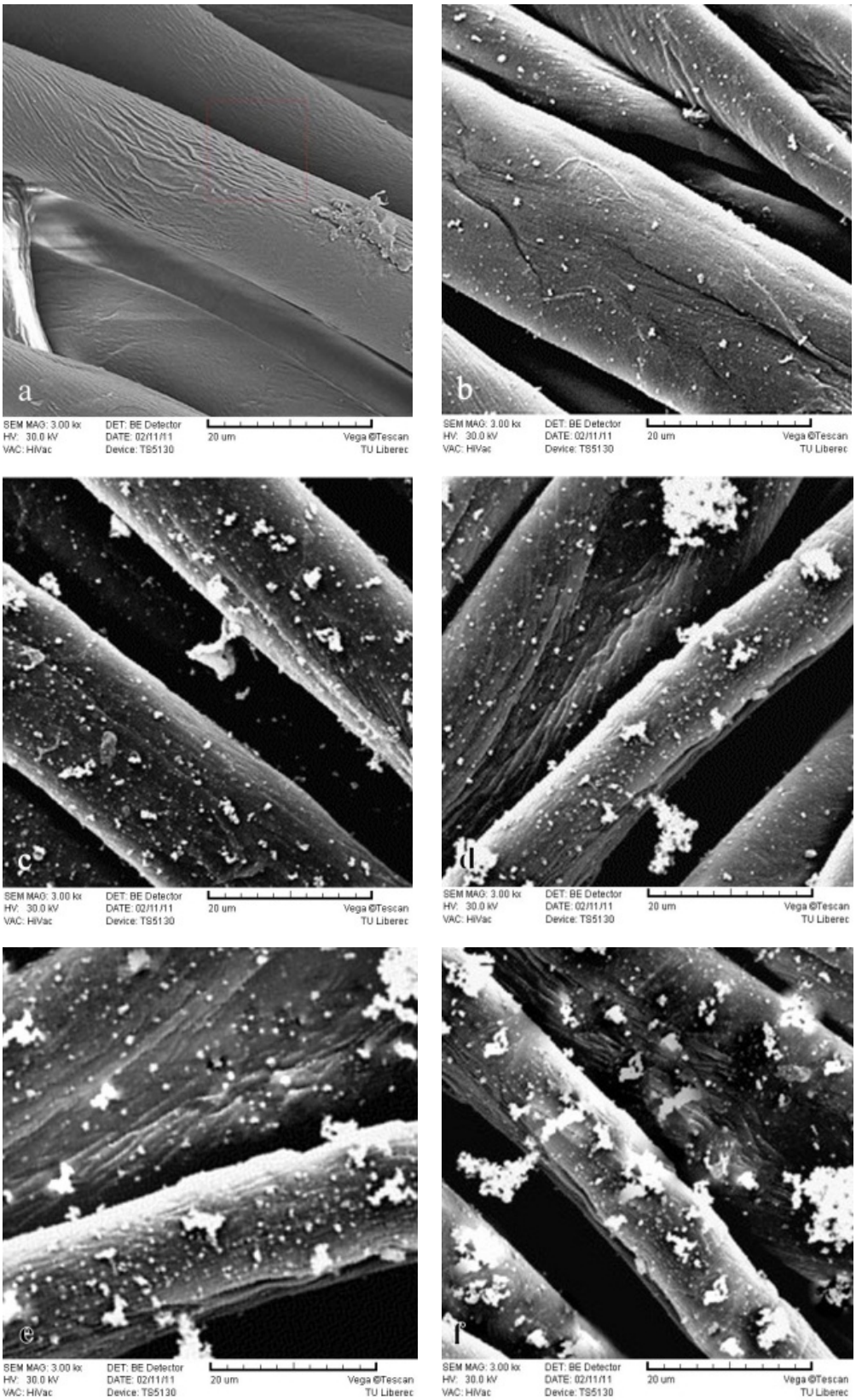

Figure 1 SEM micrographs of PPy coated cotton fibers (a) untreated A0 (b) A1 (c) A2 (d) A3 (e) A4 and (f) A5

Table 2 Electrical and thermal properties of PPy coated cotton denim fabric samples

Sample #	Volume Electrical Resistivity ρ [Ω/cm]	Volume Electrical Resistivity ρ [Ω/cm]	Surface Electrical Conductivity σ [S/cm]	Surface Electrical Conductivity σ [S/cm]	Thermal Conductivity λ x10^3 [Wm^{-1}K^{-1}]	Thermal Resistance R x 10^3 [m^{2}KW^{-1}]
A0	7.9672E+10	1.2551E-11	3.9853E+12	2.5092E-13	50.5	18.1
A1	3.8409E+07	2.6036E-08	5.4783E+08	1.8254E-09	54.8	15.3
A2	9.8000E+06	1.0204E-07	2.3470E+07	4.2608E-08	55.4	15.2
A3	5.5582E+06	1.7991E-07	9.3722E+06	1.0670E-07	53.6	16.3
A4	2.4736E+06	4.0427E-07	8.9736E+06	1.1144E-07	53.4	16.5
A5	2.0966E+06	4.7696E-07	7.6432E+06	1.3084E-07	55.7	15.4

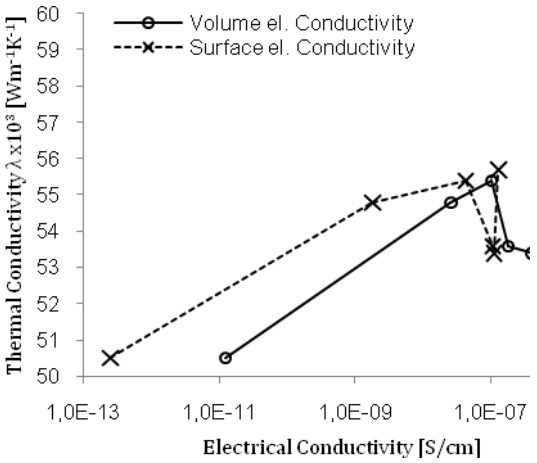

Figure 2 Thermal conductivity plotted against volume and surface electrical conductivity

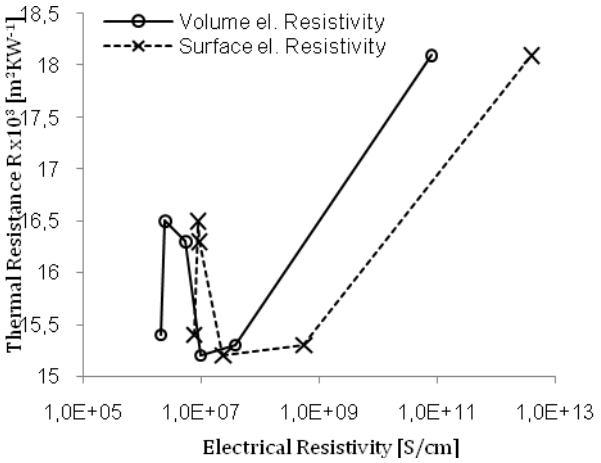

Figure 3 Thermal resistance plotted against volume and surface electrical resistivity

From the micrographs it can also be seen that there is no noticeable change in the surface morphology of the cotton fiber after deposition of PPy on it but tiny particles of PPy stick with the surface only.

Thermal conductivity of a material works by energy transfer through the material by excitation of one or more of the following ways: electrons, phonons, photons and molecules [12]. In this particular work, there is noticeable increase in thermal conductivity of untreated fabric sample and the sample treated with lowest concentration of pyrrole can be observed but there is no relationship has been found between concentration of PPy and thermal conductivity (Figure 2). Surface and volume electrical conductivity values can be seen in Table 2.

Similar effect was observed while plotting relationship between Thermal Resistance and volume and surface electrical resistivity of fabric samples as shown in Figure 3.

4 CONCLUSION

PPy was synthesized of cotton denim fabric by in situ polymerization in the presence of surfactant dopant. Electrical and thermal properties were measured and it was found that small amount of PPy particles which were formed on the surface of the cotton fiber cause a significant increase in thermal conductivity. Further increase in particle concentration cause drastic increase in electrical conductivity but it doesn't affect thermal conductivity so much. Therefore the relationship between thermal and electrical conductivity for PPy coated fabric does not follow a simple Wiedemann-Franz proportionality over this range of

concentration and/or for this technique of polymerization of PPy which is presented in this work.

Acknowledgement: *I would like to express my sincere gratitude to Prof Militky for his supervision and guidance to conduct this research. Financial support of this work was covered from student grant scheme in Technical University of Liberec, Czech Republic.*

5 REFERENCES

1. Heisey C.I., Wightman J.P., Pittman E.H., Kuhn H.H.: Text. Res. 63, 1993, 247-256
2. Frommer J.E., Chance R.R.: Electrically conductive polymers and composites: High performance polymers and composites, Kroschwitz J.I., Ed., John Wiley, NY, 1991, 174-219
3. Gregory R.V., Kimbrell W.C., Kuhn H.H.: Conductive textiles, Synth. Met. 28, 1989, C823-C835
4. Hosseini S.H., Entezami A.A.: Polym. Adv. Technol. 12, 2001, 482-493
5. Chiang C.K., Fincher C.R., Park Y.W., Heeger A. J., Shirakawa H., Louis E.J., Gau S.C., and MacDiarmid A.G.: Phys. Rev. Lett. 39, 1997, 1098
6. MacDiarmid A.G.: Synthetic Metals 84, 1997, 27
7. Cao Y., Smith P., Heeger A.J.: Synthetic Metals 57, 1993, 3514-3519
8. Milliken and Co., http://www.milliken.com
9. Kanazawa K.K., Diaz A.F., Krounbi M.T., Street G.B.: Synth. Met. 4, 1981, 119-130.
10. Goldsmid H.J..: in "Thermal Properties of Solids", Routledge and Kegan Paul, London, 1965, 49-62
11. Parrott J.E., Stukes A.D.: in "Thermal Conductivity of Solids", Pion, London, 1975, 101-104 and 110-119
12. Qi T.G.: Thermal properties of inorganic materials, Shanghai Sci. & Tech. Press 1981

ELEKTRICKÉ A TEPELNÉ VLASTNOSTI BAVLNĚNÝCH TEXTILIÍ S OBSAHEM POLYPYRROLU

The translation of article
Electrical and thermal properties of polypyrrole coated cotton fabric

Chemicky syntetizovaný polypyrrol na bavlněných textiliích zajišťuje zvýšenou elektrickou a tepelnou vodivost. Takové textilie se mohou použít pro stínění elektromagnetických polí. V práci je sledováno pronikání částic polypyrrolu do vláken a jsou hodnoceni vybrané vlastnosti výsledných bavlnářských textilií.

ANALYSIS OF CONVENTIONAL AND ORGANIC COTTON REGARDING RESIDUAL PESTICIDES

Syed Zameer Ul Hassan and Jiri Militky

Dept. of Textile Materials, Technical University of Liberec, Czech Republic
zameer_51214@hotmail.com

Abstract: *This study is focused on the measurement of bio-electrical signals caused by enzymatic inhibition of acetylcholinesterase (AChE) for the detection of organophosphorous and carbamate pesticides. These pesticides are the strong inhibitors of AChE and prevent its normal function of the rapid removal of acetylcholine (ACh). Biosensor Toxicity Analyzer (BTA) was used for the testing and enzyme activity was determined by acetylthiocholine chloride (ATCCl) as enzyme substrate. The monitoring of changes in bio-electrical signals caused by the interaction of biological substances and residues were evaluated. Two samples of conventional and organic cotton were analyzed. The method shows reasonable results and can successfully be utilized for the detection of residual pesticides on different types of cotton.*
Keywords: *Acetylcholinesterase, Acetylcholine, Acetylthiocholine chloride, Biosensor Toxicity Analyzer.*

1 INTRODUCTION

Cotton has always been a major part of the textile industry and today provides almost 38% of the world textile consumption, second only to polyester, which recently took the lead [1]. Cotton not only produces the natural fibers used in textiles and clothing but also yields a high grade vegetable oil [2]. Cotton production is highly technical and difficult because of pest pressures and environment, e.g. drought, temperature and soil nutritional conditions. The total area dedicated to cotton production accounts approximately 2.4% of arable land globally and cotton accounts for an estimated 16% of the world's pesticide consumption [3]. Pesticides are widely used for the control of weeds, diseases, and pests all over the world, mainly since after Second World War, and at present, around 2.5 million tons of pesticides are used annually and the number of registered active substances is higher than 500. Humans can be exposed to pesticides by direct or indirect means. Direct or primary exposure normally occurs during the application of these compounds and indirect or secondary exposure can take place through the environment or the ingestion of food [4].

This is why development of natural biological methods of insect control was initiated. Cotton grown without the use of insect control was initiated. Cotton grown without the use of any synthetically compounded chemicals (i.e. pesticides, fertilizers, defoliants, etc.) is considered as ''organic'' cotton. It is produced under a system of production and processing that seeks to maintain soil fertility and the ecological environment of the crop [5]. Pesticides are toxic compounds that may cause adverse effects on the human and the environment. Benzoylureas, carbamates, organophosphorous compounds, pyrethroids, sulfonylureas and triazines are the most important groups [6]. The organophosphates and carbamates are powerful inhibitors of acetylcholinesterase [7]. They can irreversibly inhibit acetylcholinesterase (AChE) which is essential for the function of the central nervous system [8], resulting in the build-up of the neurotransmitter acetylcholine which interferes with muscular responses and in vital organs produce serious symptoms and eventually death [9].

Inhibition of AChE by any xenobiotic compound is used as a tool for assessment

of toxicity of some pesticides such as organophosphates and carbamates [10]. As the pesticide residue is a potentially serious hazard to human health, the control and detection of pesticide residue plays a very important role in minimizing risk. Many methods have been developed in the last few years for the detection of organophosphorous pesticides. The most widely used methods are gas chromatography (GC), high-performance liquid chromatography (HPLC), gas chromatography-mass spectrometry (GC-MS), immune assay and fluorescence. However, these techniques, which are time consuming, expensive and require highly trained personnel, are available only in sophisticated laboratories [11].

Biosensors based on the inhibition of acetylcholine esterase (AChE) have been widely used for the detection of OP compounds [12]. Electro analytical sensors and biosensors provide an exciting and achievable opportunity to perform biomedical, environmental, food and industrial analysis away from a centralized laboratory due to their advantages such as high selectivity and specificity, rapid response, low cost of fabrication, possibility of miniaturization and easy to integrate in automatic devices [13]. Electrochemical biosensors for measurement of these pesticides are based on the inhibition of AChE and the inhibition degree is proportional to the pesticide concentration [14].

In this paper, we report another method for the determination of Organophosphorous and Carbamates pesticides based on acetylcholinesterase inhibition using AC1.W2.R1/ACCHE sensors with the help of Biosensor Toxicity Analyzer (BTA). Compared with other kinds of electrochemical AChE biosensors, this method is simple, fast and more sensitive for pesticide determination with much lower detection limit.

Principle of BTA

The target for many insecticides is an enzyme called acetylcholinesterase (AChE) [15]. Acetylcholinesterase's (AChE) biological role is the termination of impulse transmissions at cholinergic synapses within the nervous system of the insects and mammals by rapid hydrolysis of the neurotransmitter acetylcholine. Pesticides block the catalytic activity of the active center, thus acting as inhibitors of AChE. This results in the accumulation of acetylcholine in the synaptic membrane, which blocks the nerves to process the signals properly [16].

Figure1 Biosensor toxicity analyzer with microflow unit

Biosensor toxicity analyzer (BTA) works on the above mentioned principle and monitors the activity of the inhibition of AChE with the help of sensors which are equipped with an enzymatic membrane of AChE enzyme which is immobilized. It consists of two major parts, one of which is the Microflow unit and the other is Bioanalyzer. The microflow unit has the capillary arrangement which allows precise and constant flow of the liquid onto the active surface of the AChE sensor for a high level of repeatability and sensitivity in the measurements. The module has an integrated chamber in which the sensor can easily be placed or replaced as shown in Figure 1.

2 EXPERIMENTAL

2.1 Materials

Two samples of Egyptian cotton variety Giza 86 were collected from the cultivation season 2009/2010. One of them was the classical conventional cotton and the other was organic cotton without utilizing the synthetic pesticides.

2.2 Reagents and Apparatus

HPLC grades Hexane and dichloromethane solvents were used for the extraction procedure. Anhydrous and granular sodium sulfate was used as dehydrating agent throughout the extraction process. Glass wool was used as supporting material in soxhlet extraction after cleaned with acetone. A round flask (250 ml) with soxhlet and condenser glassware was used to conduct the soxhlet extraction. MOPSO sodium salt was used for the preparation of buffer solution in BTA, where as Acetylthiocholine chloride (ATCCl) as enzyme substrate and Neostigmine methyl sulfate as enzyme inhibitor. AC1.W2.R1/ACCHE Sensors were used for the monitoring of AChE inhibition.
All the above experiments were done at the Technical University of Liberec, University of Pardubice and Bvt technologies, Czech Republic.

2.3 Sample Preparation

The determination of pesticides in samples at low concentrations is always a challenge. The main aim of any extraction process is the isolation of analytes of interest from the selected sample by using an appropriate extracting phase. The development of an appropriate sample preparation procedure involving extraction, enrichment, and cleanup steps becomes mandatory to obtain a final extract concentrated on target analytes. It is always necessary to carry out some pretreatments to get a homogeneous and representative subsample [4]. Even if the sample is apparently homogeneous, that is, an aqueous sample, it will be at least necessary to perform a filtration step to remove suspended particles, which could affect the final determination of target analytes [15].

Cryogenic Homogenization

Both samples of conventional cotton and organic cotton were arranged inside of a pre-chilled Teflon mill in the form of pallets which contains a concentric Teflon ring and Teflon puck in liquid nitrogen surrounding. Each sample was milled for approximately 10 minutes with an interval of 2 min for grinding and 1 min for cooling. After the milling the resulting powder was sampled, cleaned and stored for analysis. Once the entire sample was homogenized and blended, the powder was sampled, cleaned and stored for analysis.

Soxhlet Extraction (SOX)

The Soxhlet Extraction method was used for the extraction from both of the samples. Two different solvents hexane and dichloromethane were used for each of the sample. A total of 1.0 gm homogenized sample was transferred to the Soxhlet thimble in between two layers of dehydrated sodium sulfate over a glass wool layer. The thimble was placed in the extraction apparatus charged with 230 ml of both the solvents, separately. Samples were extracted for overnight. The extract then concentrated by turbo evaporator and stored for further analysis.
Biosensor Toxicity Analyzer (BTA) equipped with AC1.W2.R1/ACCHE sensors was used for the monitoring of AChE inhibition. MOPSO sodium salt was used for the preparation of buffer solution in BTA, where as Acetylthiocholine chloride (ATCCl) as enzyme substrate and Neostigmine methyl sulfate as enzyme inhibitor.

3 RESULTS AND DISCUSSION

All the above mentioned four extracts were injected in BTA for analysis. For the convenience we will describe the results with respect to the solvent used for the extraction process.

Hexane

Both the samples of conventional cotton and organic cotton were tested on BTA. After putting the sensor in the slot and starting the pump, the buffer solution is added in the microflow unit. After some stabilization the sample is added and then the inhibitor, Neostigmine methyl sulfate, is added in the solution to compare the inhibition of the sample with the standard inhibitor. The resultant graphs of the whole activity are shown in Figure 2 and Figure 3 for conventional cotton and organic cotton, respectively. In these graphs the response of current (nano amperes) is on Y axis and the time (seconds) is on X axis.

Dichloromethane

The same procedure as mentioned in the case of the solvent hexane is repeated for the second solvent i.e. dichloromethane and the resultant graphs are shown in Figure 4 and Figure 5. It is quite visible in these graphs that there is a clear response on the addition of both the samples which can be compared with the slope of the standard inhibitor. We measure this response (ΔI) and also the relative inhibition (R_i), which is calculated to quantify inhibiting effect of an inhibitor to the enzyme. Inhibiting effect is proportional to the slope of current time dependence after the inhibitor or sample addition. The calculated values are shown in Table 1.

It can be observed that although both conventional and organic cotton samples show the change in the intensity of the current but the organic cotton sample shows more response and more inhibition with each solvent. Although the use of synthetic pesticides and sprays are prohibited in the cultivation of organic cotton but the presence of these xenobiotic compounds indicate the improper storage, organic fields surrounded by the conventional cotton fields or may be some negligence in the organic cotton production line.

Figure 2 Conventional cotton sample with hexane

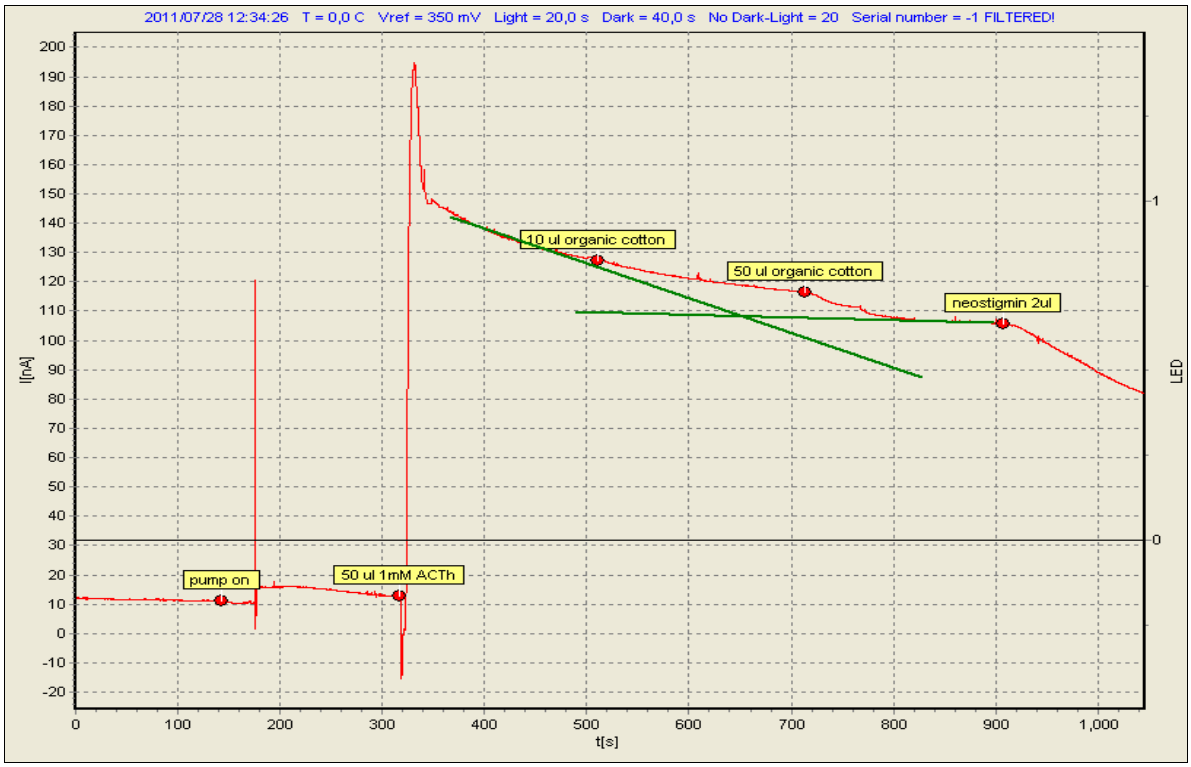

Figure 3 Organic cotton sample with hexane

Figure 4 Conventional cotton sample with DCM sample

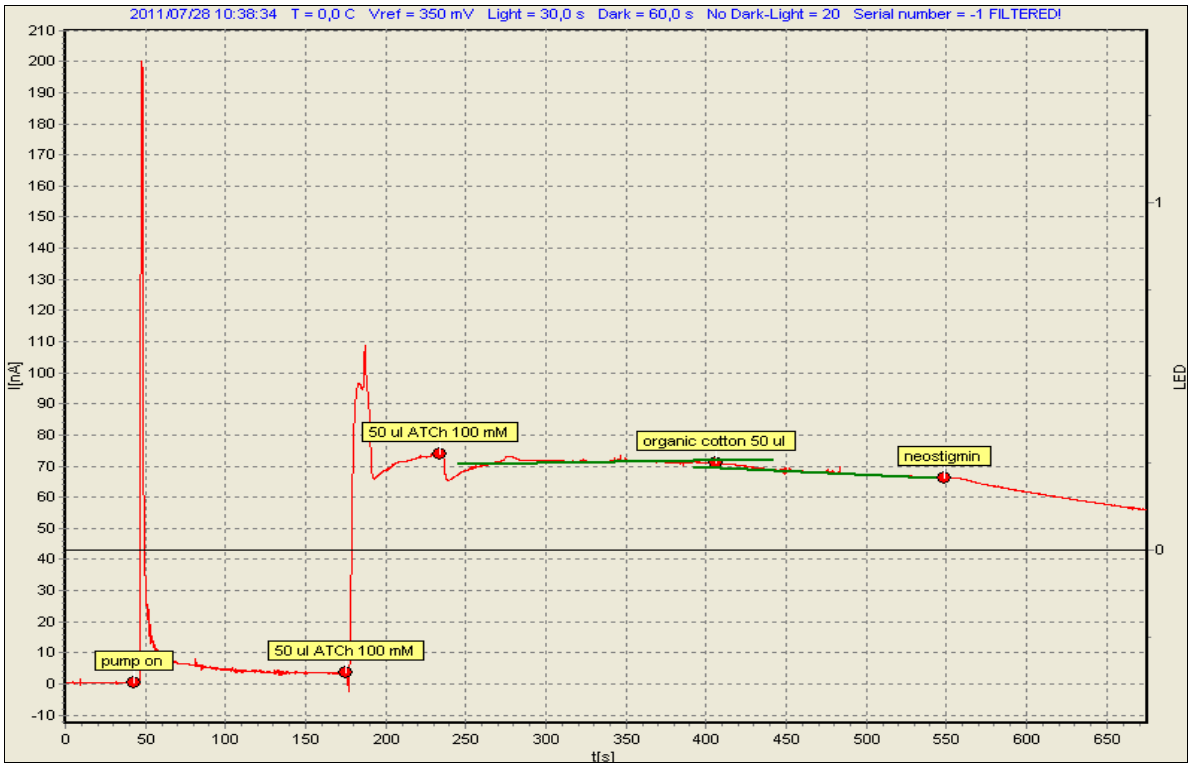

Figure 5 Organic cotton with DCM

Table 1 Response and Relative Inhibition for conventional and organic cotton

Solvents	Conventional cotton		Organic cotton	
	Response [ΔI(nA)]	Relative Inhibition [Ri]	Response [ΔI(nA)]	Relative Inhibition [Ri]
Hexane	1.416	-0.0002855	6.527	-0.0000745
Dichloromethane	3.208	-0.0004602	3.524	-0.0003441

4 CONCLUSION

This study presents a method based on AChE inhibition. Contrary to other sophisticated methods, this is an easier, faster and cheaper method. It is a method that offers to different investigators an easy way to detect the presence of organophosphorous and carbamate pesticides.

As there is worldwide interest in organic cotton as a potentially environmentally friendly way to produce cotton so this method can be helpful for analyzing the truth of the statement.

Further research must be needed to verify the usefulness of the method presented here for the screening of pesticides on some more varieties of cotton of different regions.

Acknowledgements: *The Authors would like to thank Dr. Jan Krejci, CEO of Bvt Technologies, for his support. This work was supported under Student Grant Scheme (SGS) by Technical University of Liberec, Czech Republic.*

5 REFERENCES

1. Myers D.: Organic Cotton, In Organic Cotton, edited by Dorothy Myers, London, Intermediate Technology Publications Limited, 1999
2. Robertson W.C., Roberts B.A.: Integrated Crop Management for Cotton Production in the 21st

Century, [ed.] M. Rafiq Chaudhry Phillip J. Wakelyn, Cotton:Technology for the 21st Century, First. Washington DC : International Cotton Advisory Committee, 2010, 475
3. Blackburn R.S.: Life Cycle and Environmental Impact In Sustainable Cotton Production, edited by L. Gose, Cambridge, Wood head Publishing Limited, 2009
4. Turiel E.: Sample Handling of Pesticides in Food and Environmental Samples, In Analysis of Pesticides in Food and Environmental Samples, edited by José L. Tadeo, CRC Press, 2008
5. Gordon S., Hsieh Y-L.: ed. Cotton: Science and Technology, Cambridge, Wood Head Publishing Ltd, 2007
6. Alder L.: Residue Analysis of 500 High Priority Pesticides: Better by GC – MS or LC – MS/MS?, Wiley InterScience 25, 2006, 838-865
7. El-Naggar A.E., Abdalla M.S., El-Sebaey A.S., Badawy S.M.: Clinical findings and cholinesterase levels in children of organophosphates and carbamates poisoning, Eur J Pediatr 168, 2009, 951-956
8. Hu, Haoyu: A novel chemiluminescence assay of organophosphorous pesticide quinalphos residue in vegetable with luminol detection, Chemistry Central Journal, 2010
9. Mulchandani A.: Biosensors for direct determination of organophosphate pesticides, Biosensors & Bioelectronics 16, 2001, 225-230
10. Hannam M.L.: Characterisation of esterases as potential biomarkers of pesticide exposure in the lugworm Arenicola marina (Annelida: Polychaeta), Environmental Pollution 152, 2008, 342-350
11. Mulchandani P.: Biosensor for direct determination of organophosphate nerve agents. 1. Potentiometric enzyme electrode, Biosensors & Bioelectronics 14, 1999, 77-85
12. Deo R.P.: Determination of organophosphate pesticides at a carbon nanotube/organophosphorous hydrolase electrochemical biosensor, Analytica Chimica Acta 530, 2005, 185-189
13. Buerk D.G.: Biosensors: Theory and Applications, Technomic Publishing Company, Inc., 1993
14. Arvinte A.: Development of a Pesticides Biosensor Using Carbon-Based Electrode Systems," In Chemicals as Intentional and Accidental Global Environmental Threats, by Lubomir Simeonov and Elisabeta Chirila, edited by Lubomir Simeonov and Elisabeta Chirila, Springer, 2006, 337-343
15. Tadeo J.L.: Pesticides: Classification and Properties, In Analysis of Pesticides in Food and Environmental Samples, edited by José L. Tadeo, CRC Press, 2008
16. Mulchandani A.: Microbial Biosensors for Organophosphate Pesticides, Applied Biochemistry and Biotechnology, 2011

ANALÝZA ZBYTKŮ PESTICIDŮ V KONVENČNÍ A ORGANICKÉ BAVLNĚ

Translation of the article
Analysis of Conventional and Organic Cotton Regarding Residual Pesticides

Jednou ze základních deklarovaných výhod organické bavlny je nepoužívání pesticidů při jejím pěstování. Řada výrobců produktů z organické bavlny je přesvědčena, že produkty z konvenční bavlny obsahují toxické zbytky pesticidů. Tato práce je věnována měření bio-elektrických signálů vyvolaných enzymatickou inhibicí acetylcholinesterazy (AChE) umožňujících detekci zbytků pesticidů na bázi organofosfátů a karbamátů. Oba typy pesticidů jsou silné inhibitory AChE a zabraňují její normální funkci, tj. rychlému odstranění acetylcholinu (ACh). Pro testování enzymatické aktivity byl jako substrát použit acetylthiocholine chlorid (ATCCl) a měřeni bylo provedeno na zařízení Biosensor Toxicity Analyzer (BTA). Byly analyzovány dva vzorky konvenční a organické bavlny. Výsledky ukazují, že zbytky pesticidů jsou na obou druzích bavln, což indikuje zřejmě znečištění ovzduší během sklizně a manipulace s organickou bavlnou.

THE OPTIMIZATION OF EXPERIMENTAL PARAMETERS FOR JET-RING SPINNING

Guocheng Zhu, Sayed Ibrahim and Dana Kremenakova

Department of Textile Technologies, Faculty of Textile Engineering, Technical University of Liberec, Liberec, Czech Republic, 46117

Abstract: *The application of air-jet nozzle in ring spinning system has been turned up in the last decade, and the greatest advantage reported is the reducing of hairiness. In this paper, an attempt has been made to optimize the utility of a single air-jet nozzle in ring spinning system. Some parameters, such as air pressure, the distance between front roller nip line and air-jet nozzle inlet, and the number of orifices were adjusted to get a better quality yarn. In order to confirm the role of these parameters, the properties of ring and jet-ring spun yarns were compared. All the samples were characterized in terms of count, twist, irregularity, hairiness and strength. The results showed that the air pressure and the distance have a significant influence on irregularity; all the experimental parameters have a significant influence on hairiness. By multi-objective programming method, a set of optimal experimental parameters was found, and the properties of jet-ring spun yarn were improved significantly.*

Key words: *Ring spinning; Air-jet nozzle; Irregularity; Hairiness; Optimization*

1 INTRODUCTION

Ring spinning has been a widely used method of yarn production, but is disadvantaged due to several limitations, one of which is the poor integration of many fibers that protrude from the yarn surface causing yarn hairiness [1-2]. Yarn hairiness has been shown to negatively affect the properties of the resultant fabric, particularly in terms of pilling propensity [3-5]. Generally, the hairiness of yarn can be reduced either by sizing or singeing in the short staple field and by Solo-spun or two-folding in the long staple field [6], but either higher costs or time consumption. Another method for reducing yarn hairiness is jet-ring spinning system that applied air-jet nozzle into ring spinning system, which was proved to be an effective method [7-11].

Jet-ring spinning was first reported by Wang et al [7]. In their work, an upward swirling flow of air against the yarn movement was introduced, and the result showed that the yarn hairiness was significantly reduced [7]. Subsequently, Cheng et al [8] studied the effect of some experimental parameters on yarn hairiness, and stated the relationships between yarn hairiness and twist level, spindle speed and air pressure. But their work showed that the evenness and imperfection of jet-ring spun yarns are worse than ring spun yarn, and they thought the distance between front roller nip line and air-jet nozzle inlet hardly affects the yarn hairiness [8]. Ramachandralu et al [9-11] presented that the air vortex in the direction same as the yarn twist gives better hairiness reduction. And he introduced twin air-jet nozzle into ring spinning system. The results demonstrated that the qualities of yarns were improved in 0.25 bar air pressure of first 'S' nozzle and 0.5 bar air pressure of second 'Z' nozzle. Zeng et al [10] presented their report about the properties of jet-ring spun yarns by adjusting air pressure and orifice angle of the air-jet nozzle, the results showed that hairiness will be reduced in a higher air pressure and a smaller orifice angle, but unfortunately, the evenness of yarn deteriorated.

In this work, our objectives are:

1. to assess the effect of some experimental parameters, which are air pressure, the distance between front roller nip line and air-jet nozzle inlet, and the number of orifices, on the jet-ring spun yarn properties,

2. to find the optimal experimental conditions by multi-objective programming method.

We use Box-Behnken experimental design to examine the effects of different spinning parameters on yarn properties. In order to evaluate the performance of Jet-ring spinning, we tested both conventional ring and jet-ring spun yarns and compared with them in evenness, imperfection, hairiness, and tensile properties.

2 MATERIALS AND METHODS

A cotton roving was provided by Velveta Company. The yarns were produced in a spinning system which combined ring spinning with a single air-jet nozzle. In order to determine the role of air pressure, the distance between the front roller nip line and nozzle inlet, and the number of orifices in obtaining optimum yarn characteristics, three levels of air pressure, 0.25, 0.5, 0.75 bar, three kinds of distance, 1, 2, 3 cm, and also three different orifice's number, 2, 3 and 4 were selected. The nozzle schematic diagram was showed as Figure 1, the direction of nozzle inlet face toward the front roller. And the parameters of jet nozzle were: chamber diameter is 3.5 mm, orifice diameter is 0.7 mm, orifices angle is 450.

After prepared the samples, we put the samples into the conditions of 65% humidity and 25°C temperature for 24 hours for the following testing. These samples were tested in terms of count, twist, evenness, hairiness (Zweigle G567), imperfection (Uster tester 4) and tensile property (Instron 4411, pretension was 0.125 N, gauge was 50 cm, tensile speed was 100 mm/min).

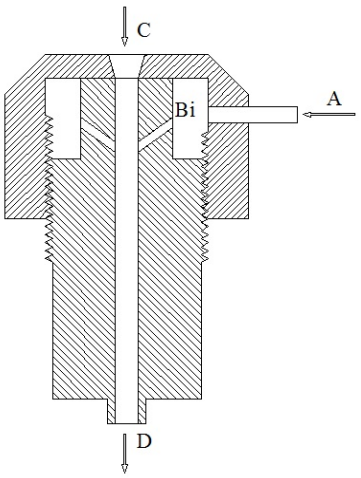

Figure 1 The schematic of air-jet nozzle. (A) the inlet of compressed air; (Bi) the orifices; (C) the nozzle inlet of air; (D) the nozzle outlet of air

Box-Behnken design

A three-level three factorial Box–Behnken experimental design (constructed using Minitab 16) was used to evaluate the effects of the selected independent variables on the response. The number of experiments required to investigate the previously noted three factors at three levels would be 27 (3^3). However, this was reduced to 15 using a Box–Behnken experimental design. The results from this limited number of experiments provided a statistical model, which can help us find the optimum experimental conditions and the relationships between experimental results and parameters. The significant variables like air pressure, the distance between front roller nip line and air-jet nozzle inlet, and the number of orifices were chosen as the critical variables and designated as X1, X2 and X3, respectively. The low, middle and high levels of each variable were designated as −1, 0 and +1, respectively, and given in Table 1. And the actual design of this experiment is given in Table 2.

Table 1 Factors and factor levels investigated in Box-Behnken experimental design

Factor	Level		
	-1	0	+1
X1: Air pressure (bar)	0.25	0.5	0.75
X2: The distance between front roller nip and nozzle inlet (cm)	1	2	3
X3: The number of orifices (n)	2	3	4

Table 2 The design of this experiment

Trial No.	Air pressure (bar)	The distance (cm)	orifices number (n)
1	+1	+1	0
2	+1	-1	0
3	-1	+1	0
4	-1	-1	0
5	0	+1	+1
6	0	+1	-1
7	0	-1	+1
8	0	-1	-1
9	+1	0	+1
10	-1	0	+1
11	+1	0	-1
12	-1	0	-1
13	0	0	0
14	0	0	0
15	0	0	0

In a system involving three significant independent variables X1, X2 and X3 the mathematical relationship of the response on these variables can be approximated by the quadratic polynomial equation:

$$Y=\alpha_0 + \alpha_1 x_1 + \alpha_2 x_2 + \alpha_3 x_3 + \alpha_{12} x_1 x_2 + \alpha_{13} x_1 x_3 + \alpha_{23} x_2 x_3 + \alpha_{11} x_1^2 + \alpha_{22} x_2^2 + \alpha_{33} x_3^2 \quad (1)$$

where Y is estimate response, α_0 is constant, α_1, α_2 and α_3 are linear coefficients, α_{12}, α_{13} and α_{23} are interaction coefficients between the three factors, α_{11}, α_{22} and α_{33} are quadratic coefficients.

In this model given in equation (1), interactions higher than second-order have been neglected. A multiple regression analysis is done to obtain the coefficients and the equation can be used to predict the response.

3 RESULT AND DISCUSSION

The yarn counts and twists were close to each other, the ring yarns count and twists were 23±0.33 tex and 730±26 tpm respectively. And the value was 23±0.39 tex and 716±15.89 respectively when the nozzle direction was down. The properties of ring spun yarn were showed in Table 3.

Table 3 Properties of ring spun yarn

CV (%)	-50% TP(/km)	+50% TP(/km)	+140% TP(/km)	S_{1+2} (/m)	S_3 (/m)	Te (cN/tex)	El (%)
20.35±0.19	397±86.2	1087±130	337±41.6	160.09±6.270	16.050±1.560	17.98±1.63	5.15±0.49

*CV represents the mass unevenness of yarns; H represents the total length of fibers protruding the yarn body per centimeter yarn length; S_{1+2} represents the total number of fibers within one millimeter and two millimeters protruding from yarn body; S_3 represents the total number of fibers which equals and more than three millimeters; -50% TP, +50% TP and +140% TP represent -50% thin places, +50% and +140% thick places respectively; Te represents the tenacity of yarns; El represents the elongation of the yarns.
*at the 0.05 level, each group data was significantly drawn from a normally distributed population.

3.1 Effect of experimental parameters on CV of jet-ring spun yarn

The analysis of data according to Box-Behnken method demonstrated that the air pressure and the distance between front roller nip line and air-jet nozzle inlet have an influence on the yarn's CV. A mathematical model was built to express the relationship between them. And in order to clearly describe this mathematical model a 3D surface plots was presented (Figure 2). The minimum value of CV is 19.3212% When x_1=-0.5203 and x_3=1 by optimization method.

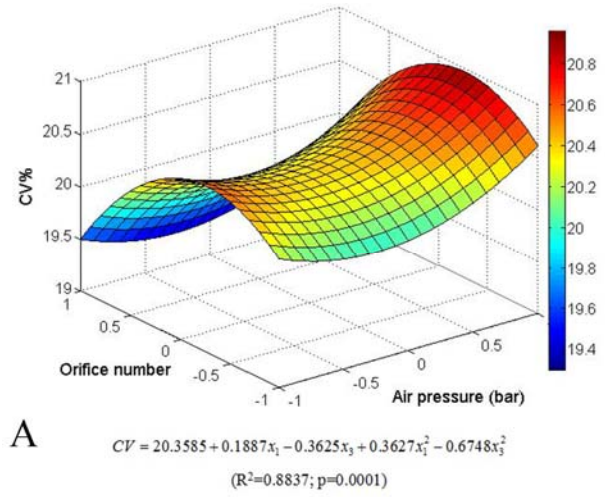

Figure 2 The mathematical model and image of CV corresponding to the experimental parameters

Although the influence of the air pressure and the distance between front roller nip line and air-jet nozzle inlet on CV is not conspicuous from the mathematical model, there are some interesting phenomena. The lower air pressure gives the lower CV value, and the CV value decrease as the increase of orifice number. The lower air pressure means that less energy and cost was needed, and the more orifice number means that uniform flow was needed. Earlier researchers reported that there was a slight deterioration in CV with jet-ring spinning, and they attributed this phenomenon to the concentration of mass in very short lengths because the surface fibers wrap around the yarn body. In our work, the results showed that in some conditions the evenness of jet-ring spun yarns were worse than ring spun yarn, but after optimization, we can find a reasonable experimental condition to improve the CV.

3.2 Effect of experimental parameters on imperfection of jet-ring spun yarn

The air pressure and orifice number have an obvious influence on imperfection, the mathematical models and images are shown in Figure 3. And the minimum value of -50%TP is 295/km when x_3=1, of +50%TP is 813/km when x_1=-1 and x_3=1, of +140%TP is 198/km When x_1=-1 and x_3=1.

Compared ring system with jet-ring system, the difference is the air flow. Therefore, the difference of thin places and thick places between ring and jet-ring spun yarn are the losing of fibers and the warping fibers caused by the air flow. We can find an interesting trend among these properties from the mathematical models, the higher the air pressure, the worse the imperfection, the more orifices, the better the imperfection. Suitable and uniform air flow field is beneficial to produce uniform yarn, otherwise, the losing of fibers make the thin places, and disorderly warping fibers make the thick places. And the more orifices, the better the uniform of air flow field.

3.3 Effect of experimental parameters on hairiness of jet-ring spun yarn

The hairiness of yarn is influenced by air pressure, distance and orifice number base on our work. Figure 4 shows the mathematical model and slice image of hairiness with the length less than 3 mm, and equation (2) expressed the relationship of hairiness with the length more than 3 mm corresponding to the experimental parameters. By the optimum method, we got the minimum value of S_{1+2} and S_3 are 112.4733/m and 2.4941/m respectively when x_1=-1, x_2=-1, x_3=1.

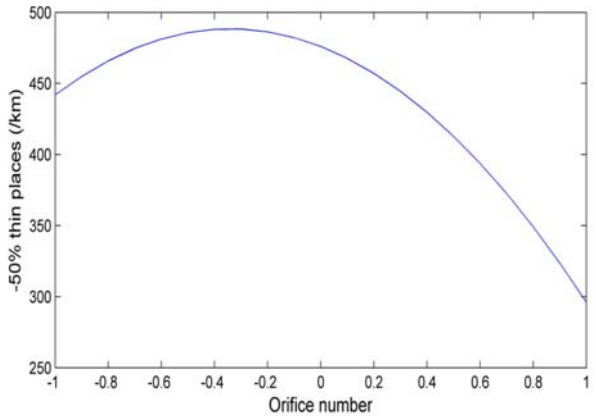

B $-50\%TP = 476.1857 - 73.325x_3 - 107.8607x_3^2$

(R^2=0.7086; p=0.0000)

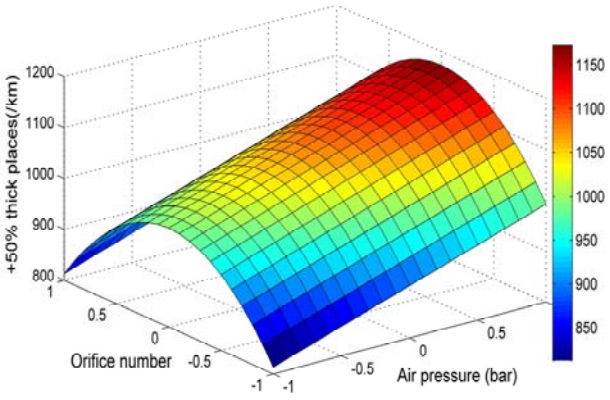

C $+50\%TP = 1083.34 + 89.6x_1 - 180.8x_3^2$

(R^2=0.5935; p=0.0045)

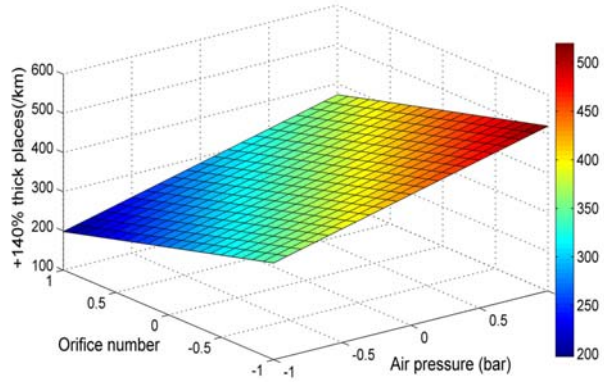

D $+140\%TP = 358.887 + 86.675x_1 - 74.575x_3$

(R^2=57.23%; p=0.0061)

Figure 3 The mathematical models and images of yarn properties corresponding to the experimental parameters, (B) -50%TP corresponding to orifice number; (C) +50%TP corresponding to air pressure and orifice number; (D) +140%TP corresponding to air pressure and orifice number

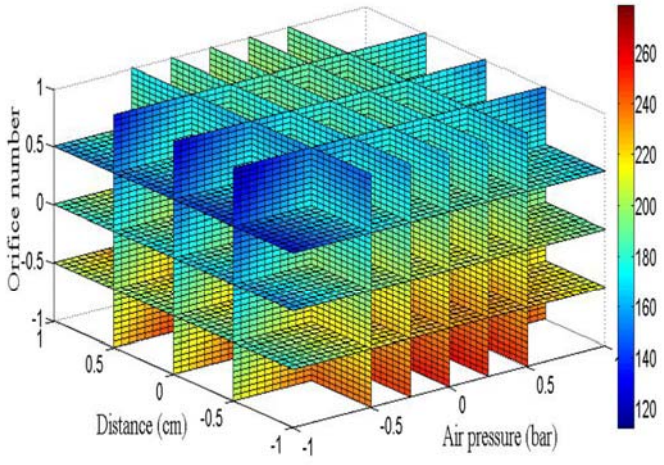

E $S_{1\text{-}2} = 219.16 + 13.9281x_1 + 13.2144x_2 - 43.9675x_3 - 35.5767x_1^2$

(R^2=0.9162; p=0.0000)

Figure 4 The mathematical model and image of yarn hairiness corresponding to the experimental parameters

$$S_3 = 21.4948 + 5.1096x_2 - 7.592x_3 - 1.7893x_1x_2 - 1.5765x_2x_3 - 3.9967x_1^2 - 2.0895x_3^2 \quad (2)$$

(R^2=0.9918; p=0.0000)

The yarns hairiness are significantly reduced when air-jet nozzle was applied, and lower air pressure, less distance and more orifice number are beneficial to reduce yarn hairiness. As to the cause of yarn hairiness, which has been attributed to the escape of fibers form the twisting action from within the spinning triangle [1, 12]. And Pillay's study demonstrated that the yarn hairiness is significantly correlated with fiber length, fineness and torsional and flexural rigidities of fibers [13]. With respect to the effect of air pressure on yarn hairiness, some researchers stated that may be more protruding fibers were wrapped into the yarn body causing by swirling air flow [7, 8]. As air pressure increases, the tangential velocity, which is responsible for wrapping the protruding surface hairs around the yarn body, increases. This leads to more wrapping fiber ends and so less hairiness. However, with increasing nozzle pressure, the recirculation zone that occurs between the inlet and the jet orifices increases. This increase is a potential source for fiber curving, so it impedes the wrapping of the protruding fiber ends [10].

The distance between front roller nip line and air-jet nozzle inlet also played a significant role in yarn hairiness, the results showed that the yarn hairiness decreases as the distance decreases. This phenomenon could be explained from several aspects, (1) the formation of yarn and hairiness were occurred in triangle zone, therefore, the yarn properties and hairiness were easy to be influenced by outer conditions; (2) the closer to the triangle zone, the more fibers warped into the yarn body; (3) some floating fibers could be blowing away.

The more orifice number, the more uniform of the air flow [14], therefore, it is important to provide the uniform air flow for improving the yarn hairiness.

3.4 Effect of experimental parameters on Yarn tensile properties

During this work, the strength and elongation properties were slightly influenced, and did not discussed because they did not to be negative effects on yarns' usage.

3.5 The optimal experimental conditions for jet-ring spun yarn

In order to get a set of reasonable experimental parameters for all of the properties of jet-ring spun yarn, we took all of the equations into account by multi-objective programming method. The best values are 19.3212, 112.4729, 2.4941, 295, 812.9 and 197.6367 corresponding to CV, $S1_{+2}$, S_3, -50%TP, +50%TP and +140%TP respectively. And the optimal experimental parameters from Matlab are

$$x_1 = -1,\ x_2 = -1,\ x_3 = 1$$

In our previous work, we applied the nozzle which produced the upward air flow into ring spinning system and built some mathematical models [15], but we did not give a set of reasonable experimental parameters for producing yarns. Therefore, in this work, we replenish this part by multi-objective programming. The minimum values from each mathematical model are 19.1, 115, 6.09, 186.5, 118.3 and 197.3 corresponding to CV, S_{1+2}, S_3, -50%TP, +50%TP and +140%TP respectively. But for holistic optimization, the optimal values are 19.2399, 134.4354, 6.17, 186.562, 126.844 and 200.0375 in turn. The optimal experimental parameters from Matlab are

$$x_1 = 1,\ x_2 = -1,\ x_3 = -0.169$$

3.6 Comparison of properties of ring and jet-ring spun yarns

The optimum experimental conditions for jet-ring spun yarn are 0.25 bar air pressure, 1 cm distance and 4 orifices when the nozzle produce the downward air flow, 0.75 bar air pressure, 1 cm distance and 3 orifices when

the nozzle produce the upward air flow. In Table 4, we give the optimum values of jet-ring spun yarn. In Figure 5, we compared these three kinds of yarns.

Table 4 Properties of jet-ring spun yarn in optimum experimental conditions

CV (%)	-50% TP(/km)	+50% TP(/km)	+140% TP(/km)	S_{1+2} (/m)	S_3 (/m)	Te (cN/tex)	El (%)
19.32	295	813	198	112.47	2.49	18.5	5.82
19.24	186	127	200	134.43	6.17	17.75	5.55

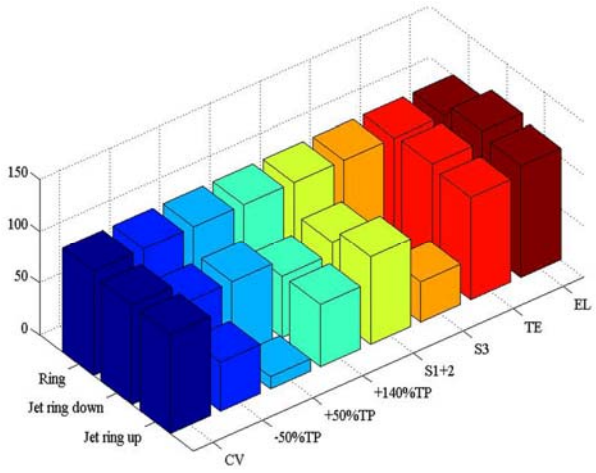

Figure 5 Comparison of ring and jet-ring spun yarns

4 CONCLUSIONS

A single air-jet nozzle is applied into ring spinning system, and a king of jet-ring spun yarn with improved quality is obtained by adjusting the air pressure, the distance between front roller and the nozzle inlet, and the orifice number of nozzle. The air pressure and the orifice number have a slight effect on yarn CV, but have a significant effect on yarn imperfection. All of the experimental parameters played important roles in yarn hairiness. And the optimal experimental conditions should be adjusted when the direction of nozzle was changed. The optimal experimental parameters are 0.25 bar air pressure, 1 cm distance and 4 orifices when the nozzle produce the downward air flow, 0.75 bar air pressure, 1 cm distance and 3 orifices when the nozzle produce the upward air flow.

5 REFERENCES

1. Wang X, Huang W., Huang X.B.: A Study on the Formation of Yarn Hairiness, J. Textile Inst. 90 Part 1, No 4, 1999, 555-569
2. Za K.: Investigation of Post-spinning Yarn Engineering, PhD Thesis, Deakin University, Australia,2003
3. Baird M.E., Hatfield P., Morris G.J.: Pilling of Fabrics a Study of Nylon and Nylon Blended Fabrics. J. Textile Inst. 47(4), 1956, 181-201
4. Timmis J.B.: How to Live with Pilling, Knitting Int. 83(9), 1976, 82-86
5. Barella A., Bardi X., Castro L.: Hairiness Modification by Yarn/Yarn and Yarn/Metal Friction, Melliand Textilber. 72(1), 1991, 3-4
6. Chang L., Wang X.: Comparing the Hairiness of Solo-Spun and Ring Spun, Textile Res. J. 73(7), 2003, 640-644
7. Wang X.G., Miao M.H., How Y.L.: Studies of JetRing spinning - Part1: Reducing Yarn Hairiness with The JetRing, Textile Research Journal 67(4), 1997, 253-258
8. Cheng K.P.S., Li C.H.L.: JetRing Spinning and Its Influence on Yarn Hairiness, Textile Res. J. 72, 2002, 1079-1087

9. Ramachandralu K., Dasaradan B.S.: Design and Fabrication of Air Jet Nozzles for Air Vortex Ring Spinning System to reduce the Hairiness of Yarn, The Journal of The Institution of Engineers (India) 84, 2003, 6-9
10. Zeng Y.C., Yu C.W.: Numerical and Experimental Study on Reducing Yarn Hairiness with the JetRing and JetWind, Text. Res. J. 74(3), 2004, 1-5
11. Ramachandralu K., Ramesh V.: Design and Development of Twin Air-jet Nozzle System for Ring Spinning, The Journal of The Institution of Engineers (India) 86, 2005, 1-5
12. Najar S.S.: An Analysis of Twist Triangle in Ring Spinning, PhD Thesis, The University of New South Wales, 1996
13. Pillay K.P.R.: A Study of the Hairiness of Cotton Yarns, Part 1: Effect of Fiber and Yarn Factors, Textile Res. J. 34, 1964, 663-674
14. Wang S., Yu X.: New Textile Yarns, ed. 1, Publishing Company of Donghua University: Shanghai, 2007, 121
15. Zhu GC, Ibrahim S., Křemenaková D.: The optimization application of air-jet nozzle in ring spinning system, In 18th International Conference STRUTEX Structure and Structural Mechanics of Textiles. 7-8th December 2011, Technical University of Liberec, Liberec, Cezch Republic